CHALMERS
UNIVERSITY OF TECHNOLOGY

# Solution Blown Conductive Cellulose Nonwovens

Master's thesis in Materials Chemistry

ELIN WESTROTH

DEPARTMENT OF CHEMISTRY AND CHEMICAL ENGINEERING
CHALMERS UNIVERSITY OF TECHNOLOGY

Gothenburg, Sweden 2020
www.chalmers.se

Master's thesis 2020:KBTX12

# Solution Blown Conductive Cellulose Nonwovens

ELIN WESTROTH


CHALMERS
UNIVERSITY OF TECHNOLOGY

Department of Chemistry and Chemical Engineering
Chalmers University of Technology
Gothenburg, Sweden 2020

Solution Blown Conductive Cellulose Nonwovens
ELIN WESTROTH

Supervisor: Ting Yang Nilsson, RISE IVF
Supervisor: Sozan Darabi, Department of Chemistry and Chemical Engineering
Examiner: Christian Müller, Department of Chemistry and Chemical Engineering

Master's Thesis 2020:KBTX12
Department of Chemistry and Chemical Engineering
Chalmers University of Technology
SE-412 96 Gothenburg

Cover: Nonwoven textile-material made from cellulose and carbon black using the solution blow spinning technique.

Written in LaTeX
Gothenburg, Sweden 2020

Solution Blown Conductive Cellulose Nonwovens
ELIN WESTROTH
Department of Chemistry and Chemical Engineering
Chalmers University of Technology

## Abstract

Conductive textiles, which have the benefit of being soft, flexible, and light, can provide many possibilities in fields such as communication, healthcare, and energy storage. The possibility of producing conductive nonwovens, from cellulose and carbon black, using the solution blow technique, was studied in this master's thesis. Nonwovens with 33, 42 and 50 wt% carbon black, based on the total amount of carbon black and cellulose, were produced to study the effect of carbon black on the nonwoven properties. The nonwoven structures, in terms of fibre diameter and surface density, were also varied to determine how the nonwoven structure affects the resistance and the mechanical properties.

It was shown that 33 and 42 wt% carbon black could be mixed into the cellulose solution while still maintaining a low enough viscosity to sufficiently solution blow the nonwoven material. 50 wt% carbon black however resulted in a remarkably high viscosity of the solution, most likely due to a percolated network of carbon black forming within the solution. The surface resistance of the nonwoven material was shown to decrease with the concentration of carbon black, the surface density, and with the fibre diameter. The decrease, with increased surface density and increased fibre diameter, showed the importance of reducing the contact resistance between the fibres to lower the overall surface resistance. The lowest resistance achieved for 42 wt% carbon black nonwovens was measured to 57 $\Omega/\square$. The mechanical properties were also affected by both the incorporation of carbon black as well as the nonwoven structure. The surface density showed an increase of both the strain at max load and the effective stress at max load with increased surface density. It was also shown that incorporation of carbon black made the fibres weaker. Carbon black/cellulose nonwovens measured lower Young's modulus and lower effective stress at max load compared to pure cellulose nonwovens. SEM imaging showed that the morphology of the fibres changed due to the carbon black, making the surface more rough and thereby also increasing the BET specific area from 2 $m^2/g$ to above 500 $m^2/g$ for 42 wt% carbon black nonwovens.

Preliminary testing was also performed to evaluate the material's future possibilities in pressures sensing and energy storage. Promising results were achieved for the testing of the material as a pressure sensor. The results showed a decrease in resistance when pressure was added on top of the material, low hysteresis was also shown as the pressure was applied and removed. For applications in energy storage, the material showed the ability of storing charge, though the measured capacitance was low. Further improvements of the material should therefore be studied, for the material to be used in energy storage. In conclusion, the master's thesis showed the possibility of producing conductive carbon black/cellulose nonwovens, using the solution blown technique, as well as providing possible future application for the produced material.

Keywords: solution blow spinning, cellulose, carbon black, nonwoven, conductive nonwoven

## Acknowledgment

I would like to thank the fibre development group at RISE IVF in Mölndal and Tobias Khönke for making it possible for me to perform my master's thesis project in the group. A big thanks to Ting Yang Nilsson who has been my supervisor throughout the project, always assisting me with any questions I have had, inspiring new ideas, and for all the help during the solution blow spinning. Also, thank you to Simonetta Granello for the help with mechanical testing, Oleksandr Nechyporchuk for the assistance with rheological measurement, Hanna Ulmefors for the help with BET specific surface area measurements, and Taoran Ma for SEM imaging. Also, to everyone else at RISE IVF who have taken the time to help me when I've had any questions and for making me feel welcome.

Thank you to Xin Wang and Matilda Taube, at RISE in Norrköping, for a good and fun collaboration during the project, and for performing all the electrical measurement and also SEM imaging.

I would also like to thank Sozan Darabi, Anja Lund and Christian Müller at Chalmers who has made it possible for me to do this project and for answering any questions I have had, as well as contributing with ideas for the project.

Elin Westroth, Gothenburg, 2020

# Contents

# 1. Introduction

An introduction to the master's thesis will be given with a background of the purpose of producing cellulose conductive textiles and why this type of material is interesting. Similar materials that are highly porous and use conductive carbon fillers are presented in a literature study. The aim, limitations and methodology used to pursue the aim in the master's thesis, are also stated in this section.

## 1.1 Background

Conductive textiles are textiles which keep their advantageous, characteristic structure and function of being soft, flexible, and light, while at the same time having the additional property of being conductive.[1, 2] Their properties of being soft, flexible and light set the conductive textiles apart from other traditionally conductive materials such as metals which are hard, stiff and heavy.

Producing conductive textiles from a bio-based source, like cellulose, provides additional benefits to the material. Cellulose is a biodegradable, renewable and biocompatible material thereby providing a sustainable alternative to inorganic electronic.[3] Cellulose, which is not conductive on its own, can be mixed with a conductive filler which transports electric charge. Conductive fillers can thus be added to make an insulating material conductive, moreover replacing metals as conductive components within a material.[4] The conductive filler carbon black is easy to blend into a solution and it is also low cost. A solution of cellulose and carbon black can be made into a fabric-like material, a nonwoven, using solution blown spinning. Through solution blown spinning, a textile material is obtained directly from the solution, the technique thereby avoids the process of first having to produce yarn, that then has to be knitted or woven into a textile. The technique also makes it possible to produce a textile-like material from weak fibres that could otherwise break if they for example were to be knitted. Thus, using the solution blown technique provides the advantage of producing material in a fast and cheap way.[1]

Other organic electronics, using conductive polymers, focus mainly on applications using thin films like displays, transistors and solar cells.[5] Conductive textiles with its fibre microstructure have the ability to move beyond these applications and also explore other areas. There is, for example, potential for electronic textiles to be used in many different fields such as communication, biomedical research, textiles, and healthcare, used as wearable electronics for heated clothing, used in light-weight energy storage device or as sensors that can monitor the environment or the human health.[2, 6–8]

The purpose of this master's thesis is to explore the ability to produce conductive textiles using cellulose, carbon black, and the solution blown technique, as this process could result in many benefits. Advantages could be achieved both in terms of production, being fast and low cost, and sustainability as the material is produced from cellulose. It also opens the door to additional research fields for organic electronics.

## 1.2 Previous Work in the Field of Porous Conductive Materials

The conductivity achieved using carbon based conductive fillers was investigated in a literature study to provide a background of what conductivity might be reachable for the carbon black/cellulose nonwoven aimed to be produced in this master's thesis project. Similar textile-inspired materials with carbon black as the conductive filler have been produced, the difference being that individual fibres were produced contrary to the nonwoven textile-like material aimed to be produced in this project. Carbon black has been used with both polyethylene and cellulose to create conductive fibres. Using carbon black, at 40 wt%, together with high density polyethylene resulted in fibres with a conductivity of 2.5 S/cm.[9] Conductive fibres out of cellulose and 50 wt% carbon black were produced by wet-spinning and resulted in a conductivity of 0.6 S/cm for the fibres.[10] The conductivity of a textile material however depends on both the resistance within the fibres as well as the contact resistance between fibres, resulting in a lower conductivity for textile materials compared to that of individual fibres (The concept of conductivity in textile materials is further explained in section 2.4.). The material produced in this project, carbon black/cellulose nonwoven, is therefore expected to have a lower conductivity than the carbon black/cellulose fibres (0.6 S/cm), as it is a textile material.

Due to its fibre structure, the textile material can be regarded as a very porous material. No material could be found that uses the same components, cellulose and carbon black, and the same method, solution blow spinning, that is to be used in this thesis project. Other conductive porous materials that use carbon particles as the conductive component were therefore investigated in the literature study, shown in Table 1. Table 1 shows the conductive filler component and matrix material used as well as the concentration of conductive filler in the material. The conductivity of the material is also presented together with a description of the material, as mentioned by authors in the respective article. The conductivity presented was measured for the whole material, not just for single fibres. Many of the porous materials presented in Table 1 are referred to as aerogels. These are materials with high porosity, low density and high inner surface area.[11] The material produced in this master's thesis is also shown in Table 1 for comparison.

Table 1: Conductivity of porous materials with carbon conductive fillers carbon nanontubes, CNT, carbon black, CB and carbon fibre, CF. A description of the material, as given by the author of respective article, is also included.

| Conductive component | Matrix material | Concentration of conductive component | Conductivity (S/cm) | Description of material | References |
|---|---|---|---|---|---|
| CNT | Cellulose | 10 wt% | 0.018 | Composite aerogel | [12] |
| CNT | Cellulose | 10 wt% | 0.022 | Composite aerogel | [13] |
| CNT | PEDOT/PSS | 5 wt% | 0.069 | Composite aerogel | [14] |
| CNT | Nanocellulose | 20 wt% | 0.01 | Aerogel | [15] |
| CNT | Bacterial cellulose | 9.6 wt% | 0.14 | MWCNT-incorporated cellulose pellicle | [16] |
| CNT | Waterborne polyurethane/ cellulose nanocrystals | 5 wt% | 0.001 | Composite foam | [17] |
| CB | Isoprene | 14 wt% | 0.015 | Stretchable conductive polymer composite | [18] |
| CB | Polyurethane | 30 wt% | 0.085 | Conducting composite | [19] |
| CB | Polyurethane | 15 wt% | 0.011 | Nanocomposite fibre web | [20] |
| CF | Polypropylene/ Polyethylene | 40 wt% | 5.5 | Nonwoven | [21] |
| CF | PDMS | 3 wt% | 0.042 | Porous nanocomposite | [22] |
| CB | Cellulose | 42 wt% | 0.027 | Nonwoven | This master's thesis |

Figure 1 shows the relationship between the concentration of the conductive filler and the measured conductivity of the porous materials. Different types of carbon fillers are represented by different symbols in the figure: carbon nanotubes (CNT) = green square, carbon black (CB) = orange circle, and carbon fibre (CF) = red triangle. The filled orange circle represents the material produced in this master's thesis. The materials having cellulose as matrix material are enclosed in a grey region.

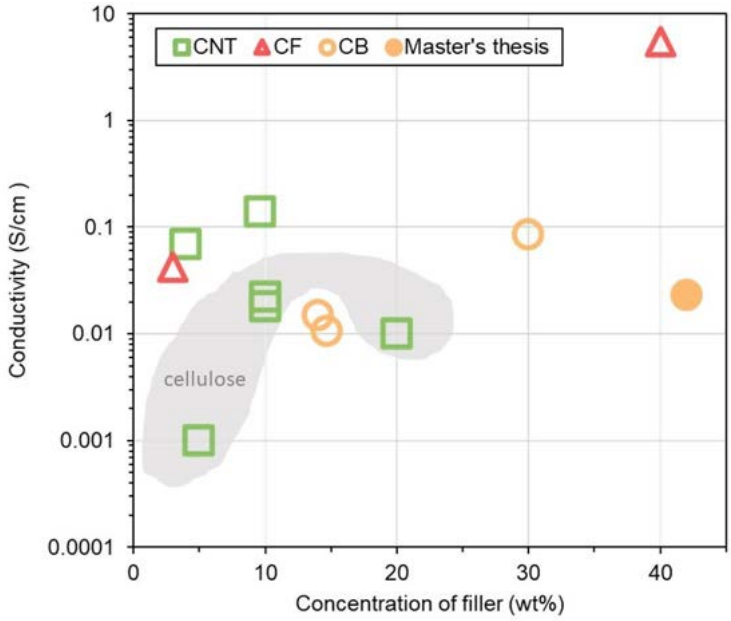


Figure 1: Relationship between concentration of filler and conductivity for porous materials with carbon based conductive fillers, carbon nanotube, (CNT, green square), carbon fibre (CF, red triangle), carbon black (CB, orange circle). The material produced in this master's thesis is shown with a filled in orange circle. All materials with cellulose as the matrix material are enclosed in a grey region. For references see Table 1.

The conductivity of the porous materials depends on the type of conductive component used, the matrix material, the amount of conductive filler loaded into the material, the porosity and also the way in which the filler is incorporated into the conductive composite.[23] The conductivity one wants to obtain also depends on the application it is aimed to be used for. For example, a sensor's main purpose is not to be as conductive as possible, but for the conductivity to change as the sensor is exposed to external stimuli. Figure 1 illustrates that the cellulose based materials generally give lower conductivity, below 0.05 S/cm, compared to using other polymer matrices. The PEDOT/PSS aerogel with CNT results in three times as high conductivity (0.069 S/cm) compared to cellulose and CNT aerogels (around 0.02 S/cm), Table 1. It is important to note that PEDOT/PSS can itself be used as an inclusion in a cellulose aerogel to improve the conductivity of cellulose, as PEDOT is a conductive polymer. Cellulose alginate aerogels functionalized with PEDOT:tosylate were reported to show a conductivity of 5.7 S/m at a concentration of 1.7 g/g mass of PEDOT:tosylate in the cellulose aerogel.[24] The higher conductivity achieved when using PEDOT/PSS as the matrix material is thereby most likely due to the conductive properties of PEDOT/PSS. However, matrix materials made from other polymers than cellulose do not possess the advantages of cellulose, like being biodegradable, biocompatibility and originate from a renewable source.

Figure 1 also shows a trend of higher concentrations of CB being used, >10 wt%, com-

pared to CNT (square), $\leq$ 10 wt%, without any difference in conductivity achieved. This may also explain why more references could be found for materials with CNT, compared to CB, as it is probably preferred hence it allows a lower concentration of filler. The lower concentration of filler required is related to the higher aspect ratio of CNT, further explained in section 2.3. CB is however chosen for this project based on the possibility of spinning nonwoven material. CB/cellulose fibres with 50 wt% CB have successfully been produced using wet spinning by Härdelin et.al.[10] The step from wet spinning to solution blow spinning is not very big as both techniques utilise a solution to make material. Thus, making the CB/cellulose solution promising for solution blow spinning.

## 1.3 Aim

The aim of the master's thesis is to produce conductive nonwoven material made from cellulose and the conductive filler carbon black, using solution blown technique. The produced nonwoven will be characterized to evaluate how the surface resistance, mechanical properties, and morphology changes with the incorporation of carbon black. The effect of the nonwoven structure, in terms of fibre diameter and surface density, on the electrical and mechanical properties will also be studied.

## 1.4 Limitations

The project will be operated at lab scale only, aiming to produce nonwoven material large enough for testing. The produced samples will also have a limited width as the width of the nine capillary nozzle, used during solution blowing, is 1.5 cm. Due to narrow samples, tensile testing in the cross direction is excluded, and tensile testing in the machine direction will solely be conducted. To achieve solutions of cellulose and carbon black that have the right viscosity for solution blowing, the ratio between the solvents EMIMAc and DMSO will be tested. The change of temperature, as a strategy to decrease the viscosity, will not be a parameter tested. The constant heating of the solution will become time consuming as several steps of heating has to be added during production of the nonwoven. The aim is instead to have solutions that are workable at room temperature. The project will only focus on one type of conductive filler, carbon black, and only one system for dissolution of cellulose, EMMIMAc/DMSO. This project will mainly focus on the production of the nonwoven material, however improvement of the nonwoven in terms of the softness and feel will not be in focus. The characterization of the nonwovens' electrical properties will be performed by collaborators at RISE in Norrköping. This master's thesis will therefore not focus on the these measuring techniques, only the results from these measurements will be obtained.

## 1.5 Methodology

To produce conductive cellulose nonwovens, the master's thesis project includes three main parts: finding a solution that can be solution blown into nonwoven material (1), producing the nonwoven using solution blown technique (2), and the analysis of the nonwoven material for evaluation of how the electrical properties, the mechanical properties, and the morphology, changes with the incorporation of carbon black (3), Figure 2. The goal is to make the nonwoven as conductive as possible to investigate the maximum conductivity, that can be reached for the nonwoven, thus being an indication of what possibilities the

material possesses, in terms of future application. Nonwovens from cellulose and 33 wt% CB (Appendix A) were produced in trials prior to the master's thesis project. Improvements of the method used in previous trials are to be made to allow incorporation of more carbon black into the nonwoven, and to make the process more time efficient.

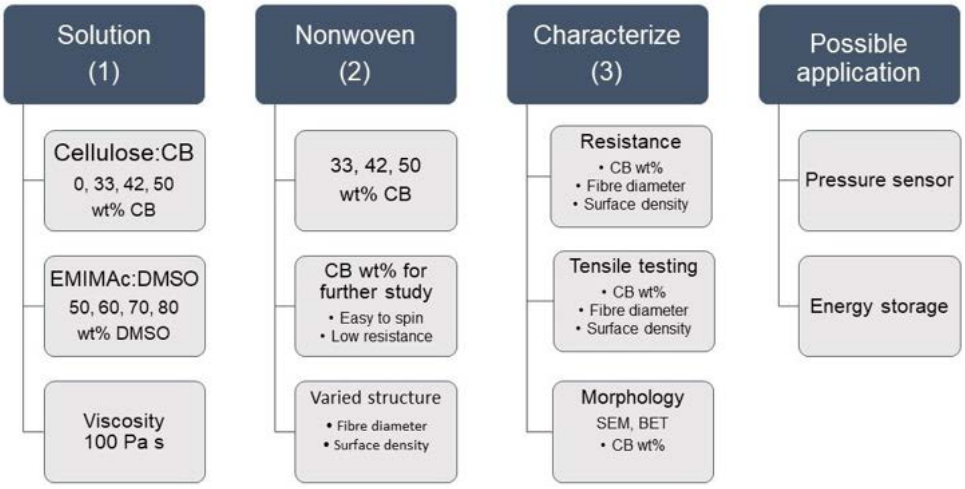


Figure 2: Methodology used in project to produce conductive cellulose nonwovens. The three main parts are: making the CB/cellulose solution (1), producing the nonwoven material (2), characterising the resistance, tensile properties and the morphology of the fibres (3).

The viscosity of the solutions, measured using rheology, is an indication of whether the solution has the ability to be solution blown or not. For solution blowing, a shear viscosity of 100 Pa s has been reported as a bench mark for achieving a spinnable solution.[25] Three ratios between cellulose and carbon black (33, 42 and 50 wt% CB) is attempted to see how much conductive filler can be incorporated into the solution. The viscosity of the solutions is tuned by varying the ratio between the solvent, 1-ethyl-3-methylimidazolium acetate, EMIMAc, and the co-solvent, dimethyl sulfoxide, DMSO (50:50, 40:60, 30:70, 20:80). One solution for each concentration of carbon black, with a viscosity close to the benchmark of 100 Pa s, is then selected for trial, using the solution blown technique, to see if it is possible to produce nonwoven material.

To further study the effect of nonwoven structure on the electrical and mechanical properties, nonwovens with different fibre diameter and different surface density are produced. The CB concentration resulting in a solution which is easy to spin into fibres, and which also results in nonwoven material with as low resistance as possible, is selected to produce the nonwovens with varied structure. Nonwovens with both varied CB concentration and varied nonwoven structure are then characterized for their electrical and mechanical properties as well as the morphology of the fibres. Both solutions and nonwovens are visualized using light microscopy in order to measure particle size and fibre diameter respectively. Scanning electron microscopy, SEM, is also for visualization of the individual fibres and their surface morphology. $N_2$ adsorption is utilized to measure the specific surface area of the nonwovens by the BET-method. The mechanical testing in the form of tensile testing is also performed to quantify the strain, strength, and stiffness of the nonwoven material. The electrical properties, surface resistance and capacitance, are measured by collaborators at RISE in Norrköping. The capacitance is measured as an indication of using the material in energy storage applications. The application of the material as a pressure sensor is also preliminary tested by measuring the resistance response to pressure.

# 2. Theory

A detailed description of how the nonwoven material is created using solution blow spinning as well as the definition of a nonwoven material is given in the theory section. Concepts to understand the components, cellulose, and carbon black, are also presented. Topics mentioned for cellulose are its structure, how cellulose is dissolved and regenerated into fibres using ionic liquid, and its role during the fibre spinning process. The principles of a conductive filler are mentioned as well as the importance of dispersing the filler in the solution. Important concepts used for characterization of the solution and the nonwoven are also presented for resistance, rheology, tensile testing and Branauer-Emmett-Teller (BET), specific surface area.

## 2.1 Solution Blow Spinning of Nonwovens

Nonwoven materials are currently found in many different products such as automotive interiors, isolation, filtration media, and in disposable fabrics such as sanitary wipes or as medical/surgical disposables.[26] The nonwoven material consists of fibres which are randomly oriented and entangled, as opposed to more traditional fabrics which have a more ordered fibre arrangement. Figure 3 shows the arrangement of fibres in woven and knitted textiles where the fibres are interloped and interlaced in a more ordered manner compared to the random orientation in the nonwoven.[27] Nonwovens are produced in one continuous process, directly from a solution or melt.[27]. Removing the first step of producing fibres, which are then processed into fabric, makes the production of nonwovens a comparably fast and cost-effective method due to reduced labour and handling cost for nonwoven materials.[1, 27] The process also makes it possible to produce textile-materials from weak fibres that could otherwise break if the fibres were to be knitted or woven into a textile.

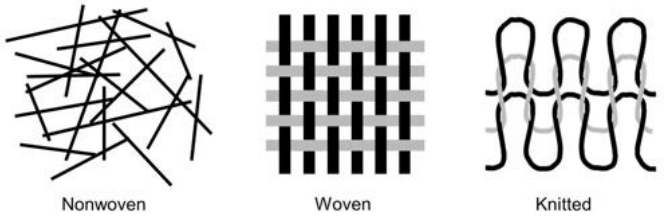


Figure 3: Schematic drawing of the inter-structure in nonwoven, woven and knitted textiles. Adapted from Stoppa et.al.[1]

Nonwovens can be produced using various fibre spinning techniques, such as melt blowing, electrospinning, and solution blow spinning. If bio-based materials are to be produced, melt blowing often proves difficult due to the fact that many bio-based materials do not melt, e.g. cellulose.[28] Electrospinning and solution blow spinning are therefore better options when producing bio-based nonwovens as a solution is used instead of a melt.[29] Electrospinning requires that a large electric field is applied and highly toxic solvents are therefore often used to provide conductivity to the solution.[30] Another disadvantage with

electrospinning is that it can be difficult to produce material in large scale. Commonly in electrospinning, only one single nozzle is used and when it comes to cellulose, only low concentrations can be used.[25] This makes electrospinning a relatively slow production technique. Solution blow spinning is therefore advantageous as it has fewer limitations than electrospinning. Producing nonwovens in larger scale is easier with solution blow spinning as the number of nozzles is directly coupled to the production speed and can be easily increased.[30] Using less toxic solvent, as well as faster production, thus makes solution blow spinning interesting when producing bio-based nonwovens.

Solution blow spinning is a fibre spinning technique where a solution is extruded through fine capillaries and rapidly drawn out into fibres by a high pressure air stream.[30] The solution is pushed through the capillaries by a pump, at which the extrusion speed is controlled. As the solution reaches the fine capillaries, the solution is drawn out into thin fibres by the surrounding air stream, flowing around the solution. The air stream also guides the solution down to the coagulation bath.[30] The fibres become randomly entangled and randomly oriented as they enter the bath and the nonwoven material is created as the solvent is replaced by the coagulant. The nonwoven can then be collected from the bath, for example using a rotating collector.[25] A schematic of the solution blow spinning process is shown in Figure 4. The schematic shows the cross-section of the solution blow apparatus.

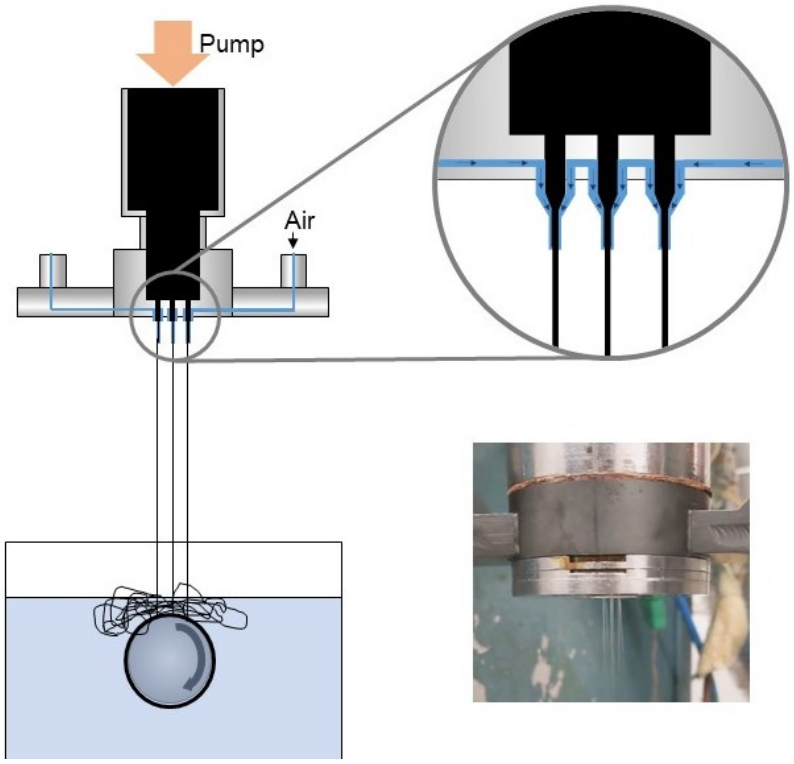


Figure 4: Schematic representation of the solution blown technique and photo of the spin die.

There are many factors that affect the spinning process, both the parameters used during the spinning as well as the composition of the solution used. For the solution to be spinnable and to be processed into fibres, it has to have a workable viscosity as well as a high enough concentration of polymer in the solution. It is important that the entanglement of chains is high enough to overcome the forces experienced by the solution when it is pushed through the fine capillaries and drawn out into fibres by the high pressure air

stream, or no fibres will form. For fibres to form, the concentration of polymer therefore has to exceed the overlap concentration, c*, at which the polymer chains within the solution start to entangle and overlap. If the concentration of polymer is below c*, beads will form instead of long continuous fibres.[30] The entanglement of polymer chains also depends on the polymer molecular weight, the length of the polymer chain. Longer chains will result in more entanglement which thereby decreases the overlap concentration.[31] For example, Zhang et.al. showed that high molecular weight cellulose resulted in more stable fibre formation and could also withstand a higher maximum air velocity compared to low molecular weight cellulose.[32]

The molecular weight and concentration of polymer also affects the viscosity and flow of the solution, something that also has to be considered during solution blow spinning. Other factors affecting the viscosity are the temperature, which reduces the viscosity, as well as the incorporation of filler, such as nanoparticles, which can increase the viscosity.[30] The solution's ability to flow will also affect the extrusion speed required to push the solution out through the fine capillaries. The viscosity is thereby important for the spinnability of the solution as well as for the ability to be produce thin fibres. A viscosity of 100 Pa s has been reported suitable to form cellulose fibres with small diameters during solution blow spinning.[25] 100 Pa s is therefore used as a benchmark when preparing solutions in this project.

By changing the parameters used during the solution blow spinning process, the structure of the nonwoven and its fibres can be altered. Parameters that can be altered are the extrusion speed of the solution, the air flow pressure, the collection time, the distance between the nozzle and the coagulation bath, as well as the temperature.[29] The thickness of the fibres is affected by the amount of solution exiting the capillaries at a given time, something which can be controlled by the extrusion speed. A higher extrusion speed will therefore result in thicker fibres as more solution is being pushed through the capillaries.[33] The pressure of the air stream will also have an effect on the fibre diameter. Higher air pressure will result in thinner fibres as the solution can be drawn out faster when falling down into the coagulation bath.[33] The mass of the sample collected is governed by the collection time of the nonwoven in the coagulation bath. A sample that is collected for a longer time will have a higher mass as well as a higher surface density (the nonwoven surface density is defined as the mass of the nonwoven divided by its surface area, Equation 3). To be able to form fibres, the extrusion speed nor the air pressure can be too high or too low. The air pressure and extrusion speed cannot be too high, or the forces experienced by the solution will prevent it from forming continuous fibres. Too low extrusion speed will also prevent fibre formation as enough polymer has to exit the capillaries for stable fibres to be formed. The window in which nonwoven material can be produced is therefore limited, as neither the extrusion speed, air pressure, nor viscosity, can be too high or too low to sufficiently produce nonwoven material from a solution. All these parameters have to be considered to successfully produce a nonwoven fibre-material from a solution.

## 2.2 Cellulose

In the quest of making sustainable bio-based materials, cellulose is an interesting alternative due to its many advantages. Cellulose is both biocompatible, biodegradable, low-cost and made from a renewable source, it is most commonly food in wood.[3] Cellulose can also

be found in other sources like bushes, bast plant, and cotton fibres, as well as in organisms such as algae, bacteria, and animal tunicates, where cellulose is naturally produced.[34] Cellulose, like many other bio-based materials, does not melt which limits the number of processing techniques that can be used to regenerate cellulose into material.[35] It is however possible to dissolve cellulose using ionic liquids.[36] Dissolving cellulose makes it possible to regenerate cellulose into fibre material by various fibre spinning techniques, such as solution blow spinning. Ionic liquids also possess advantages over more traditional solvents which are often volatile, toxic and have higher melting points.[37] Cellulose is therefore an attractive material to explore in order to produce sustainable fibre materials, like nonwovens.

### 2.2.1 Cellulose Structure

Cellulose is a linear non-branched polysaccharide, made up of glucose units (D-glucopyranose units). The glucose units are linked between carbon 1 and 4, by so called $\beta$ -1,4- glucosidic bonds, Figure 5.[38]. The glucose molecule contains a large number of free hydroxyl groups which can form both intramolecular hydrogen bonds between neighbouring glucose molecules within the chain as well as intermolecular bonds between the cellulose chains, Figure 5.[35] The large number of hydrogen bonds result in a big cellulosic network being created.[34] The intramolecular bonds are responsible for the rigidity of the cellulose chain whereas the intermolecular bonds regulates the crystal structure of the cellulose. The cellulose chains align in bundles to form microfibrils which have both ordered crystalline regions as well as unordered amorphous regions. The microfibrils then bundle up to form macrofibrils which are the building blocks of the cellulose fibre cell walls.[35] Cellulose fibres are therefore semi-crystalline, made up of both crystalline and amorphous regions. The crystalline regions are formed due to the intermolecular hydrogen bonding between chains. These hydrogen bonds are strong compared to those in the amorphous regions which are fewer and looser.[35] It is due to the strong bonds in the crystalline regions that the cellulose does not melt and which also makes cellulose insoluble in many solvents, like water.[35] Cellulose will however swell in water due to the hydrogen bonds which can form between water and the loose hydroxyl groups in the amorphous regions.[37] The semi-crystallinity of cellulose thereby makes it both hydrophilic as well as insoluble in water. As cellulose is insoluble in water, water can be used as the coagulation medium for cellulose in for example solution blow spinning.

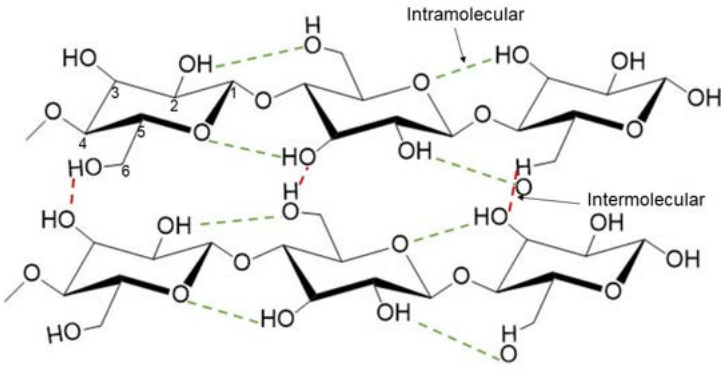


Figure 5: Molecular structure of cellulose showing intramolecular hydrogen bonds (green) and intermolecular hydrogen bonds (red). Adapted from Paquin et.al.[35]

There are different crystal structures of cellulose, the two major ones being cellulose I and

cellulose II. Cellulose I is the crystalline structure of almost all native celluloses whereas cellulose II is the crystalline structure of regenerated cellulose.[38] Regenerated cellulose is native cellulose which has been dissolved after which it is again made into cellulose material, by for example fibre spinning. The crystallinity of cellulose depends on the source of the cellulose. The degree of crystallinity is in the range of 50 - 75 % for cellulose from higher plants, such as wood, 80 % for tunicate cellulose and 25 - 40 % for regenerated man-made fibres.[38] The number of glucose units in the cellulose chain, the degree of polymerization (DP), also varies with the source of the cellulose. The DP for wood pulp is around 300 to 1700 whereas the DP for cotton, other plant fibres and bacterial cellulose is in the range of 800 to 10 000.[35]

### 2.2.2 Dissolution of Cellulose

The strong interactions between the cellulose chains, primarily in the crystalline regions, makes the cellulose hard to dissolve in many solvents.[35] For the cellulose to be dissolved, intermolecular interactions have to be broken, and the chains have to be separated from each other, something which can be achieved using ionic liquids.[36] Ionic liquids have become very interesting as solvents for cellulose in the last couple of decades as they have advantages over more traditional solvents which are volatile and toxic.[36] Ionic liquids are also preferred as they have a low melting point, generally below 100°C, and can be used under mild conditions also making them interesting from an energy perspective.[37]

Ionic liquids are organic solvents which consist of counter ions, just like salts.[37] One such compound is 1-ethyl-3-methylimidazolium acetate, EMIMAc, which can be used to dissolve cellulose. Studies suggest that both the cation, $[EMIM]^+$, and the anion, $CH_3OOH^-$, in the ionic liquid EMIMAc, can form hydrogen bonds with the hydroxyl groups on the cellulose chains, thereby causing separation of the chains and dissolution of the cellulose.[39] At least 2.5 - 3 moles of EMIMAc, to each anhydroglucose unit in the cellulose, are needed in order for the cellulose to be dissolved.[40] Ionic liquids have a much higher viscosity than many other organic solvents, making them hard to use in some processes.[37] To tune the viscosity of solvent, a co-solvent with lower viscosity can be added.[40] Dimethyl sulfoxide, DMSO, which is miscible in EMIMAc but incapable of dissolving cellulose on its own, can be used as a co-solvent when dissolving cellulose.[40] DMSO has a viscosity of 2 mPa and is much less viscous than EMIMAc, which has a viscosity of 200 mPa.[37] Adding DMSO does not reduce the ionic liquid's ability to dissolve cellulose and can therefore be used in the solvent as long as the concentration of EMIMAc is kept above the required concentration for dissolution of cellulose (2.5 - 3 moles per cellulose anhydroglucose unit).[28, 40] Changing the ratio between EMIMAc and DMSO in the solution thereby makes it possible to decrease and tune the solution's overall viscosity.[41] Replacing some of the ionic liquid with the co-solvent DMSO also comes with the advantage of reducing the overall cost of the solvent, ionic liquids being generally expensive.[28]

There are many advantages of ionic liquids compared to other traditional solvents, such as low melting point, they are less volatile and also less toxic. Their advantages and ability to dissolve cellulose make ionic liquids interesting for production of sustainable materials. However, ionic liquids are currently mostly used in research and not in up-scaled processes.[36] Aspects like the toxicity, risk for exposure, and environmental effects have to be considered further for ionic liquids to move from lab-scale to industrial production.[36] The main drawbacks hindering the use of ionic liquids are the recyclability and reusability of the solvent. These factors become crucial due to the cost of ionic liquids but also for a

sustainable process to be achieved. Hence, these challenges have to be overcome for ionic liquids to be used as solvents at an industrial scale, in a sustainable way.

## 2.3 Conductive Filler

Conductive fillers can be added to an insulating material, like plastic or cellulose, to make it conductive.[42] Examples of conductive filler are metals, like copper and silver, and carbon based fillers such as carbon black, CB, carbon nanotubes, CNT, and graphite.[43] A conductive material can only be achieved if a continuous conductive pathway is formed within the material, along which charge can flow, Figure 6b. The concentration at which the conductive pathway starts to form, and the resistivity starts to decrease, is called the percolation threshold, Figure 6a.[42] The relationship between the resistivity and the concentration of filler can be seen in Figure 6a, which shows an S-shaped curve. The resistivity does not decrease noticeably until the percolation threshold is reached. Above the percolation threshold, the resistivity starts to decrease dramatically with the increase in filler concentration until the resistivity eventually levels off, indicating that an increase in filler concentration does not improve the conductive pathway further.[42]

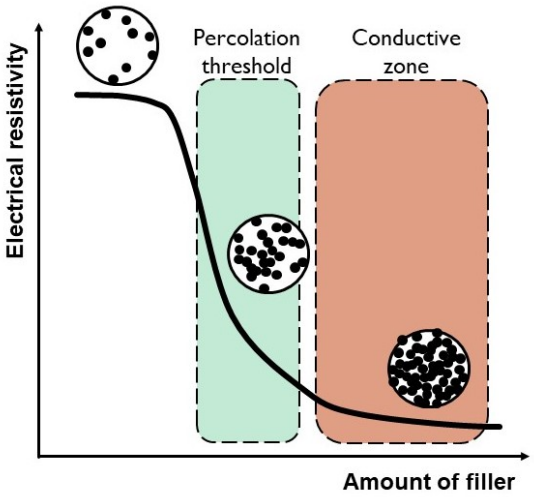


(a)

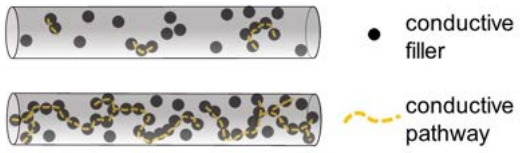


(b)

Figure 6: Definition of the percolation threshold, a. Adapted from DeArmitt.[42] Schematic showing the conductive pathway formed between conductive filler particle, b.

The conductivity and percolation threshold depend on both the size, shape, and aspect, ratio of the conductive filler.[23] Examples of fillers with different aspect ratios are CNT, which has a higher aspect ratio than CB due to its more elongated shape. The percolation threshold has been shown to decrease with increased aspect ratio.[23] Consequently, a higher concentration of CB is needed to make an insulating material conductive compared to CNT.[23]

The dispersion of filler in a solution is also important to achieve a homogeneous mixture which can be easily processed into a conductive material. Dispersion can however be difficult with nano-sized particles as they easily form aggregates which further join into larger agglomerates due to the existing Van der Waals forces between the them.[4] In solution blow spinning it is important that the aggregates within the solution are no bigger than the diameter of the fine capillaries, or clogging can occur. Having an even size

distribution of aggregates and particles in the spinning solution is also important for the continuous flow of solution when it is drawn into fibres. Large aggregates in the solution might cause breakage during the fibre spinning process.[44] The aggregates can therefore not be larger than the desired fibre diameter.

### 2.3.1 Carbon Black

The conductive filler used in this project is carbon black. Carbon black is widely used as a conductive fillers, but also as pigment and as a reinforcing filler in tires.[45] Because carbon black and other carbon based fillers are conductive they have the ability to replace metals where a conductive material has to be achieved. Carbon black is an amorphous form of carbon, with high surface area, consisting of primary nanoparticles that easily fuse together to form aggregates.[4, 45] Carbon blacks are mainly derived from fuel oil by thermal decomposition of hydrocarbons.[45] The electrical volume resistivity for most carbon black grades are in the range of $10^{-1}$ - $10^{2}$ Ωcm. As carbon black has a higher resistivity than metals the incorporation of carbon black in a polymer material will results in a lower conductivity than for traditionally conductive materials, like metals.[43] The conductivity required for a material however depends on its application thus carbon black still has the ability to replace metals in various applications though it has lower conductivity.

Moving away from metals, goes hand in hand with the quest of creating more sustainable bio-based materials. Metals have many disadvantageous from an environmental perspective. They have to be mined, and heavy metals, like copper, are known to accumulate in the environment and in organisms.[46] Eco-cost is an indicator which can be used to evaluate the sustainability of different products.[47] The value of the eco-cost is based on the impact on human health, on the ecosystem, resources used, as well as the carbon footprint.[48] Copper has an eco-cost of 8.82 €/kg and is thereby more of an environmental burden than CB, with an eco-cost of 1.28 €/kg.[48] Replacing metals with conductive carbon black is therefore beneficial in terms of sustainability.

Creating a fully sustainable material using CB, however requires consideration of both the source of carbon black as well as of where it ends up at the end of its life cycle. Producing carbon black from more sustainable raw materials than fuel oil could be a big step in making CB a more sustainable alternative. Using vegetable oil as a renewable source could be an alternative in the future, and work like this has already been conducted in the tire industry.[49] Another option could be to use oil residues from other processes where the oil would otherwise be disposed of. As carbon black is made up of nanoparticles which can have consequences if they enter the environment, it is also important to evaluate the recyclability and leakage of nanoparticles in a material with nanoparticular fillers.[47] This will not be evaluated in the master's thesis but it is important to keep in mind when talking about the sustainability of the material. Though carbon black serves useful in moving towards more sustainable products by replace metals, their own impact on the environment during their life cycle still has to be carefully considered.

## 2.4 Conductivity of Textiles with Conductive Fibres

The conductivity of a textile material made out of conductive fibres does not only depend on the fibres' conductivity, it also depends on the contact resistance between fibres.[50] A conductive textile is made up of many fibres. The current therefore has to flow, not

only within one fibre, but also from one fibre to the other, making the contact resistance between fibres very important. The contact resistance depends on both the contact area between fibres and on the number of contact points.[51, 52] Both an increase in the number of contact points as well as the contact area make it easier for charge to travel within the material. As the path travelled by the charge becomes less hindered, the resistance decreases. The contact resistance will therefore decrease as the number of contact points and the contact area between two fibres increase.[51, 52] The effect of contact resistance make conductive textiles interesting as pressure sensors. As pressure is applied onto a fluffy conductive textile both the number of contact points as well as the contact area between fibres will increase due to the fibres being forced closer together.[51] Applying pressure will thereby cause a decrease in resistance. Hence, making the conductive textiles suitable as pressure sensors.

Textiles are very porous compared to other conductive materials.[53] Due to the porosity, the thickness of the material can be very hard to measure. Flat conductive materials like conductive textiles, and thin films, are therefore often characterized using surface resistance, where the thickness of the sample is ignored.[53]. The surface resistance is given in the unit "ohm per square", $\Omega/\square$, and is often measured using a so called four-point probe.[53, 54]

## 2.5 Rheology

During the solution blowing process, the solution is subjected to a lot of shear, for example during mixing, pumping, and drawing of the solution into fibres. The viscosity and flow of a solution therefore becomes interesting in terms of fibre spinning as the suitability of the solutions for fibre spinning is highly dependent on the flow of the material. Rheological measurements are used to study the deformation and flow of a material.[31] Materials behave differently depending on if they are elastic solids or viscous liquids. An elastic solid behaves like a perfect spring and will deform immediately when opposed to stress. When the stress is released it will immediately return to its original shape.[55] The deformation of a viscous liquid, on the other hand, is time dependent as the viscous liquid resists flow.[55] Materials, like polymers, that have both viscous and elastic properties are called viscoelastic.[56] Due to the long polymer chains, the polymer solution will exhibit so called shear thinning behaviour. The viscosity will decrease with increased shear rate.[57] When the shear rate is low, it will be hard for the polymer chains to disentangle and slide past each other, resulting in high viscosity. The high viscosity will remain constant as the shear rate increases until it eventually becomes sufficiently high for the polymer chains to disentangle and move, decreasing the viscosity.[57]

The viscoelastic properties of a polymer solution can be measured by performing a rheological oscillatory test. An oscillatory shear test is where the solution is opposed to oscillatory stress, and the oscillatory response is recorded.[31] The linear viscoelastic region is the region where the viscosity is independent of the deformation of the solution.[57] By performing an experiment in the linear viscoelastic region, information about the molecular structure can be given.[31, 57] The complex modulus, G*, is the ratio between the applied stress and the measured strain during testing. The complex modulus is made up of two parts, the elastic modulus, G', and storage modulus, G", Figure 7.[57] G' will dominate in an elastic solid and the phase angle, $\delta$ (defined in Figure 7), will be equal to 0° for a completely elastic solid, whereas for completely viscous liquid, G" will dominate and $\delta =$

90°.[56] The phase angle thereby indicates whether a material is more liquid- or solid-like, depending on if $\delta$ is closer to 90 or 0°.

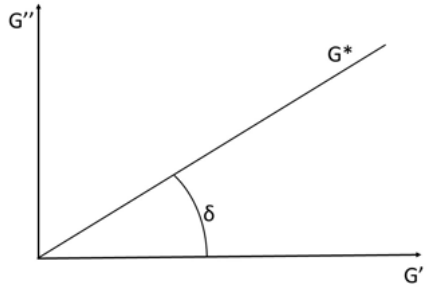


Figure 7: Definition and relationship between the rheological terms complex modulus, G*, elastic modulus, G', the storage modulus, G", and the phase angle, $\delta$.

Rheology can also be used to evaluate the percolation in a polymer/filler system as the filler changes the rheological behaviour of the solution.[58] A more percolated network causes the solution to shift from a solid towards liquid.[59] This shift can be seen in a so-called Van Gurp-Palmen plot where the phase angle, $\delta$ is plotted against the complex modulus, G*.[60] For the phase angle, a value closer to 90° is an indication of a liquid whereas $\delta$ closer to 0° indicates solid-like behaviour.[59–61]. The change from a liquid- to a more solid-like state can therefore be seen in the Van Gurp-Palmen plot, by examining the shape of the curve and the change in the phase angle.[60] A shift from a high $\delta$ towards a lower $\delta$, in the low G* region, is therefore an indication of the solid-like elastic response increasing due to the formation of a network, in this case the percolated network.[61]

## 2.6 Mechanical Testing of Nonwoven

Tensile testing is a type of mechanical testing which can be used to measure the elongation, stiffness, and strength, of a material. During tensile testing, the sample is pulled at two opposite ends by a force, and the deformation, the strain, of the material is recorded.[62] This test generates a stress/strain curve, Figure 8, from which values of strain at max load, tensile stiffness and tensile strength can be derived.[62] Different materials thus show different behaviour when opposed to tensile testing, depending on the material's strength and stiffness.

The stress, $\sigma$, is defined as the force, F, divided by the cross-sectional area, A (Equation 1). Strain, $\varepsilon$, is defined as the elongation, $\Delta$l, which is the change in length $l - l_0$, divided by the original length of the sample, $l_o$ (Equation 2).[63] The Young's modulus, which is a measurement of the stiffness of the material, is calculated from the slope of the curve in the linear elastic region where the strain is proportional to the applied stress.[31]

$$\sigma = \frac{F}{A} \tag{1}$$

$$\varepsilon = \frac{l - l_0}{l_0} = \frac{\Delta l}{l_0} \tag{2}$$

A Nonwoven is a material with randomly entangled fibres that are not interlaced like woven or knitted materials.[27] The arrangement and entanglement of the fibres affect the mechanical properties of the nonwoven itself. During the process of solution blow spinning of nonwovens, the material can, for example, be collected on a rotating collection cylinder. As the cylinder rotates, it simultaneously provides some orientation to the fibres, aligning them in the direction of the collector's rotation, the machine direction (MD). The nonwoven properties are therefore anisotropic i.e. they wary with the direction in which the nonwoven is tested.[64] Perpendicular to the MD, is the cross direction, CD, running across the fibres. Performing tensile testing on nonwovens results in a clear differences in strength and strain, depending on the direction in which the material is tested.[64] In the machine direction, the strain is low but the tensile strength at break is high. The fibres run parallel to the MD and the strain is therefore low due to the minimal reorientation of fibres as they are pulled in the MD. The tensile strength at break in the MD is mainly due to the failure of the individual fibres, and not to the nonwoven structure breaking. The nonwoven is more loosely held together in the CD, resulting in high strain and low tensile strength.[64]

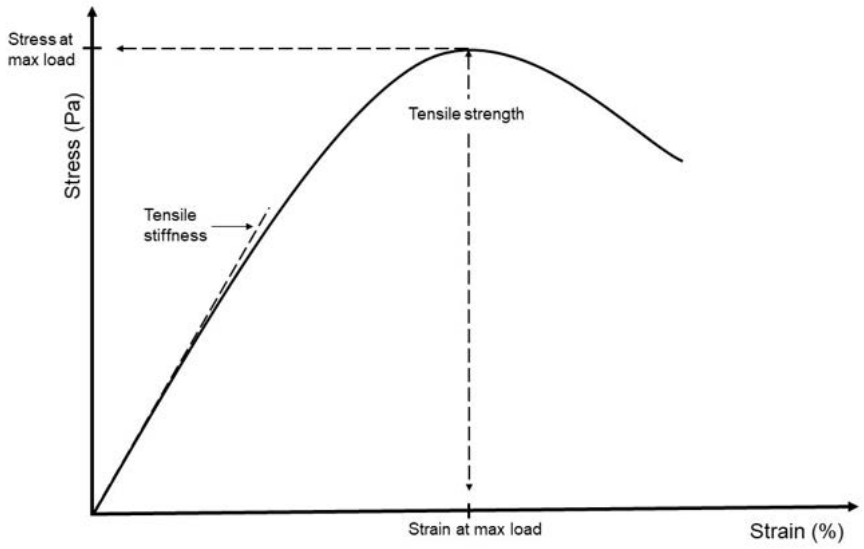


Figure 8: Typical stress-strain curve showing definitions of tensile strength, tensile stiffness and strain at max load. Adapted from Hutten.[62]

Apart from the orientation of the fibres, the entanglement within the nonwoven has proven to be a very important factor which affects both the strain, and the strength, of the nonwoven material.[65, 66] Tausif et.al. studied nonwovens where the entanglement within the material was controlled by the amount of needle punching of the material. Increased punch density, giving more entanglement, resulted in increased strain at break and increased tensile strength, showing that entanglement greatly affects these properties.[65] When assessing the mechanical properties of nonwovens it is therefore important to consider both the direction at which the nonwoven is tested, as well as both the effect of the strength of the individual fibres and the entanglement of the fibres.

## 2.7 BET Specific Surface Area

The specific surface area can be calculated using the physisorption isotherm.[67] The amount of molecules, usually $N_2$, that adsorb to the surface of the material with increased pressure is recorded as the physisorption isotherm, Figure 9.[62, 67] The physisorption isotherm will look different depending on the surface of the material. The physisorption isotherm can be divided into six different types, based on the shape of the curve.[67] For example, Type II shows the physisorption given by a macroporous or nonporous surface, whereas Type VI is given by a highly uniform nonporous surface, Figure 9.[67]

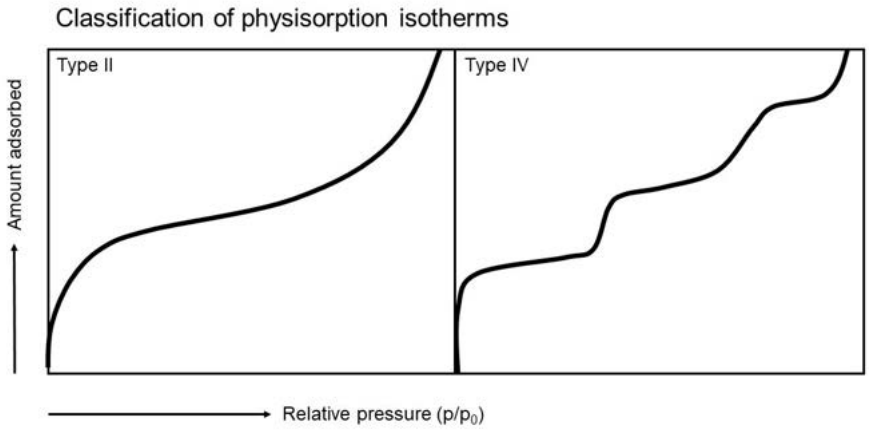


Figure 9: Type II and Type IV physisorption isotherms. Reproduced from Thommes et.al.[67]

The specific surface area can be calculated from the physisorption isotherm using the Brunauer-Emmet-Teller theory, BET. Using the BET method, the amount of gas to form a monolayer on the surface can be determined from the physisorption isotherm. The surface area can then be calculated as the amount of adsorbed molecules in the monolayer multiplied by the space taken up by one molecule.[67]

# 3. Material and Method

## 3.1 Material

A cellulose hardwood dissolving pulp ("Södra purple", Södra, Sweden) was used as the main fibre material together with high molecular weight tunicate cellulose (DP = approx. 4000). The solvent used was 1-ethyl-3-methylimidazolium, EMIMAc, (Sigma-Aldrich, Switzerland, $\geq$ 95%, $M_w$ = 170.21 g/mol, density = 1.101 g/cm$^3$) together with the co-solvent dimethyl sulfoxide, DMSO, (Sigma-Aldrich, China, $\geq$ 99%, $M_w$ = 78.13 g/mol, density = 1.10 g/cm$^3$). The conductive filler used was carbon black, CB, ("KETJEN-BLACK EC-600JD", AkzoNobel, The Netherlands, BET surface area = 1400 m$^2$/g, bulk density = 100-120 kg/m$^3$, pore volume (DPB) = 480 - 510 ml/100g). The surfactant sodium dodecyl sulfate, SDS ("Sodium Dodecyl Sulfate (Lauryl)", Thermo Scientific, USA, $M_w$ = 288.42 g/mol), was used in the coagulation bath during solution blow spinning. Ethanol ("F-sprit 95%", CCS Healthcare AB, Sweden, $\geq$ 95%) was used for washing of the nonwoven material.

## 3.2 Preparation of Solution

All cellulose was dried in an oven at 100 °C and the dissolving pulp was rotor milled to a powder-like material ($\leq$ 2 mm). Cellulose pulp and high MW cellulose were weighed to a total cellulose concentration of 4 wt% in solvent, in order to stay above the overlap concentration, c*. High MW tunicate cellulose was added, for its longer polymer chains, to achieve more stable fibre formation. The concentration of tunicate cellulose in the total amount of cellulose was kept at 5 wt% for all solutions. The solvents EMIMAc and DMSO were used at EMIMAc:DMSO-ratios 50:50, 40:60 or 30:70 and 20:80. The cellulose was dissolved in the EMIMAc/DMSO-solvent at 75 °C and stirred using an overhead mixer for approximately 1-2 h until all cellulose was dissolved and a visually homogeneous solution was obtained. The carbon black was then added at 0, 33, 42 and 50 wt%, based on the total amount carbon black and cellulose. Calculations of mass for cellulose, CB, EMIMAC, and DMSO, are shown in Appendix B. The complete solution was then stirred with ceramic balls over night at room temperature. The CB/cellulose-solution was then heated again, to around 60°C, to reduce loss when the solution was transferred from the reaction beaker. A high shear mixer (T 18 digital ULTRA TURRAX®, IKA®) was used prior to solution blow spinning in order to reduce the size of carbon black aggregates formed in the solution. The solution was mixed at 8000 rpm for approximately 10 - 15 min until the biggest carbon black aggregates, visualized in the solution using a light microscope (Nikon Eclipse Ci-POL, Nikon Instruments Co., Ltd.), were no bigger than 50 µm. The solution was centrifuged (PLC-322, Hemel) at 2000 rpm for 5 min to remove any air bubbles before using the solution to make nonwoven material by solution blow spinning.

A pure cellulose-solution with 5.8 wt% of cellulose, based on the total amount of cellulose

and solvent, was also prepared. The EMIMAc:DMSO-ratio in the solvent used was 30:70 and the tunicate concentration, based on the total amount of cellulose, was kept at 5 wt%. The cellulose was dissolved at 75°C and stirred with an overhead mixer overnight to achieve a visually homogeneous solution.

## 3.3 Solution Blow Spinning of Nonwoven Material

The prepared solution was solution blown into nonwoven material by solution blow spinning. The solution was loaded into a cylinder with a diameter of either 26 or 32 mm, depending on how much solution was to be used. A die (Biax Fiberfilms, Greenville, WI, USA) with nine capillaries (inner diameter 220 µm) was used for solution blow spinning, Figure 4. The distance between the coagulation bath and the spinneret die was kept at 30 cm. The solution was blown into a coagulation bath of 0.1 wt% SDS in water and collected on a rotating cylinder with a circumference of 25 cm, rotating at approximately 4.5 rpm. The SDS was used in the coagulation bath to prevent fibres from sticking together, based on results from trails prior to the thesis project. The same distance between the spinneret and the nozzle, the same coagulation bath, and the same cylinders, were used for all experiments. The extrusion speed, collection time and air pressure were however altered between samples.

Solutions containing 33, 42 and 50 wt% were selected to study the spinnability of solutions with different concentrations of carbon black. The extrusion speed and air pressure were varied to determine the parameters required for fibres to be solution blown from the solutions. The lowest extrusion speed required, together with the air pressure used to sufficiently draw out fibres from the solution, was recorded.

Nonwovens with varied fibre diameter and varied surface densities were also produced from the CB/cellulose-solution containing 42 wt% CB and an EMIMAc/DMSO-ratio of 30:70, by changing the parameters during the solution blow spinning (this experiment will be referred to as the "parameter-experiment"). The nonwoven surface density is defined according to Equation 3, where m is the mass of the nonwovens sample and w and l is the width and length of the sample respectively. The fibre diameter and surface density were altered by the extrusion speed and collection time respectively, while the air pressure was kept constant at 0.8 bar. The collection time was varied between 117 and 176 s, while keeping the extrusion speed at 5.72 ml/min, in order to vary the surface density between samples. To vary the fibre diameter between samples, an extrusion speed between 5.72 and 8.72 ml/min was used. For these samples, the collection time was calculated to be varied between 77 and 117 s in order to keep the volume of solution collected at 16.8 ml. Example calculations of the extrusion speed and collection time as well as the parameters used for all samples collected in the "parameter-experiment" are presented in Appendix C.

A pure cellulose nonwoven was also solution blown to be able to compare cellulose and CB/cellulose nonwovens. The solution blow parameters were calculated to achieve the same surface density and the same fibre diameter as for one of the nonwovens produced in the "parameter-experiment", Appendix C. The cellulose nonwoven was solution blown

at an extrusion speed of 6.72 ml/min, an air pressure of 0.8 bar and collected for 115 s.

$$\rho_{surf} = \frac{m}{w \times l} \tag{3}$$

## 3.4 Washing and Drying of Nonwoven

After collecting fibre mats from the coagulation bath, the samples were placed in water overnight to wash out the solvents. The samples were then washed in 1 litre of ethanol per sample for approximately 7 hours before they were dried in room temperature overnight, pinned to a styrofoam board. For the"parameter-experiment" the samples were pinned to the board at a set width of 2.5 cm in order to maintain a constant width for all samples made.

## 3.5 Rheological Evaluation of Solution

Rheology measurements were conducted to evaluate the viscosity of the cellulose and CB/cellulose-solutions. The measurements were performed using a rheometer (NOVA, Rheologica Instruments AB, Sweden) with a concentric cylinder, having cone and plate geometry at the bottom. The inner and outer diameter of the cylinder was 25 and 27 mm respectively with a cone angle of 5.4°. The sample was pre-sheered at a sheer rate of 100 $s^{-1}$ for 1 min and equilibrated for 5 min to introduce the same sheer history to all samples. A stress sweep was executed in the range $10^{-4}$ to $10^{+2}$ Pa at a frequency of 1 Hz to determine the linear viscoelastic region. A value of stress in the linear viscoelastic region was then selected at which the frequency sweep was performed between frequencies $10^{-2}$ to $10^{+2}$ Hz. All measurements were conducted at 23°C.

## 3.6 Light Microscopy Imaging

Solutions and nonwoven fibres were visualized using optical microscope Nikon Eclipse Ci-POL (Nikon Instruments Co., Ltd., Tokyo, Japan) with a Nikon TV-lens (C-0.38x) digital camera. The size of carbon black aggregates, and the diameter of fibres, were measured and visualized using the imaging software NIS-elements BR. The solution or fibre to be visualized was placed between a glass plate and cover slip for visualization.

The CB/cellulose-solutions contain bigger aggregates as well as smaller particles with a diameter less than 1 µm. The smallest particles are very difficult to visualize using the light microscope and were therefore not measured. Instead, only the size of the largest CB aggregates, found in the solution, were measured, as an indication of how well distributed the carbon black was in the solution. The fibre diameter was also measured for nonwoven samples. To be able to visualize the nonwoven fibres, using light microscopy, the samples were taken from the edge of the nonwoven. The fibres were also manually separated, to create more space between individual fibres, in order to be able to visualize and measure the fibre diameter. The fibre diameter was measured at x4 magnification. Only fibres crossing the diagonal of the image were measured, Figure 10. A minimum of 100 measurements were made for each nonwoven sample and the mean diameter was obtained from the imaging software, NIS-elements BR.

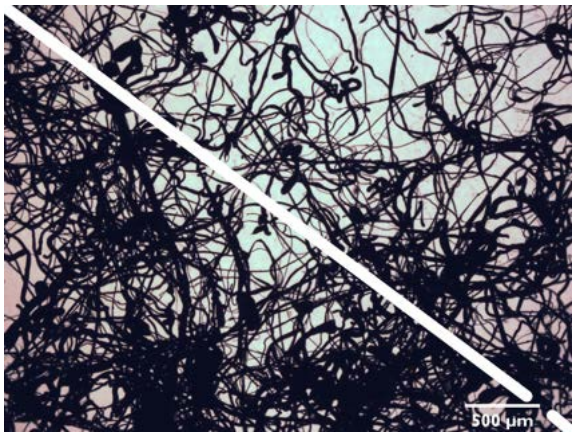


Figure 10: The diagonal of the light microscopy image (white) along which measurements of the fibre diameter were made.

## 3.7 Surface Resistance Measurement

Four-point bar measurements of the surface resistance for nonwoven samples were performed by collaborators at RISE Norrköping, using a prototype probe fixture, Figure 11. A 500 g brass weight was applied on the sample during the measurement through an insulating plate. The applied pressure was applied to ensure good contact between the sample and the bars. For nonwovens produced in the "parameter-experiment", five measurements were made at different places on each nonwoven, from which the mean surface resistance was calculated.

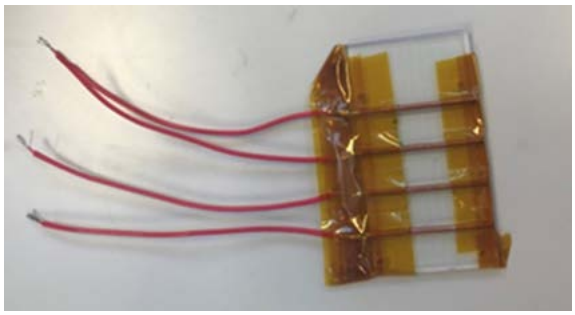

Figure 11: Prototype probe fixture for four-point bar measurements of surface resistance.

## 3.8 Mechanical Measurement - Tensile Testing

The mechanical properties strain at max load, Young's modulus, and effective stress at max load, were measured for nonwoven samples. The measurements were performed by tensile testing (Instron 5966, Instron Engineering Corporation, USA) with a load cell of 500 N. The samples were conditioned in 65% relative humidity and 22°C for 24 h prior to testing. The nonwovens were stamped into a rectangular shape, with a width of 10 mm, and clamped at a distance of 20 mm between the clamps. All samples were also cut in half, creating two specimens for each nonwoven to be tested. The samples were pulled apart in the machine direction, using applied tensile force at a rate of 100 mm/min, until break and the force required was recorded. The Young's modulus was calculated by the software Bluehill (Instron), and the effective stress $\sigma_{\text{eff}}$ was calculated as the force at max load, $F_{\text{max}}$, divided by the effective area of the nonwoven, $A_{\text{eff}}$, Equation.4. The effective area represents the area of the actual fibre material in the nonwoven, if the

nonwoven would be non-porous. The effective area was calculated by the nonwoven's surface density, $\rho_{\text{surf}}$, the density of the fibres in the nonwoven, $\rho_{\text{fib}}$, and the width of the sample, w, see Equation 4.[25] The surface density, $\rho_{\text{surf}}$ was calculated as the mass of the sample divided by its surface area, Equation 3. The density of the fibres were approximated to 1.5 g/cm$^3$, for pure cellulose nonwovens, and 1.61 g/cm$^3$ for 42 wt% CB/cellulose nonwovens (approximations were made using: cellulose density = 1.5 g/cm$^3$, carbon black density = 1.8 g/cm$^3$).[68, 69]

$$\sigma_{eff} = \frac{F_{max}}{A_{eff}} = \frac{F_{max} \times \rho_{fib}}{\rho_{surf} \times w} \tag{4}$$

## 3.9 Specific Surface Area - BET-method

The specific surface area was determined by the $N_2$ adsorption isotherm using surface analyzer Gemini® VII 2390 (Micromeritics Instrument Corporation, USA). Samples were dried in an oven at 80°C for 24 h prior to BET testing. The samples were then weighed and put in glass tubes, in which they were degased, with $N_2$ at 80°C, prior to sampling for at least 1 h. 11 data points for adsorption in the relative pressure range 0 to 0.3 were used. The specific surface area was calculated according to the BET-method using the Gemini VII software.

## 3.10 SEM imaging

SEM imaging of pure cellulose fibres, and 33 wt% CB/cellulose fibres at 35000x magnification, was performed at RISE IVF using JSM-7800F (JEOL, Tokyo, Japan) SEM. The microscope was operated at an acceleration voltage of 5 kV. The pure cellulose fibres required a coating to be visualized with SEM. The cellulose samples were mounted on carbon conductive tabs and coated with PELCO® conductive liquid silver paint (Ted Pella, Inc., USA). The samples were thereafter sputtered with a Pt layer of 1.5 nm using Cressington Sputter Coater 208HR (Cressington Scientific Instrument Ltd., UK). The SEM imaging of fibres containing 42 wt% CB was performed by collaborators at RISE in Norrköping using Sigma 500 Gemini (Zeiss). The sample was attached to a holder via a double-sided copper tape and the instrument was operated at an acceleration rate of 5 kV.

## 3.11 Capacitance Measurements

Measurements of the capacitance of the nonwoven material was performed by collaborators at RISE in Norrköping. The electrolyte used was 1-ethyl-3-methylimidazolium ethyl sulfate, EMIM:ES. And a cyclic voltammetry scan was performed at scan rates between 1 mV/s - 200 mV/s.

## 3.12 Pressure - Resistance Preliminary Testing

A preliminary pressure-resistance test was performed to evaluate the material's ability to function as a pressure sensor. Two manual tests were set up where the material's ability to respond to pressure was measured. The material was cut into strips with a width of 1 cm. The strip was placed in a circuit with the electrodes 5 cm apart, shown in Appendix

D. Weights were added onto the nonwoven material to increase the pressure exerted on the nonwoven. The pressure exerted by the weight was calculated according to equation 5 where P is the pressure, F is the force, A is the area on which the pressure is exerted, m is the mass and g is the gravitational acceleration 9.82 $m/s^2$ (in Sweden). The area on which the pressure was exerted on the sample was approximated to 3 $cm^2$, which is the approximate area where the weight is in contact with the sample, see Appendix D. Two different type of weights were used, one out of cardboard, $m_{cardboard}$, with a weight of 0.3 g, and one out of metal, $m_{metal}$, weighing 21 g. The experiments were performed on nonwovens with 33 wt% CB and a surface density of 9.6 $mg/cm^2$. For illustrations and photo of the set up used for the pressure-resistance preliminary testing see Appendix D.

$$P = \frac{F}{A} = \frac{mg}{A} \tag{5}$$

One test was performed where the metal and cardboard weights were added continuously on top of the sample. The resistance was recorded for each weight when the value of the resistance had stabilized. 7 metal weights and 7 cardboard weights were added one by one, starting with the cardboard weights, to increase the pressure on the nonwoven. The resistance was recorded as each weight was added. After all weights had been added, the resistance was also recorded as the weights were removed one by one, starting with the metal weights.

A manual, dynamic test was also performed where sets of weights were added onto the material. A total of 7 individual metal weights (21 g each), were used, giving 7 different sets of weight weighing between 21 and 147 g, depending on the amount of individual weights used in each set. One set of weights was added onto the nonwoven and the resistance was noted down. The set of weights was then removed, and the resistance was again recorded. This, adding and removing of weights, was repeated three times for each set of weights.

# 4. Results and Discussion

To produce conductive cellulose nonwovens, a solution which can be solution blown into nonwoven material is foremost required. There are three main requirements for the solution. The requirements regard the viscosity of the solution, the size of the aggregates and that enough carbon black must be added in the solution to make the nonwoven conductive. To achieve the requirements, the method of preparing the solution was altered compared to previous trials, Appendix A, and the solution's viscosity was studied using rheology. When an acceptable solution had been obtained it was solution blown into nonwoven material. The produced nonwovens were then characterized for their electrical properties (the surface resistance), the mechanical properties, and the morphology of the fibres, to evaluate how both the structure of the nonwoven and the amount of CB affected said properties. Two possible applications of the material were preliminary tested to show future possibilities for the material.

## 4.1 Improvement of Method

The "original" method of preparing the CB/cellulose solution, Appendix A, was improved in order to make the process more time efficient and to be able to increase the concentration of CB in the solution while still achieving efficient mixing of the solution. An additional step of high shear mixing was incorporated to improve the dispersion of CB and to reduce the size of CB aggregates in the solution. Light microscopy was used to evaluate if the improved "new" method could give as good CB dispersion as the "original" method. SEM imaging was also used to determine whether the different preparation methods resulted in a different fibre structure in the nonwoven.

### 4.1.1 Dispersion of Carbon Black

In the "original" method, Appendix A, the CB and DMSO were ball milled for two days before this CB/DMSO mixture was added to the cellulose that had been dissolved in EMIMAc. The final solution was then mixed, and ball milled overnight. A more time efficient way of preparing the solution was obtained by excluding the two-day mixing of the CB and DMSO. The cellulose was instead dissolved in both solvents, EMIMAc and DMSO, before the carbon black was added into the dissolved cellulose solution. The obtained solution was then only ball milled overnight, reducing the preparation time by two days. Another issue with the solution prepared by the "original" method, apart from being time consuming, was that it resulted in high viscosity for both the DMSO/CB solution and the cellulose/EMIMAc solution, as they were mixed separately before being combined and mixed together. If a too high concentration of CB was used, the DMSO/CB solution resulted in a very thick paste, making ball milling very difficult as the balls were not able to move within the thick paste. By instead mixing all the components together at once, the issue of too high viscosity could be avoided and the mixing of solution was made easier. This also made it possible to mix in higher concentrations of CB without being restricted by a thick paste forming.

Not much of a difference can be seen for the CB aggregate size between solutions prepared by the "original" (Figure 12a) and "new" method (Figure 12b), even though the CB was ball milled for a much shorter time using the "new" method (two days less). The solutions compared in Figure 12 both contain 33 wt% CB but have different concentrations of cellulose in solvent, 4 wt% cellulose for the solution prepared by the "new" method and 2.7 wt% for the "original". A higher concentration of cellulose was used in the "new" method, to safely stay above the cellulose overlap concentration, c*, when more CB was to be added. Both solutions show a quite even dispersion of the CB aggregates. No aggregates bigger than 40 µm could be found in the solution prepared by the "original" method, Figure 12a, whereas the biggest aggregate found in the solution prepared with the "new" method, Figure 12b, was 46 µm. The similar aggregate size distribution of the solutions indicate that the "new" method is still sufficient in breaking up the CB aggregates even though the CB is only ball milled overnight.

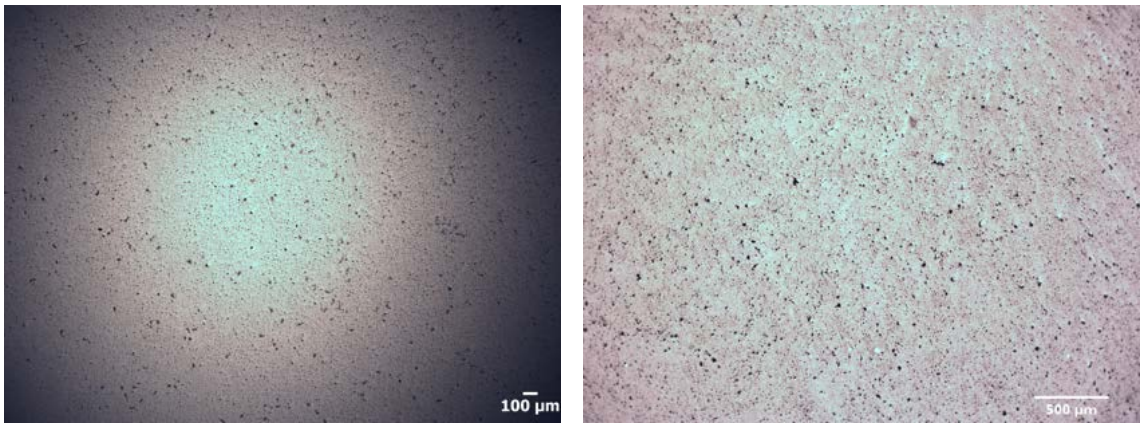


(a) (b)

Figure 12: Light microscopy images of carbon black carbon black aggregates in solutions prepared by the "original" method, a, and the "new" method, b. The images are taken at x4 magnification, the scale bar represents 100 and 500 µm in a and b respectively.

High shear mixing was also added as an additional step in preparing the solution, to reduce the CB aggregate diameter even further. Light microscopy images of the solution (4 wt% cellulose, 42 wt% CB and 70 wt% DMSO) before and after high shear mixing are shown is Figure 13. The solution was mixed using a high shear ultra turrax mixer for a total of 15 min at 8000 rpm, resulting in a clear difference in the carbon black aggregate size. Aggregates of approximately 100 µm can clearly be seen before high shear mixing, Figure 13a, whereas the biggest aggregate found in the solution after 15 min of high shear mixing is around 20 µm, Figure 13b. High shear mixing was therefore deduced efficient to reduce the aggregate size of CB, in the CB/cellulose/EMIMAc/DMSO-solution, as the high shear mixer clearly appears to be breaking up larger aggregates in the CB/cellulose solution.

### 4.1.2 Fibre Appearance

SEM images show fibres solution blown from solutions prepared by the "original" method, Figure 14a, and the "new" method, Figure 14b. It appears as though the fibres prepared using the "new" method have just as even fibre diameter as the ones prepared by the "original" method. The fibres produced by the "new" method appear more stretched out, and there are less curly fibres seen within this nonwoven. There are also less lumps, and

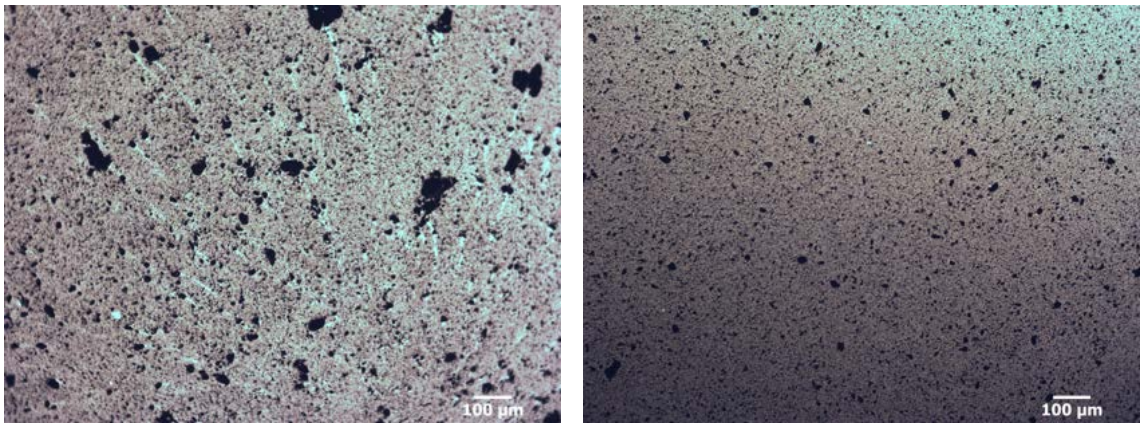


(a) (b)

Figure 13: Light microscopy images of carbon black aggregates in solutions before, a, and after 15 min of high shear ultra turrax mixing, b. Both images are taken at x10 magnification, the scale bars represent 100 µm.

thinner fibres seem to have been able to form using the "new", 14b, method compared to the "original", 14a. The fibre appearance thereby indicates a more stable fibre formation process when the "new" method was used. The "new" method can thus be confirmed to be just as good, if not better, when it comes to producing the nonwoven material. Its advantages during the preparation of the solution however, stand out as the "new" method makes it easier to mix solutions with a high concentration of CB. With the "new" method, the solution can also be prepared in a more time efficient way, without compromising the dispersion of carbon black.

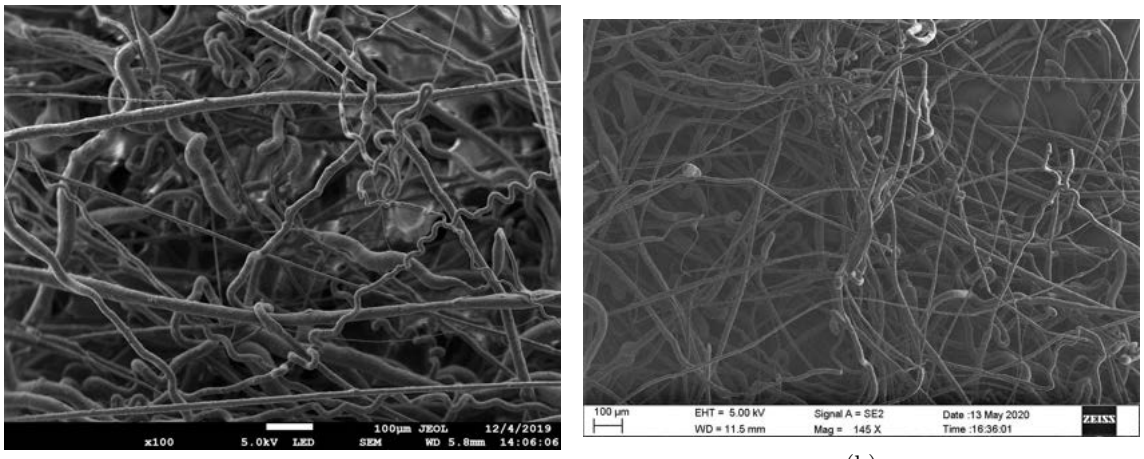


(a) (b)

Figure 14: SEM images of nonwoven fibres prepared by the "original" method, a, and the "new" method, b. Image a is taken at x100 magnification with the scale bar representing 100 µm. Image b is taken at x145 magnification with the scale bar representing 100µm.

## 4.2 Rheological Behaviour of Solutions

The suitability of the solutions for fibre spinning is highly dependent on the flow of the material. During the solution blowing process, the solution is subjected to a lot of shear, for example during mixing, pumping, and drawing of the solution into fibres. The rheological

behaviour of the solution is thereby a very important factor for fibre spinning of the solution. A rheology library of solutions was created to identify solutions with appropriate viscosity, 100 Pa s, for solution blow spinning of nonwovens. Two different parameters were varied in the rheology library: the ratio of carbon black to cellulose and the ratio of the solvents, EMIMAc:DMSO.

The rheology library extends over solutions with 0, 33, 42, and 50 wt% CB, where the DMSO to EMIMAc ratio was varied between 50, 60, 70 and 80 wt% DMSO. The complex viscosity, obtained at 0.01 Hz, for the different solutions respectively, are shown in Figure 15. The viscosity, G', G", and phase angle, obtained for each solution, in the frequency range 0.01 to 20 Hz, are presented in Appendix E. Figure 16 also shows the shear-thinning behaviour of the solutions, common for polymer solutions.[57] The viscosity of all solutions, in Figure 16, decreases as the shear rate increases. The shear thinning behaviour is also worth noting, as it will affect the viscosity of the solution when it is subjected to shear during the spinning process.

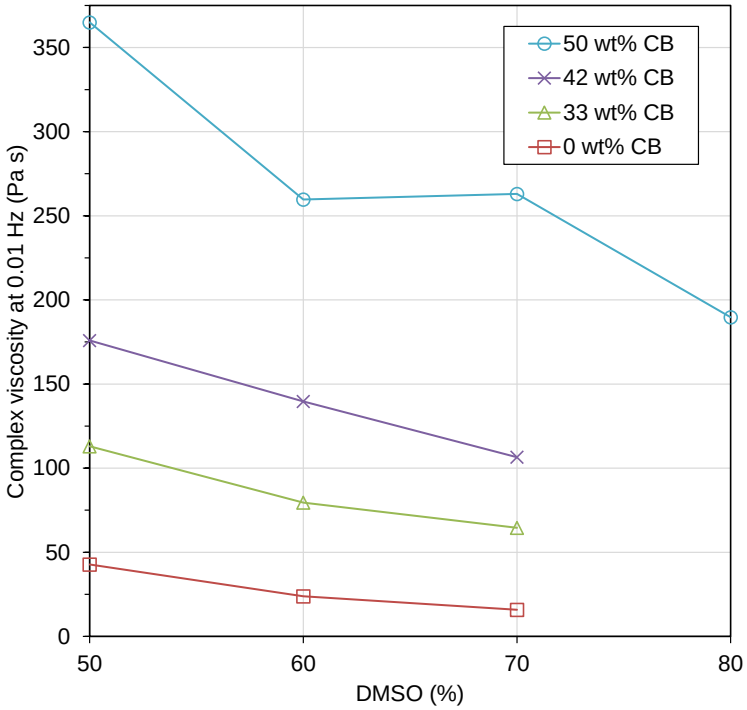


Figure 15: Complex viscosity at 0.01 Hz for carbon black/cellulose solutions with 0 (red square), 33 (green triangle), 42 (purple cross) and 50 wt% carbon black (blue circle). The solutions contain varying amounts of DMSO in the solvents, 50, 60, 70 and 80%.

### 4.2.1 DMSO's Effect on Viscosity

A trend of decreasing viscosity with an increasing amount of DMSO can be seen in Figure 15. For example, for the solution with 42 wt% CB, the viscosity decreases from 176 Pa s to 107 Pa s as the concentration of DMSO is increased from 50 to 70 wt%. These results coincide with the results found in other studies, which all report a lower viscosity with an increasing ratio of DMSO in the total amount of solvent.[28, 40, 70] Replacing some of the EMIMAc with DMSO, by adjusting the solvent:co-solvent ratio, lowers the viscosity of the final solution. This is because the viscosity of the co-solvent itself, DMSO, is lower (2 mPa s) compared to that of the ionic liquid, EMIMAc, (200 mPa s).[37] A deviation

from the decreasing trend is however seen for solutions with 50 wt% CB. No decrease in the viscosity is seen as the DMSO is increased from 60 to 70 wt%, Figure 15. The reason might be due to the fact that the high viscosity, for solutions with 50 wt% CB, made it harder to prepare the solutions in terms of achieving efficient mixing and dispersion of CB. This makes it harder to achieve the same dispersion of CB for all solutions with 50 wt%. A trend with increasing DMSO concentration might therefore be harder to see, compared to the clear trends seen for 0, 33 and 42 wt% CB.

### 4.2.2 Carbon Black's Effect on Viscosity

An increase in viscosity is seen as the amount of CB, in the solution, increases from 0 to 50 wt%, Figure 15. For example, for solutions with 70 wt% DMSO, an increase in viscosity, from 16 Pa s to 263 Pa s, can be seen as the concentration of CB increases from 0 to 50 wt%, Figure 15. The increasing viscosity due to increasing CB concentration was also seen in a study where CB/cellulose solutions were prepared for wet spinning of fibres.[10] The increase in viscosity is majorly due to the increase of dry weight in the solution. As more dry weight, in the form of carbon black, is added to the solution, the viscosity of the solution will naturally increase. A more profound increase in viscosity is seen between 42 and 50 wt% CB as the viscosity increases from 106.5 Pa s to 263 Pa s, for solutions with 70 % DMSO, Figure 15 (more clearly shown in Figure 19). Härdelin et.al. reported a dramatic increase in viscosity above 3 vol% of CB in the spinning solution.[10] In this thesis, the CB/cellulose ratio 42:58 wt/wt, above which the dramatic increase is seen, corresponds to a CB concentration of approximately 1.6 vol% (2.8 wt%) in the total solution (for calculation of volume percentage see Appendix B). The pronounced increase in viscosity is a sign of a percolated network forming within the solution, and the concentration at which this happens is the percolation threshold. The percolation threshold in this project appears to be around 1.6 vol%. This is lower than that shown by Härdelin et.al., 3 vol%, but still of the same magnitude. The slight difference is probably due to different types of carbon black being used.

### 4.2.3 Percolated Network in Solution

A percolated network induces a shift in the solution behaviour, making it more solid-like i.e. increasing the viscosity.[61] This shift can be seen by looking at the shape of the rheology curve, and not just values of the viscosity at one specific frequency. Figure 16 shows the viscosity over the frequency range 0.01 to 20 Hz for solutions with 0, 33, 42 and 50 wt% CB and 60% DMSO. 50 wt% shows a very small deviation from the curve shape exhibited by 0, 33, and 42 wt% CB, in the low frequency region. The decrease in viscosity between 0.01 and 0.02 Hz is much steeper for 50 wt%, compared to the solutions with lower concentrations of CB, Figure 16.

The difference in viscosity with CB concentration is however difficult to see in the complex viscosity-frequency plot, Figure 16. A Van Gurp-Palmen plot, Figure 17, can instead be used to show these differences more clearly.[60] The formation of a percolated network can be seen in a Van Gurp-Palmen plot, Figure 17, where the phase angle is plotted against the complex modulus. Figure 17 shows that the phase angle for solutions with 0, 33, and 42 wt% CB, is approaching a high value of around 90° in the low G* region. 90° being an indication of liquid-like behaviour.[57] For 50 wt% CB however, the curve deviates from those with a lower CB concentration, and the phase angle is instead decreasing or flattening, indication more solid-like behaviour. This change in the rheological behaviour

with 50 wt% CB is thereby an indication of the formation of a solid-like network, the percolated network.[58, 60, 61] The indication of a solid-like network forming for solutions with 50 wt% CB coincides with the results in Figure 15, where a more dramatic increase in viscosity was seen between 42 and 50 wt% CB than between 33 and 42 wt%. This again points towards 1.6 vol%, of CB in the solution, being the percolation threshold in the solution. The formation of the percolated network in the solution with 50 wt% CB, resulting in high viscosity of the solution, further provides difficulties for solution blow spinning as the complex viscosity is above the benchmark of 100 Pa s for all ratios of EMIMAc to DMSO tested.

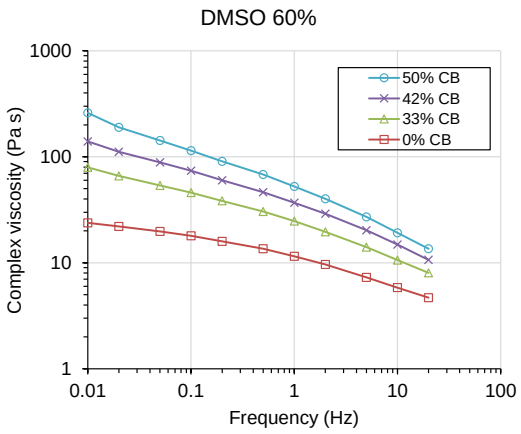


Figure 16: Frequency sweep showing the complex viscosity for solutions with 0 (red square), 33 (green triangle), 42 (purple cross) and 50 wt% CB (blue circle).

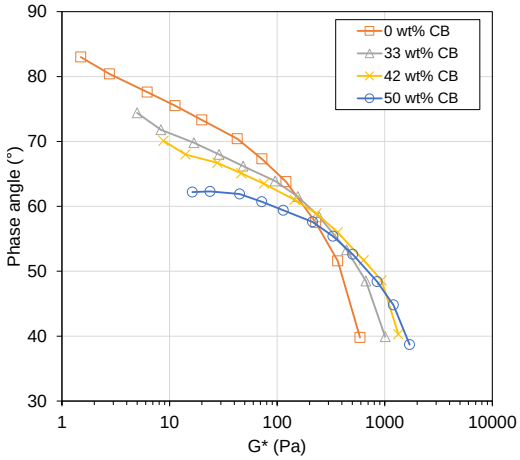


Figure 17: Van Gurp-Palmen plot for solutions with 0 (orange square), 33 (grey triangle), 42 (yellow cross) and 50 wt% CB (blue circle) with 60% DMSO in the solvent.

### 4.2.4 Selection of Solutions for Solution Blow Spinning

Solutions that were to be attempted to be solution blown into nonwoven material were picked out from the rheological library evaluation. One solution for each concentration of CB (33, 42 and 50 wt% CB) was selected with the benchmark of 100 Pa s for the viscosity. The solutions chosen are summarized in Table 2. The selected solutions will be referred to as CBX_DMSOY where X is the weight percentage of carbon black, based on the total amount of filler and cellulose, and Y is the weight percentage of DMSO in the total amount of solvent. Solutions with viscosities around 100 Pa s were chosen for 33 and 42 wt% CB. The selected solution with 33 wt% CB and 70% DMSO, CB33_DMSO70, gave a viscosity of 79 Pa s, and the solution with 42 wt% CB and 70% DMSO gave a viscosity of 106 Pa s, Table 2. For the solutions with 50 wt%, no solution with a viscosity close to 100 Pa s could be found in the rheology library, Figure 15. The 50 wt% solution still proved interesting as it showed signs of a percolated network forming within the solution. The 50 wt% CB solution with the lowest viscosity in the rheology library, 190 Pa s with 80 wt% DMSO, was therefore chosen, though its viscosity was almost double that of the benchmark for a spinnable solution.

Table 2: Viscosity of solutions with 33, 42 and 50 wt% CB, chosen for solution blowing.

| Sample code | CB (wt%) | DMSO (wt%) | Complex viscosity at 0.01 Hz (Pa s) |
|---|---|---|---|
| CB33_DMSO60 | 33 | 60 | 79 |
| CB42_DMSO70 | 42 | 70 | 106 |
| CB50_DMSO80 | 50 | 80 | 190 |

## 4.3 Solution Blow Spinning of Nonwovens

CB/cellulose nonwovens with CB concentrations 33, 42, and 50 wt%, were produced using solution blow spinning. The nonwovens were produced from the solutions CB33_DMSO60, CB42_DMSO70, and CB50_DMSO80, selected from rheological evaluations of the viscosity, section 4.2, Table 2. One of the produced nonwovens was then selected for further testing, based on its surface resistance as well as its ability to spin nonwoven material, where nonwovens of different fibre diameters and different surface densities were to be made. The parameters used during solution blow spinning of the nonwovens as well as the selection of one nonwoven for further study are presented in this section of the report.

### 4.3.1 Nonwovens with Different Concentrations of Carbon Black

All of the solutions selected for solution spinning, CB33_DMSO60, CB42_DMSO70 and CB50_DMSO80, resulted in nonwoven material. Light microscopy images, showing the surfaces of the produced nonwovens, are shown in Figure 18. The lowest extrusion speed, at which fibres could be produced during solution blow spinning, is shown in Table 3. Table 3 also shows the average fibre diameter, surface density, and measured surface resistance, of the produced nonwoven material from each solution, respectively.

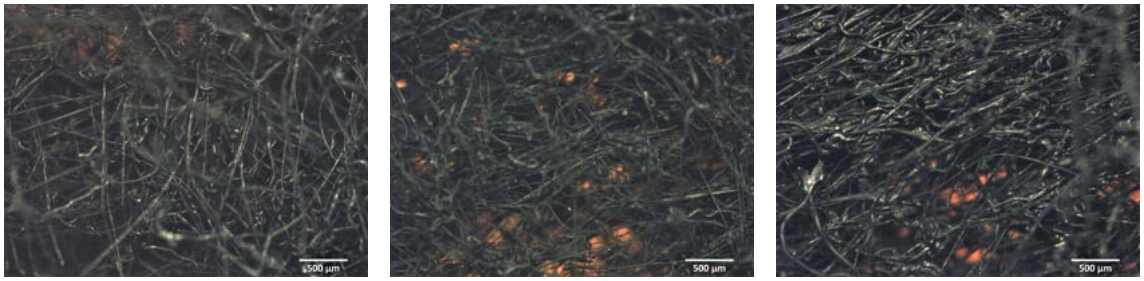


(a) (b) (c)

Figure 18: Light microscopy images showing the surface of nonwoven samples with 33 (a), 42 (b) and 50 wt% CB (c). The images were taken at x4 magnification, the scale bar represents 500 µm.

#### 4.3.1.1 Solution Blow Spinning Ability of Solution

The ability of the solution to produce nonwoven material was evaluated based on two things, if the viscosity made it easy to work with and if a low enough extrusion could be used, which would allow alterations of the fibre diameter in further testing. 9.7 ml/min is the highest extrusion speed that could be obtained with the equipment used during this project. The extrusion speed required to produce nonwovens should thus be below 9.7 ml/min for the fibre diameter to be altered by an increased extrusion speed. The highest extrusion speed, required to make nonwoven material, was found for the solution CB50_DMSO80, 9.7 ml/min. CB50_DMSO also has the highest concentration of CB, 50

wt%, and the highest viscosity, 190 Pa s, Table 2. The high viscosity of CB50_DMSO50 has been shown to be a result of the percolated network forming, due to the high concentration of CB, section 4.2. For CB33_DMSO60 and CB42_DMSO80 the viscosity was chosen to be around 100 Pa s. The extrusion speeds required for these solutions, 4.1 and 6.7 ml/min respectively, are thus below 9.7 ml/min, would therefore allow alteration of the fibre diameter. The increase in extrusion speed required, with a higher viscosity, is due to the solutions inability to flow. Less flow of the solution, due to high viscosity, makes it harder to draw the solution out into fibres and it thereby requires more force, in the form of a higher extrusion speed. The concentration of cellulose in the solution is also important as the cellulose concentration has to be above the overlap concentration, c*.[30] As the ratio of CB:cellulose increases in the solution, the concentration of cellulose decreases. A higher concentration of CB thereby makes it harder to spin fibres, as the cellulose will come between cellulose chains and hinder them from bonding and entangling.

Table 3: Lowest extrusion speed required, fibre diameter, surface density, and surface resistance, for nonwovens with 33, 42 and 50 wt% carbon black.

| Sample code | Lowest extrusion speed (ml/min) | Fibre diameter (µm) | Surface density ($mg/cm^2$) | Four bar measurement surface resistance ($\Omega/\square$) |
|---|---|---|---|---|
| CB33_DMSO60 | 4.1 | 21 ± 12 | 10 | 660 |
| CB42_DMSO70 | 6.7 | 17 ± 11 | 11 | 102 |
| CB50_DMSO80 | 9.7 | 29 ± 11 | 11 | 53 |

#### 4.3.1.2 Effect of Carbon Black on the Surface Resistance

The measured surface resistance, for the three nonwovens, show a decrease with increased concentration of CB. The surface resistance decreases from 660 to 102 to 53 $\Omega/\square$ as the CB concentration increases from 33 to 42 to 50 wt% CB, Table 3. The lower values of 102 and 53 clearly show that the conductive properties of the material could be improved by additional incorporation of CB. Compared to previous trials with 33 wt% CB (Appendix A), the surface resistance of the material shows an improvement from 760 $\Omega/\square$, to around and below 100 $\Omega/\square$, as 42 and 50 wt% CB were successfully incorporated in the cellulose nonwoven. Figure 19 illustrates the change in viscosity of the solution (blue cross) and the change in surface resistance for the nonwoven (orange circle) with the concentration of carbon black. The decrease in resistance reassembles the S-curve behaviour of the resistance, Figure 6a, as a percolated network has formed.[42] The vast decrease in surface resistance between nonwoven with 33 and 42 wt% CB, from 660 to 102 $\Omega/\square$, thereby indicates that a fully conductive path has formed. The decrease between 42 and 50 wt% is not as big, implying that a sufficient conductive pathway has already formed for 42 wt%, in the nonwoven material, Figure 19. The change in both the viscosity, and the resistance, has been derived back to the formation of a percolated network in the solution and in the nonwoven, respectively. Increasing the concentration of CB above that of 42 wt% results in a big increase in the viscosity of the solution but a minor decrease in the surface resistance. This is shown in Figure 19, as the increase of the CB concentration, between 42 and 50 wt% CB, results in an increase in the viscosity from 106 to 190 Pa s and a decrease in surface resistance of 102 to 53 $\Omega/\square$.

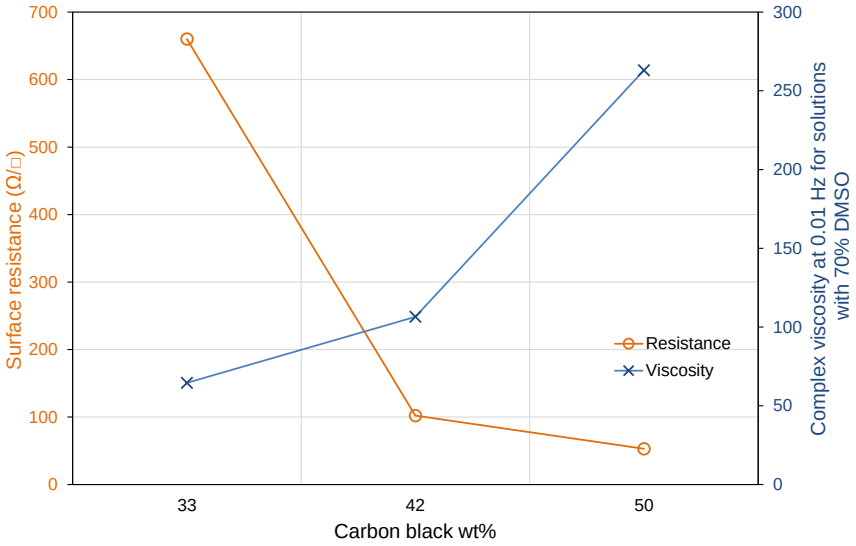


Figure 19: Complex viscosity at 0.01 Hz for solutions with 70 wt% DMSO in solvent (blue cross) and surface resistance of nonwoven containing 33, 42 and 50 wt% CB (orange circle).

#### 4.3.1.3 Selection of Solution for Further Study

Further study of how the electrical properties depend on the structure of the nonwoven was to be conducted using the most suitable CB/cellulose solution. The most promising solution was chosen based on the criteria of being easy to solution blow, with the ability to change the extrusion speed in order to vary the fibre diameter, as well as exhibiting a low surface resistance, indicating that a percolated network had formed. Solution CB33_DMSO60 was excluded as the produced nonwoven had a much higher surface resistance than 42 and 50 wt% CB, Figure 19. Though the nonwoven with 50 wt% CB shows the lowest surface resistance, its disadvantages in solution blow spinning, like high viscosity and the need for high extrusion speed, excluded the solution CB50_DMSO80 from further study in this project. Solution CB42_DMSO70 was thereby chosen for its viscosity (106 Pa s) around the benchmark of 100 Pa s and a low enough extrusion speed of 6.7 ml/min (lower than the maximum extrusion speed of the equipment, 9.7 ml/min), providing the ability to alter the fibre diameter. CB42_DMSO70 also showed indications of a sufficient conductive path forming in the material, resulting in a low surface resistance of 102 Ω/□.

### 4.3.2 Nonwovens with Varied Fibre Structure

To study how the surface resistance and mechanical properties depend on the nonwoven structure, nonwovens with different fibre diameter and surface density were produced from the chosen solution CB42_DMSO70. The fibre diameter was altered in four different samples by alteration of the extrusion speed between 5.72 and 8.72 ml/min. The resulting mean fibre diameters of the four nonwovens samples were measured to 14 ± 6, 16 ± 8, 25 ± 9 and 28 ± 11 µm respectively, Table 4. The samples will be referred to as NW_fibdimA where A is the measured average fibre diameter. Figure 20 shows light microscopy images of nonwoven NW_fibdim14, Figure 20a, and NW_fibdim28, Figure 20b, where a difference in the fibre diameter between the samples is seen, NW_fibdim28 showing thicker fibres compared to NW_fibdim14. Appendix F shows light microscopy images of all nonwovens NW_fibdimA, Figure F-2, and NW_surfdensB, Figure F-1, together with the measured fibre diameter distribution for each nonwoven, Figure F-3.

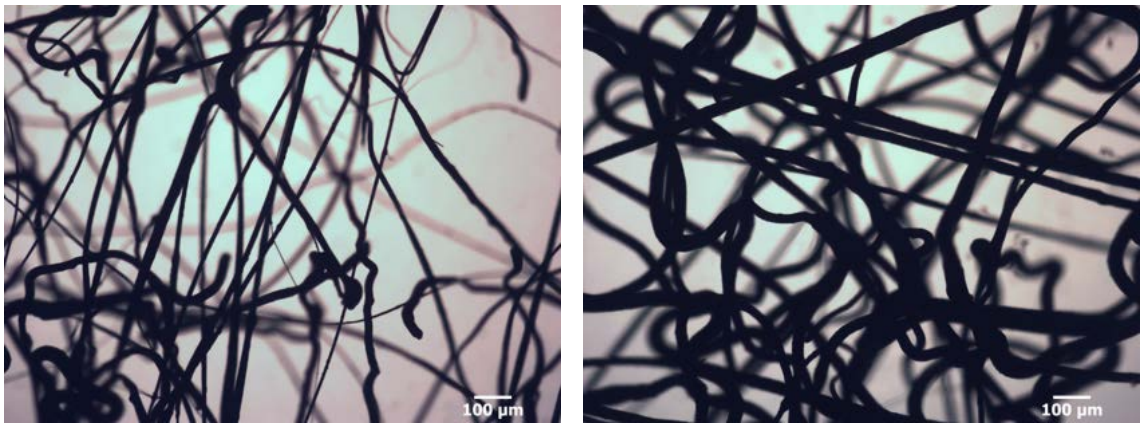


(a) (b)

Figure 20: Light microscopy images showing fibres from nonwoven samples NW_fibdim14, a, and NW_fibdim28, b. The mean fibre diameter is 14 and 28 µm for the samples respectively. Both images are taken at x10 magnification, the scale bar represents 100 µm.

The surface density was altered between three nonwoven samples to 16, 20 and 33 mg/cm$^2$, by increasing the extrusion speed from 117 to 176 s. The samples will be referred to as NW_surfdensB where B is the calculated surface density of the samples. Measurements and calculation of the surface density is shown in Appendix G. The surface density and fibre diameter, obtained by tuning the extrusion speed and sample collection time, is summarized in Table 4 for the nonwoven samples produced. Calculations of the parameters used during the solution blown process, to produce nonwovens with different fibre diameter and surface density, are presented in Appendix C.

Table 4: Nonwovens with varied fibre diameter and surface density, produced by variation of the extrusion speed and collection time during the solution blow spinning process.

| Sample | Extrusion speed (ml/min) | Sample collection time (s) | Fibre diameter (µm) | Surface density (mg/cm$^2$) |
|---|---|---|---|---|
| NW_fibdim14 | 5.72 | 117 | 14 ± 6 | 22 |
| NW_fibdim16 | 6.72 | 100 | 16 ± 8 | 21 |
| NW_fibdim25 | 7.72 | 87 | 25 ± 9 | 21 |
| NW_fibdim28 | 8.72 | 77 | 28 ± 11 | 20. |
| NW_surfdens17 | 5.72 | 117 | 13 ± 8 | 17 |
| NW_surfdens21 | 5.72 | 147 | 16 ± 8 | 21 |
| NW_surfdens33 | 5.72 | 176 | 13 ± 10 | 33 |
| NW_cell | 6.72 | 115 | 16 ± 9 | 25 |

Due to the solution blow spinning process being quite a chaotic, with many parameters affecting the outcome of the nonwoven, it proved somewhat difficult to alter the nonwoven structure. The alteration of the fibre diameter, with extrusion speed, proved difficult and the mean fibre diameter for some of the samples turned out pretty similar, 14 ± 6 and 16 ± 8 µm for NW_fibdim14 and NW_fibdim16. However, a general correlation of an increased fibre diameter with increased extrusion speed can still be seen for samples NW_fibdimA, Table 4. Factors such as the loss of sample during the collection in the coagulation bath may also be the reason why NW_fibdim14 and NW_surfdens17 show a big difference in surface density, 22 mg/cm$^2$ for NW_fibdim14 and 17 mg/cm$^2$ for NW_surfdens17, even

though the same parameters were used during the spinning process. An increase in the surface density is however still shown for samples NW_surfdensB. To further study the effect of surface density and fibre diameter, the difference between NW_fibdim14 and NW_surfdens17 was concluded not to be important, nor affect the correlations studied. One pure cellulose nonwoven, referred to as NW_cell, was also produced to be able to compare the mechanical properties between nonwovens with and without CB. This pure cellulose nonwoven was made to have the same surface density and fibre diameter as sample NW_fibdim16. The mean fibre diameters of NW_fibdim16 and NW_cell were both 16 µm, and the surface densities obtained were 21 and 24 mg/cm$^2$, Table 4. The higher surface density of NW_cell is most likely due to less loss of fibres during the collection of the nonwoven in the coagulation bath.

## 4.4 Resistance of Carbon Black Nonwovens

It has already been shown, in section 4.3.1, that the surface resistance of CB/cellulose nonwovens decreases with increasing concentration of carbon black, Table 3. The effect of the nonwoven structure, in terms of fibre diameter and surface density, on the surface resistance was also studied, and is presented in this section. The mean surface resistance, with the standard deviation represented by error bars, is presented for nonwovens with different fibre diameter, and different surface density, in Figure 21. Data obtained from the measurements are shown in Appendix H. Nonwovens are quite uneven materials. The measured surface resistance as well as the fibre diameter will therefore vary a bit throughout the sample, causing a variation in the resistance measured at different locations of the samples. The unevenness is seen in the standard variations of the measurement. Some general trends can still be seen for the effect of fibre diameter and surface density on the surface resistance. Figure 21 shows a big decrease in surface resistance, approximately 50%, when the surface density doubles, compared to a decrease of approximately 20% as the fibre diameter doubles. The lowest surface resistance reached, 57 Ω/□, obtained by the sample with the highest surface density, NW_surfdens33. Its surface resistance is in the same range as the surface resistance of the nonwoven produced from the solution with 50 wt% CB, CB50_DMSO80, 53 Ω/□, Table 3. An estimation of the conductivity of the porous nonwoven material was made to $1 \div (R_{\text{surf}} \times t)$, where $R_{\text{surf}}$ is the mean surface resistance and t is the mean thickness of the nonwoven sample, shown in Appendix H.[71] The average surface resistance for samples NW_fibdimA and NW_surfdensB is 0.023 S/cm. The 42wt% CB/cellulose nonwoven thereby shows a similar value to cellulose aerogels with 10 wt% CNT, showing a conductivity of 0.018 and 0.022 S/cm, Table 1 and Figure 1.

### 4.4.1 Influence of Surface Density

An overall trend of a decreased surface resistance with increasing surface density is shown in Figure 21a. As the surface density increases from 17 to 33 mg/cm$^2$, the surface resistance decreases from 107 to 57 Ω/□. This is an approximate decrease in the surface resistance by 50 %, as the surface density is increased by a factor two. The resistance within a material with conductive fibres depends on the contact resistance between fibres.[52] The decrease in contact resistance is therefore most likely due to the decrease in contact resistance between fibres. Figure 22 shows a schematic drawing of the influence of surface density on the number of fibre-fibre contact points (red dots). Figure 22 can be interpreted as a 2-dimensional representation of a thin sheet of the nonwoven, being visualized from above.

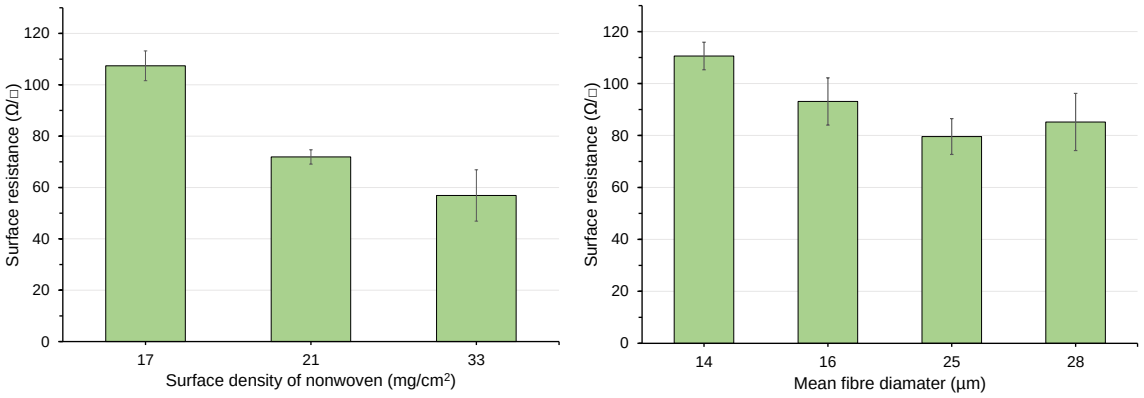


Figure 21: Surface resistance for nonwovens with varied surface density, a, and varied fibre diameter, b. The surface density is varied between 17, 21 and 33 mg/cm$^2$. The mean fibre diameter varies between 14, 16, 25 and 28 µm.

A higher surface density is represented by more individual fibres per square. When the number of individual fibres in the square is increased from 25 to 69, the number of contact points also increase from 38 to 166, illustrating an increase in the number of contact points with an increase in surface density. However, the nonwoven has a 3D structure. The contact between fibres within the whole material will therefore also depend on how pressed together the nonwoven is. The contact resistance between fibres will decrease as more contact points are established, making it easier for charge to be transported in the material.[52] The number of contact points, and thereby the surface density, will therefore decrease with the surface resistance.

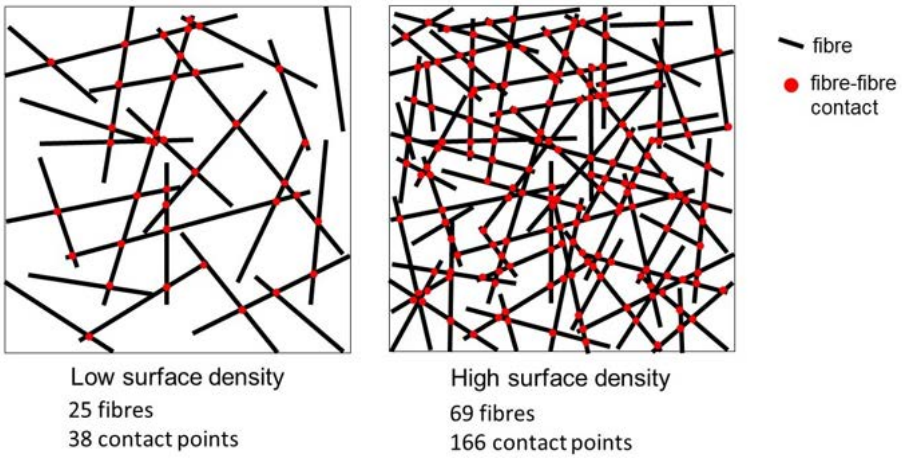


Figure 22: Schematic drawing of the influence of surface density on the number of fibre-fibre contact points.

### 4.4.2 Influence of Fibre Diameter

An overall trend indicating a decreased resistance with increased fibre diameter can be observed in Figure 21b. The surface resistance decreases from 111 to 85 Ω/□ as the fibre diameter increases from 14 to 28 µm. The increase in surface resistance with increased fibre diameter between sample NW_fibdim25 and NW_fibdim28 however, is most likely due to the unevenness of the nonwoven samples. The difference in fibre diameter is also small, 25 and 28 µm, and might not induce a big, noticeable change in the surface resistance.

The biggest difference in surface resistance is seen between sample NW_fibdim14 and NW_fibdim25 measuring 115 and 79 Ω/□ respectively. A feasible explanation for the decrease in surface resistance with the increase in fibre diameter is that the fibre-fibre contact area increases. An increased fibre-fibre contact area reduces the contact resistance between fibres, creating less resistance for the charge to move within the material.[51] Figure 23 shows a schematic drawing of the influence of fibre diameter on the contact area between two fibres. When the fibre diameter doubles, from 10 to 20 µm, the contact area between two fibres quadruples, from 100 to 400 $\mu m^2$, illustrating that the fibre diameter has a huge influence on the fibre-fibre contact area. However, as the fibre diameter increases there will also be fewer individual fibres in the nonwoven, as the density is kept constant for samples with varied fibre diameter. With a lower number of fibres, the number of contact points will decrease, resulting in an increased surface resistance (as previously shown in section 4.4.1) as the fibres become wider. The increase in fibre diameter thereby leads to both an increased contact area as well as a decreased number of contact points. These two opposing factors could explain why the surface density seems to have a bigger impact on the surface resistance, compared to the fibre diameter.

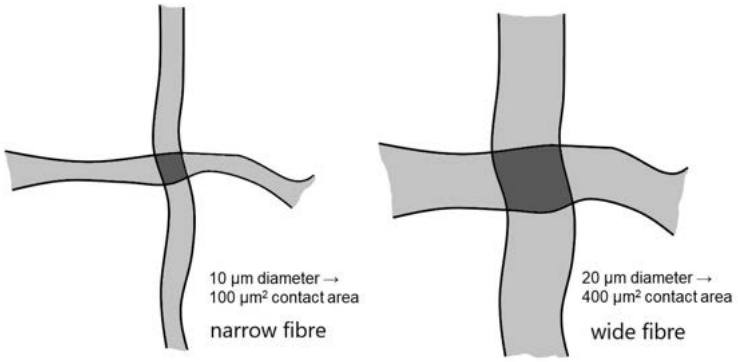


Figure 23: Schematic drawing showing the influence of fibre diameter on the contact area between fibres.

## 4.5 Mechanical Testing of Carbon Black Nonwovens

Mechanical characterization in the form of tensile testing, where the nonwovens are pulled apart by a constant force, was carried out to study how the mechanical properties change with the inclusion of carbon black in cellulose nonwovens, and with the nonwoven structure, i.e. the fibre diameter and the surface density. The tensile properties measured were strain, stiffness, and strength. Two replicate samples were used for each nonwoven which showed that there is some unevenness in the material. Because the nonwovens are uneven, more replicas would have been beneficial for the results of the mechanical testing. Still, correlations between the mechanical properties and both the nonwoven structure, and the incorporation of the CB, can be deduced from the tensile testing. Data obtained from the measurements made during tensile testing are shown in Appendix I.

### 4.5.1 Effect of Nonwoven Structure

Results for the strain at max load, Young's modulus, and effective stress at max load, for nonwovens with altered fibre diameter and surface density is shown in Figure 24.Two specimens were measured for each type of nonwoven. The mean value, between the two specimens, are shown in Figure 24, together with the standard deviation between the specimens, represented by error bars.

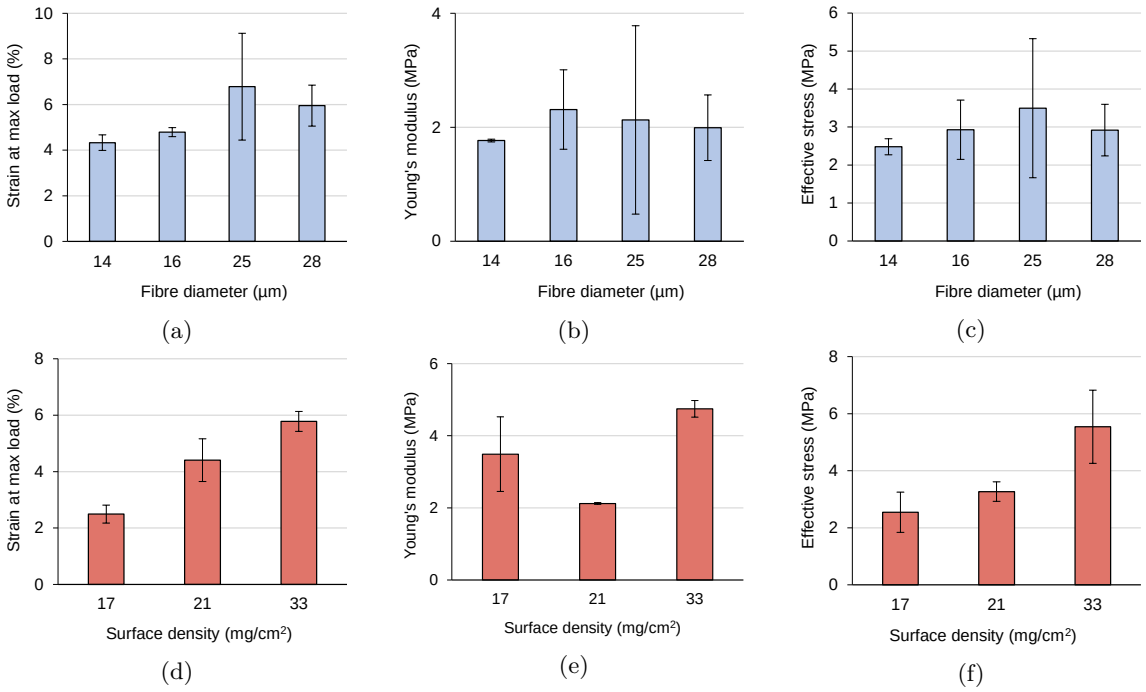


Figure 24: Measurement of the mechanical properties strain at max load (a and d), Young's modulus (b and e), and effective stress at max load (c and f), for nonwovens with varied fibre diameter, a, b, c, and varied surface density, d, e, f.

#### 4.5.1.1 Fibre Diameter and Mechanical Properties

The results show that there does not seem to be a correlation between the fibre diameter and any of the mechanical properties tested. The strain at max load for the nonwovens with different fibre diameters (NW_fibdimA) all have a value around 5 %, Figure 24a. The Young's modulus is around 2 MPa, Figure 24b, and the effective stress is around 3 MPa, Figure 24c, for all samples NW_fibdimA. The fibre diameter has however been shown to affect both the strain and strength of nonwoven polyurethane material.[65] An increase in strain and the overall strength of the nonwoven with decreasing fibre diameter was reported. The increase being a result of increased surface area of the fibres, which can provide additional fibre adhesion within the matrix, thus making the nonwoven stronger.[65] The inability to see a trend involving the fibre diameter and the mechanical properties might be due to the unevenness of the nonwoven structure in the samples, which can be seen as the standard deviations for the mechanical measurements are quite big for some of the sample. The strain at max load for NW_fibdim25, with a fibre diameter of 25 µm, varies between 5.13 % and 8.44% for the two specimens tested. The change in fibre diameter, from 14 to 28 µm, compared to the unevenness of the nonwovens, might therefore be too small for any effect on the mechanical properties to be noticeable. As the nonwovens prove to be uneven, and therefore produce big standard deviations between the two replicas tested, more replicate tests would have to be conducted to draw any definite conclusions regarding the fibre diameter's effect on the mechanical properties of the nonwoven. A bigger difference in fibre diameter might also be required for any effect to be observed.

#### 4.5.1.2 Surface Density and Mechanical Properties

More pronounced trends can however be seen regarding the effect of surface density on the strain at max load and the effective stress. For the samples with different surface densities (NW_surfdensB), an increase in the strain at max load, as well as an increase in effective stress at max load, can be observed with the increase in surface density. The strain at max load increases from 2.5 to 5.8 %, Figure 24d, and the effective stress at max load from 2.5 to 5.5 MPa, Figure 24f, as the surface density is increases from 17 to 33 mg/cm$^2$. An effect of the surface density on the Young's modulus is however hard to discuss as no general trend can be seen. The Young's modulus both decreases (between 17 to 21 mg/cm$^2$) and increases (between 21 to 33 mg/cm$^2$) with increasing surface density, Figure 24e. The lack of trend could be due to calculation errors of the Young's modulus by the software as the linear region is picked out.

The stress at max load is an indication of the strength of the material. Naturally, the stress will increase with increased surface density, as there are more fibres holding the nonwoven together, over which the force can be distributed. The effective stress however, which is normalized to the surface density (Equation 4), also increases with surface density, indicating that there is another factor contributing than just the number of fibres. It has been shown that an increased degree of entanglement results in increased strain at break, and increased tensile strength, in a nonwoven material.[65] The increase in strain and effective stress could thereby be explained with the assumption of increased fibre entanglement as the surface density increases. Due to more entanglement, and thereby more crossover points between fibres, the force will divide over a bigger area, resulting in the nonwoven being able to withstand more stress. More entanglement would also allow the nonwoven to deform more before the fibres start breaking, resulting in a larger strain at max load. The mechanical testing for CB/cellulose nonwovens shows that the surface density has a bigger influence on the mechanical properties than the fibre diameter. Even though some trends and lack of trends can be eluded from the results, more replicas would be beneficial for definite conclusions to be drawn from the results as there is unevenness in the nonwoven structure.

### 4.5.2 Comparison with Pure Cellulose Nonwovens

A comparison of the mechanical properties between a pure cellulose nonwoven and a nonwoven with 42 wt% CB was made. Nonwovens with similar fibre diameter and surface density were chosen for the comparison. Both nonwovens chosen had an average fibre diameter of 16 µm and a surface density of 21 and 25 mg/cm$^2$, for CB/cellulose and pure cellulose nonwovens respectively. Results for the strain at max load, the Young's modulus, and the effective stress at max load, is presented in Figure 25. Two replicas were again used for each nonwoven sample, and big standard deviations can similarly be seen in the results due the unevenness in the nonwoven structure.

The results show that the strain is not affected by the incorporation of carbon black into the nonwoven fibres. The strain at max load, for both the cellulose and CB/cellulose nonwoven, is around 5 %, Figure 25a. The nonwovens ability to deform before break is thereby the same with and without CB. This coincides with results previously shown in section 4.5.1, that the strain is affected by the surface density and entanglement of the fibres in the nonwoven. As the nonwovens compared were chosen to have approximately

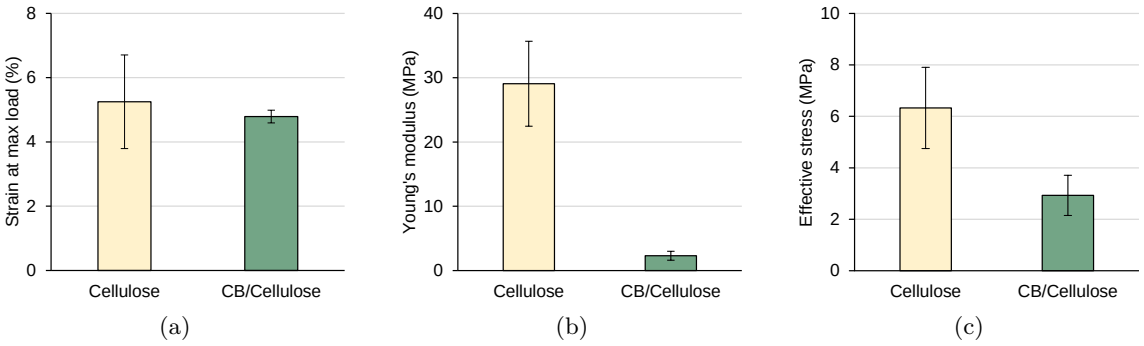


Figure 25: Comparison of the mechanical properties strain at max load, a, Young's modulus, b, and effective stress at max load, c, for cellulose and CB/cellulose nonwovens.

the same surface density, this would also mean that they would have the same amount of entanglement within the nonwoven. The same degree of entanglement thereby results in the same strain at max load, seen in Figure 25a.

Figure 25b shows a big difference in the Young's modulus between the cellulose and CB/cellulose nonwoven, 29 and 2 MPa respectively. The Young's modulus represents the stiffness of the material.[31] This indicates that the cellulose nonwovens are stiffer and stronger than CB/cellulose nonwovens, and more force is therefore needed to achieve the same amount of strain. The effective stress at max load also displays a big difference between nonwovens with and without CB, with values of 6.3 and 3.0 MPa respectively, Figure 25c. This again implies that more force is needed to break the pure cellulose nonwovens, and that this nonwoven is stronger than the CB/cellulose nonwoven. Assuming that the entanglement of the fibres for both nonwovens is the same, as they were chosen to have the same surface density, the difference in strength is probably due to the inclusion of carbon black into the fibres, and not due to structural macroscopic change within the nonwovens. As the carbon black is added into the fibres the concentration of cellulose in the fibres will also decrease, making the fibres weaker as there is less material holding the fibre together. Additionally, the carbon black may disrupt bonding between cellulose chains. With less intermolecular bonding between the cellulose, the fibres become weaker, resulting in a lower effective stress. Yang et.al. has shown that the tensile strength of regenerated cellulose fibres increases with the crystallinity of the cellulose.[72]. The decrease in effective stress, between the nonwovens without and with CB, could therefore also indicate a decrease in crystallinity of the cellulose in the nonwoven samples. To further investigate the effect of CB on the crystallinity in the nonwoven samples, other characterization techniques, as for example X-Ray diffraction analysis, XRD, could be used.[73] The comparison of cellulose and CB/cellulose nonwovens has shown that the strain achieved before break depends on the nonwoven structure, the surface density, and entanglement, whereas the effective stress at max load depends on the strength of the individual fibres.

## 4.6 Morphology of Nonwoven Fibres

The effect on the surface of the fibres, with incorporation of carbon black, was studied using SEM imaging, for visualization of the surface, and by comparing the BET specific surface area for cellulose and CB/cellulose nonwovens.

### 4.6.1 SEM imaging

To visualize the difference in surface morphology between cellulose and CB/cellulose fibres, SEM imaging was used. SEM images of a pure cellulose nonwoven, a CB/cellulose nonwoven with 42 wt% (NW_fibdim14), as well as an image of the surface of a CB/cellulose nonwoven with 33 wt% CB, are shown in Figure 26. Figure 26a shows a very smooth surface for the pure cellulose fibres within the nonwoven. Figure 26b and 26c on the other hand, showing images of the nonwoven with 42 wt% CB, show a much more rough surface contrary to the smooth surface of the pure cellulose fibres. The image with 35000x magnification, showing 33 wt% CB/cellulose fibres, Figure 26d, also illustrates the roughness of the fibre surface as a result of incorporation of CB. The BET specific surface area was also measured to quantify how the roughness of the surfaces changes when CB is added into the fibres.

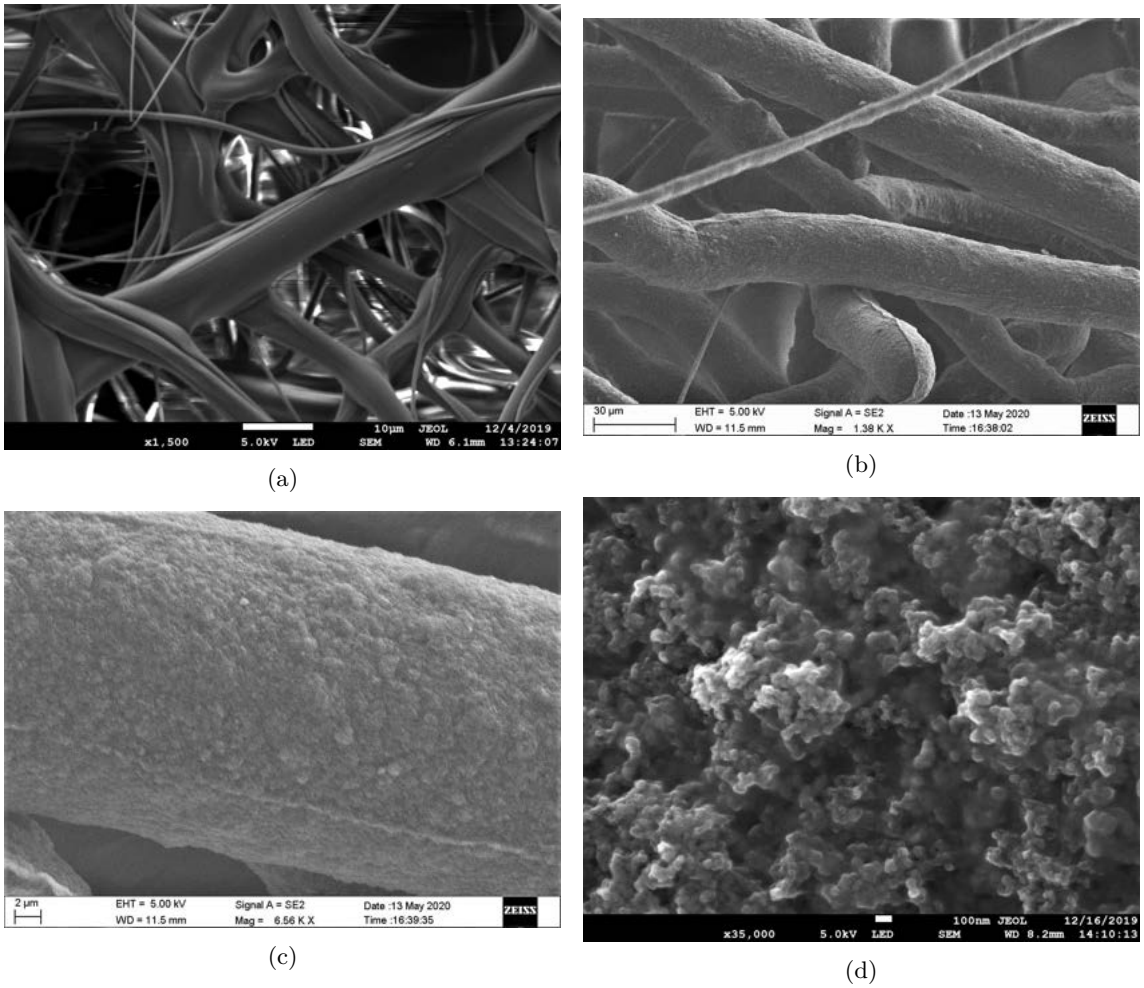


(a) (b) (c) (d)

Figure 26: SEM images of fibres within nonwoven samples. Cellulose fibre (x1500 magnification, scale bar 10 µm), a, 42 wt% CB/cellulose fibre (x1500 magnification , scale bar 10 µm), b, 42 wt% CB/cellulose fibre (x1380 magnification, scale bar 30 µm), c, and 33 wt% CB/cellulose fibre (x35000 magnification, scale bar 100 nm), d.

### 4.6.2 BET Specific Surface Area

The BET specific surface area for pure cellulose, and CB/cellulose nonwovens with 42 wt% and 50 wt% CB, was measured using $N_2$ adsorption, shown in Table 5. The surface area

of nonwovens with different fibre diameters, NW_fibdimA, and different surface densities, NW_surfdensB, were measured for the nonwovens with 42 wt% CB.

The measured BET specific surface area is around 500 $m^2/g$ for all of the nonwovens containing 42 wt% CB, Figure 5. Both an increase and a decrease in the specific surface area can be seen as the fibre diameter and surface density increases. Thinner fibres would theoretically give a larger surface area for samples of the same weight as the surface to volume ratio increases for thinner fibres. However, no correlation could be seen for the surface area with neither the fibre diameter nor the surface density. The difference in fibre diameter between samples might be too small to be detected using the BET method. There is also a broad distribution of the fibre diameter within the nonwoven samples, shown in Appendix F, Figure F-3. The broad distribution of fibre diameters might also contribute to why it would be hard to see a possible correlation between the fibre diameter and the BET specific surface area.

Table 5: BET specific surface area, measured using $N_2$ adsorption, for nonwovens with 0, 42 and 50 wt% CB.

| Sample code | CB (wt%) | BET specific surface area ($m^2/g$) |
|---|---|---|
| NW_cell | 0 | 2 ± 0.1 |
| NW_fibdim14 | 42 | 522 ± 2 |
| NW_fibdim16 | | 515 ± 2 |
| NW_fibdim25 | | 505 ± 2 |
| NW_fibdim28 | | 510 ± 2 |
| NW_surfdens17 | | 490 ± 1 |
| NW_surfdens21 | | 540 ± 2 |
| NW_surdens33 | | 502 ± 2 |
| CB50_DMSO80 | 50 | 571 ± 2 |

The average BET specific surface area was calculated to 512 $m^2/g$ for all samples with 42 wt% CB, and was used to compare the surface area with the nonwovens with 0 and 50 wt% CB. The BET specific surface area for 0 and 50 wt% CB was measured to 2 and 571 $m^2/g$ respectively, Table 5. The surface area of NW_cell is in the same order of magnitude as that of similar porous cellulose materials, the surface area reported being less than 10 $m^2/g$.[74–76] For example, the BET surface area of an electrospun nonwoven cellulose fibre mat, with an average fibre diameter of 380 ± 40 nm, is 4.86 ± 0.05 $m^2/g$.[76] Looking at the adsorption isotherm of NW_cell, Figure 27, it resembles the Type VI adsorption isotherm, Figure 9, which is obtained for uniform non-porous surfaces.[77] The shape of the adsorption isotherm thereby confirms why the specific surface area of NW_cell is very low, and that the fibres are very smooth and non-porous. The same conclusion could be drawn from the SEM imaging, showing smooth fibres within the pure cellulose nonwoven, Figure 26a. Comparing the average value of 512 $m^2/g$ for the surface area of nonwovens with 42 wt% CB, with that of pure cellulose and 50 wt% CB, an increase in the surface area can be seen with the amount of carbon black. The surface area changes from 2 $m^2/g$ for nonwoven without CB (0 wt% CB) to above 500 $m^2/g$ for nonwoven with CB. Addition of carbon black thus results in a huge increase in the specific surface area. The BET specific surface area of the carbon black used (KETJENBLACK EC600 JD) is 1400 $m^2/g$. Consequently, inclusion of 42 wt% CB in the cellulose nonwoven has a huge impact on the surface area of the nonwoven fibres.

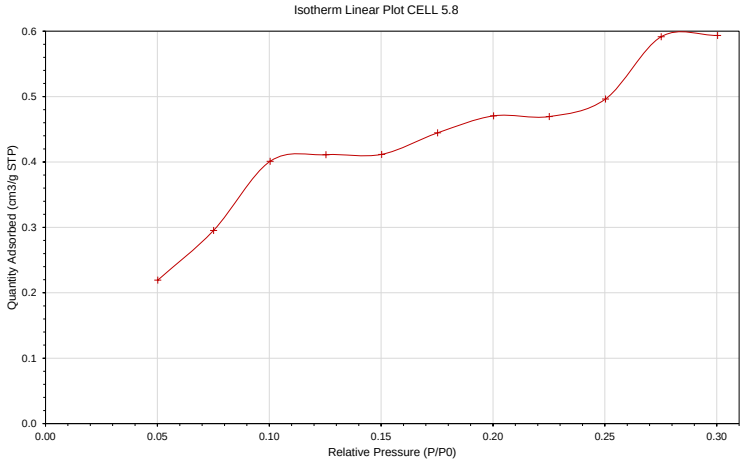


Figure 27: Amount of $N_2$ adsorbed in the pressure range 0-0.3 $p/p_0$ for cellulose nonwoven.

## 4.7 Possible Applications

Preliminary experiments were conducted to evaluate the possibility of using the nonwoven material for two different applications, as a pressure sensor or as an electrode in an energy storage device. The experiments are just rough test and more testing and evaluation should be conducted to fully evaluate the material's possible applications further. The purpose of the results in this section is to show future possibilities for the material.

### 4.7.1 Pressure Sensor

For a material to work as a pressure sensor it has to be able to respond as the pressure changes. Two preliminary experiments were conducted to evaluate the possibility of using the nonwoven material as a pressure sensor. Nonwovens with 33 wt% CB were used for these experiments. A manual dynamic test, with three repetitions for each set of weights added onto the material, shows how the resistance changes when pressure (in the form of a weight) is added and removed. The dynamic test was conducted to evaluate the material's ability to return to its original state after pressure is released and added, shown in Figure 28. The resistance at 0 Pa, measured after pressure is released, is close to the original value of 7.55 kΩ for cycles even up to 2.75 kPa. After a pressure of 3.44 kPa is applied, the resistance at 0 Pa drops to 7.13 kPa. A similar resistance is also seen after the higher pressures, 4.12 and 4.81 kPa, are removed. The decrease in resistance, after a pressure of 3.44 kPa or higher is applied, indicates that the material does not return fully to its original state and shape. As more pressure is applied to the material it might need a longer time to fully recover. The material's inability to return to its original fluffiness thereby result in a decreased resistance as more fibre-fibre contact is being established between fibres.[52] The material still shows promising results, consistently returning to 94% of the original pressure, or above, after pressure is removed. The maximum pressure, or weight, which can be applied to the material without it permanently deforming is therefore also an important factor which should be studied further.

Figure 29 shows how the resistance changes when pressure, in the form of a weights, is added continuously to the sample (blue circle), causing an evident decrease in the measured resistance. When weight is removed (orange cross), the curve follows a similar path as

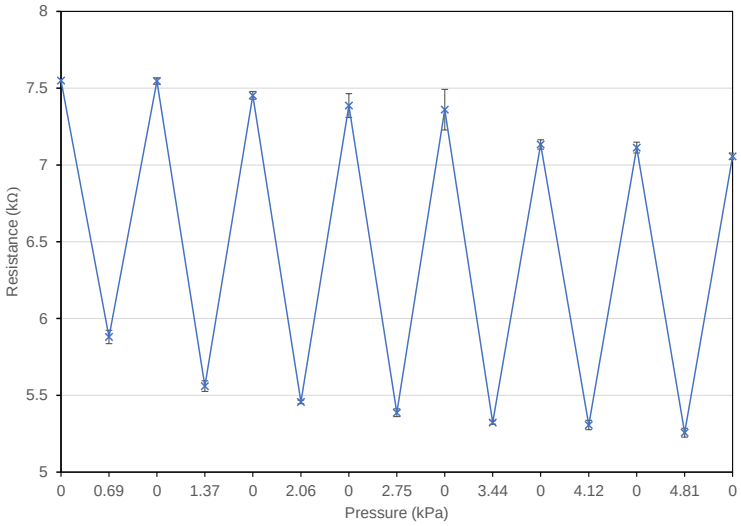


Figure 28: Dynamic manual test of how the pressures on the nonwoven material affects the resistance.

to when the weight was added. This is a good indication that the material was not damaged and give consistent values. The difference in resistance between when pressure is removed and added could be due to the material not having time to recover and become as fluffy as originally, also seen in the dynamic test, Figure 28. As the material stays more compact a lower resistance is measured than if the material would have fully returned to its fluffier state. This is seen in Figure 29 as the curve for removed pressure (orange cross) is persistently below the curve for the added pressure (blue circle).

When a pressure of 2 kPa is added, the resistance decreases to 5.43 kΩ, which is approximately 70% of the original value. The decrease in resistance with pressure is likely due to the improved fibre-fibre contact, and thereby the decreased contact resistance, between fibres within the material.[52] The effect of fibre-fibre contact on the surface resistance was also shown in section 4.4.1, where the effect of surface density on the resistance was studied. The nonwoven material has a 3D-structure. One could look at the material as being built up of sheets, created during the collection of the nonwoven on the spinning collector in the coagulation bath. One sheet corresponds to one rotation of the collector. The fibres within each sheet are well entangled whereas the entanglement and contact between sheets are not as big. When the nonwoven is pressed down by the weights, more contact between the sheets is established. More contact results in lower contact resistance between the fibres in the material, hence reducing the overall resistance of the material. The decrease in resistance is not as evident when additional pressure above 2 kPa is added. An explanation for this could be that the fibres have already reached close to maximum contact between themselves. Thus, adding extra pressure will not have a significant impact on the resistance. The fluffiness of the samples also becomes important when evaluating the change in resistance with pressure. The fluffiness will correlate to the change in the number of contact points with pressure. The fluffiness of the sample could be quantified by the volume density of the samples, providing that the thickness of the samples can be measured. An example of calculated volume density is seen in Appendix G (Table G-3) for nonwovens with 42 wt% CB. No value for the volume density of the 33 wt% CB nonwoven, used in this pressure sensor experiment, was obtained.

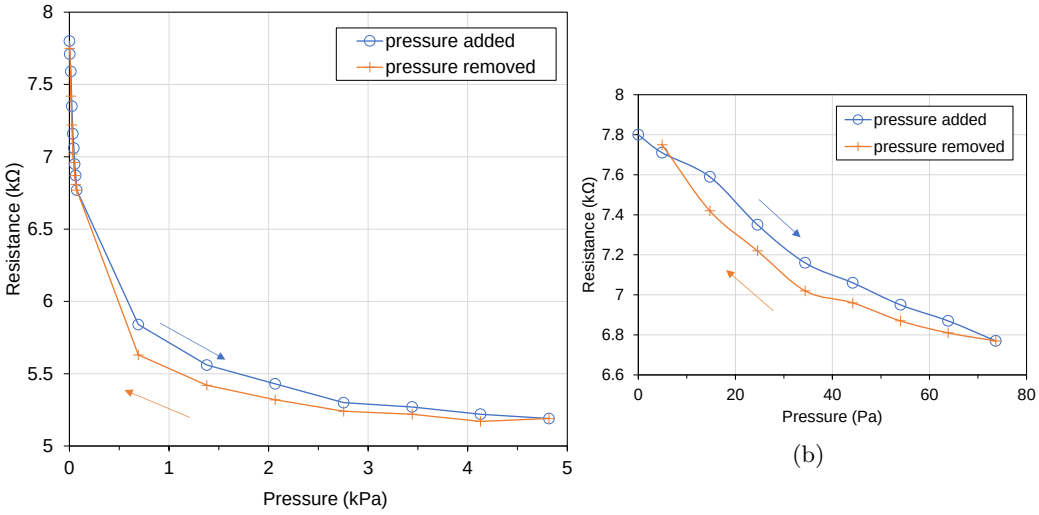


Figure 29: The pressure influence on resistance of nonwoven as the pressure is added (blue circle) and removed (orange cross) in the pressure range 0-5 kPa, a, and 0-80 Pa, b.

For a material to work as a pressure sensor it is most important that the material is able to respond to pressure. It is also important that a consistent response is given as pressure is added and removed. The conducted tests, Figure 28 and 29, show that the surface resistance of the material decreases as pressure is added, and increases again after the pressure is removed. The material also exhibits low hysteresis as a low variation in resistance is seen when the pressure is added and removed. Both these properties show the materials potential of functioning as a pressure sensor. The requirement of the pressure sensor is not that it must be as conductive as possible, but rather that the change in resistance has to be big. It is therefore possible that even less CB than 33 wt%, tested in this experiment, is adequate for the material to show a respond to pressure. Less CB might possibly increase the mechanical properties of the material, making the material less brittle and less prone to breakage. The effect of CB on the mechanical properties was presented in section 4.5.2 where a decrease in stiffness and strength could be seen as the CB concentration was increased from 0 to 42 wt%. Less breakage of the material would be beneficial as the resistance response might otherwise change over time, as the material breaks due to the pressure.

### 4.7.2 Energy Storage

Capacitance was measured for one of the nonwoven samples with 42 wt% carbon black, NW_fibdim14. The capacitance was measured to 16.86 F/g, based on the mass of CB in the nonwoven used during testing. The material thereby shows some capacitance and it has the possibility to store charge even though the capacitance is not very high. In comparison, fibres which were electrtospun, using carbon nanotubes and cellulose, resulted in a nanocomposite supercapacitor with a reported capacitance of 145 F/g, based on the mass of active material in the electrode.[78]. Carbon black has relatively low capacitance, $< 5$ F/g, compared to graphene, 80 - 170 F/g.[79] Replacing the carbon black with graphene has for example been shown to increase the capacitance.[79] The results obtained for the CB/cellulose nonwoven are just preliminary. Further testing has to be performed and with optimization it might be possible to use the material as a capacitor.

The nonwoven was also tested for its flame-retardant properties. Figure 30 shows that the cellulose nonwoven started burning, the whole sample had disappeared within 15 s. The CB/cellulose nonwoven, on the other hand, did not ignite and it did not start to burn. After being exposed to the open flame for 20 s it was however more brittle than before, indicating that cellulose had been removed from the sample. This makes sense as there is not a completely closed protective layer of carbon black on the outside of the fibres. The flame-retardant property is useful if the material was to be used as electrodes in energy storage, where a lot of heat could be created. It is then important that the electrodes do not ignite, and that the flammability of the electrode is reduced.

(a) (b)

Figure 30: Pure cellulose nonwoven, a, and CB/cellulose nonwoven, b, when exposed to an open flame for 6 seconds.

# 5. Future Work

Producing nonwovens that are conductive has proven possible by the thesis work. The CB/cellulose nonwoven could be studied even further, both in terms of producing the nonwoven, and in terms of testing possible applications of the material, to better understand the incorporation of CB and to improve the material.

Further improvements could be made to achieve an even better solution and to achieve even thinner fibres. Filtration of the solution, to remove bigger aggregates left in the solution, even after high shear mixing, could be tested to see if it makes it possible to produce even thinner fibres. Raising the temperature, to reduce the viscosity, could perhaps decrease the extrusion speed that has to be used and thereby decrease the fibre diameter.

For the material to be able to be used in an industrial scale, it is necessary that bigger nonwovens can be produced. The mechanical testing showed that the CB/cellulose nonwovens are quite brittle, and the fibres are weak. Creating bigger nonwovens, using a die with more capillaries, would therefore be interesting to see if it would be possible to produce larger material without it breaking.

More replicate samples would also be beneficial for the mechanical testing as the nonwoven samples are quite uneven. Having more replicates than two would make it easier to draw definite conclusions regarding the carbon black effect, and the effect of the nonwoven structure, on the mechanical properties. The correlation between cellulose crystallinity and the incorporation of CB could also be interesting as the decrease in tensile strength can be a sign of decreased crystallinity. How the crystallinity of cellulose changes with the DMSO concentration could also be interesting in order to see if an increased DMSO concentration reduces a solutions ability to spin strong fibres. Crystallinity of cellulose in the nonwoven could for example be studied using XRD.

Further study regarding the possible applications for the material would also be interesting for the future of the material. More testing of the material to be used as a pressure sensor, not just a manual test, preferably using dynamic mechanical analysis, DMA, could be performed. The possibility of using the material as other type of sensors, such as a humidity or a heat sensor, are other applications that could be tested. Further testing would also be beneficial to evaluate the possibility of using the nonwoven in energy storage. Making more compact nonwovens, possible by using other drying methods, could be tested to see if it affects the capacitance of the material. Replacing some of the CB with graphene could also be tried in order to increase the capacitance.

# 6. Conclusion

In conclusion, it was possible to produce conductive cellulose nonwoven material out of cellulose and carbon black, using the solution blown technique. The method from previous trials, the "original" method, could be improved, which allowed incorporation of 42 and 50 wt% CB, as well as a surface resistance below 100 Ω/□ being achieved compared to the previous achieved value of 760 Ω/□. The lowest surface resistance achieved with 42 wt% CB was 57 Ω/□.

Properties of the nonwoven could also be characterized, showing that CB affects the electrical and mechanical properties as well as the morphology of the fibres. The surface resistance decreases with increased CB concentration in the nonwoven. Incorporating 42 wt% CB proved efficient in decreasing the surface resistance while the solution, at the same time, was easy to work with during solution blow spinning. The surface resistance also decreases with increased fibre diameter, and the surface density, mainly due to the contact resistance between fibres being reduced. The mechanical properties are influenced by the incorporation of CB which makes the fibres weaker. The surface density also affects the mechanical properties strain and effective stress at break, due to an increased entanglement of fibres. The surface of the fibres is also affected by the incorporation of CB. CB makes the surface more rough, resulting in a BET specific surface area 100 times larger than without CB. The material also showed promise as a pressure sensor as well as showing ability to store charge.

Further testing of applications is interesting as this conductive textile could be produced from the sustainable, biodegradable material cellulose, using the fast solution blown technique.

# References


[1] Stoppa, M. and Chiolerio, A. "Testing and evaluation of wearable electronic textiles and assessment thereof". In: *Performance Testing of Textiles: Methods, Technology and Applications*. Elsevier Ltd., 2016. Chap. 4, pp. 65–101. DOI: 10.1016/B978-0-08-100570-5.00005-0.

[2] Stoppa, M. and Chiolerio, A. "Wearable electronics and smart textiles: A critical review". In: *Sensors (Switzerland)* 14.7 (2014), pp. 11957–11992. DOI: 10.3390/s140711957.

[3] Wang, S., Lu, A., and Zhang, L. "Recent advances in regenerated cellulose materials". In: *Progress in Polymer Science* 53 (2016), pp. 169–206. DOI: 10.1016/j.progpolymsci.2015.07.003.

[4] Huang, J. C. "Carbon black filled conducting polymers and polymer blends". In: *Advances in Polymer Technology* 21.4 (2002), pp. 299–313. DOI: 10.1002/adv.10025.

[5] Forrest, S. R. and Thompson, M. E. "Introduction: Organic electronics and optoelectronics". In: *Chemical Reviews* 107.4 (2007), pp. 923–925. DOI: 10.1021/cr0501590.

[6] Pacelli, M., Loriga, G., Taccini, N., and Paradiso, R. "Sensing fabrics for monitoring physiological and biomechanical variables: E-textile solutions". In: *Proceedings of the 3rd IEEE-EMBS International Summer School and Symposium on Medical Devices and Biosensors, ISSS-MDBS 2006* (2006), pp. 1–4. DOI: 10.1109/ISSMDBS.2006.360082.

[7] Hertleer, C., Rogier, H., Vallozzi, L., and Van Langenhove, L. "A textile antenna for off-body communication integrated into protective clothing for firefighters". In: *IEEE Transactions on Antennas and Propagation* 57.4 PART. 1 (2009), pp. 919–925. DOI: 10.1109/TAP.2009.2014574.

[8] Bao, L. and Li, X. "Towards textile energy storage from cotton T-shirts". In: *Advanced Materials* 24.24 (2012), pp. 3246–3252. DOI: 10.1002/adma.201200246.

[9] Nilsson, E., Rigdahl, M., and Hagström, B. "Electrically conductive polymeric bicomponent fibers containing a high load of low-structured carbon black". In: *Journal of Applied Polymer Science* 132.29 (2015), pp. 1–9. DOI: 10.1002/app.42255.

[10] Härdelin, L. and Hagström, B. "Wet spun fibers from solutions of cellulose in an ionic liquid with suspended carbon nanoparticles". In: *Journal of Applied Polymer Science* 132.6 (2015), pp. 1–7. DOI: 10.1002/app.41417.

[11] Hüsing, N. and Schubert, U. "Aerogels - Airy Materials: Chemistry, Structure, and Properties". In: *Angewandte Chemie - International Edition* 37.1-2 (1998), pp. 22–45. DOI: 10.1002/(SICI)1521-3773(19980202)37:1/23.0.CO;2-I.

[12] Huang, H. D., Liu, C. Y., Zhou, D., Jiang, X., et al. "Cellulose composite aerogel for highly efficient electromagnetic interference shielding". In: *Journal of Materials Chemistry A* 3.9 (2015), pp. 4983–4991. DOI: 10.1039/c4ta05998k.

[13] Qi, H., Mäder, E., and Liu, J. "Electrically conductive aerogels composed of cellulose and carbon nanotubes". In: *Journal of Materials Chemistry A* 1.34 (2013), pp. 9714–9720. DOI: 10.1039/c3ta11734k.

[14] Zhang, X., Liu, J., Xu, B., Su, Y., et al. "Ultralight conducting polymer/carbon nanotube composite aerogels". In: *Carbon* 49.6 (2011), pp. 1884–1893. DOI: 10.1016/j.carbon.2011.01.011.

[15] Wang, M., Anoshkin, I. V., Nasibulin, A. G., Korhonen, J. T., et al. "Modifying native nanocellulose aerogels with carbon nanotubes for mechanoresponsive conductivity and pressure sensing". In: *Advanced Materials* 25.17 (2013), pp. 2428–2432. DOI: 10.1002/adma.201300256.

[16] Yoon, S. H., Jin, H. J., Kook, M. C., and Pyun, Y. R. "Electrically conductive bacterial cellulose by incorporation of carbon nanotubes". In: *Biomacromolecules* 7.4 (2006), pp. 1280–1284. DOI: 10.1021/bm050597g.

[17] Zhang, S., Sun, K., Liu, H., Chen, X., et al. "Enhanced piezoresistive performance of conductive WPU/CNT composite foam through incorporating brittle cellulose nanocrystal". In: *Chemical Engineering Journal* 387.October 2019 (2020), p. 124045. DOI: 10.1016/j.cej.2020.124045.

[18] Chen, J., Li, H., Yu, Q., Hu, Y., et al. "Strain sensing behaviors of stretchable conductive polymer composites loaded with different dimensional conductive fillers". In: *Composites Science and Technology* 168.October (2018), pp. 388–396. DOI: 10.1016/j.compscitech.2018.10.025.

[19] Li, F., Qi, L., Yang, J., Xu, M., et al. "Polyurethane/conducting carbon black composites: Structure, electric conductivity, strain recovery behavior, and their relationships". In: *Journal of Applied Polymer Science* 75.1 (2000), pp. 68–77. DOI: 10.1002/(SICI)1097-4628(20000103)75:1<68::AID-APP8>3.0.CO;2-I.

[20] Hwang, J., Muth, J., and Ghosh, T. "Electrical and mechanical properties of carbon-black-filled, electrospun nanocomposite fiber webs". In: *Journal of Applied Polymer Science* 104.4 (May 2007), pp. 2410–2417. DOI: 10.1002/app.25914.

[21] Lu, L., Xing, D., Xie, Y., Teh, K. S., et al. "Electrical conductivity investigation of a nonwoven fabric composed of carbon fibers and polypropylene/polyethylene core/sheath bicomponent fibers". In: *Materials and Design* 112 (2016), pp. 383–391. DOI: 10.1016/j.matdes.2016.09.096.

[22] Wu, S., Zhang, J., Ladani, R. B., Ravindran, A. R., et al. "Novel Electrically Conductive Porous PDMS/Carbon Nanofiber Composites for Deformable Strain Sensors and Conductors". In: *ACS Applied Materials and Interfaces* 9.16 (2017), pp. 14207–14215. DOI: 10.1021/acsami.7b00847.

[23] Xue, Q. and Sun, J. "Electrical Conductivity and Percolation Behavior of Polymer Nanocomposites". In: *Polymer Nanocomposites*. Ed. by X. Huang and C. Zhi. Springer, Cham, 2016, pp. 1–351. DOI: 10.1007/978-3-319-28238-1.

[24] Françon, H., Wang, Z., Marais, A., Mystek, K., et al. "Ambient-Dried, 3D-Printable and Electrically Conducting Cellulose Nanofiber Aerogels by Inclusion of Functional Polymers". In: *Advanced Functional Materials* 30.12 (2020). DOI: 10.1002/adfm.201909383.

[25] Jedvert, K., Idström, A., Köhnke, T., and Alkhagen, M. "Cellulosic nonwovens produced via efficient solution blowing technique". In: *Journal of Applied Polymer Science* 137.5 (2020), pp. 1–9. DOI: 10.1002/app.48339.

[26] Tobler-Rohr, M. I. "The supply chain of textiles". In: *Handbook of Sustainable Textile Production*. Ed. by M. I. Tobler-Rohr. Cambridge, UK: Woodhead Publishing Limited, 2011. Chap. 2, pp. 45–149. DOI: 10.1533/9780857092861.45.

[27] Smith, P. A. "Technical fabric structures – 3. Nonwoven fabrics". In: *Handbook of Technical Textiles*. Ed. by M. Pritchard, R. W. Sarsby, and S. C. Anand. Cam-

bridge: Woodhead Publishing Limited, 2000. Chap. 6, pp. 130–151. DOI: 10.1533/9781855738966.372.

[28] Lv, Y., Wu, J., Zhang, J., Niu, Y., et al. "Rheological properties of cellulose/ionic liquid/dimethylsulfoxide (DMSO) solutions". In: *Polymer* 53.12 (2012), pp. 2524–2531. DOI: 10.1016/j.polymer.2012.03.037.

[29] Kumar, A. and Sinha-Ray, S. "A review on biopolymer-based fibers via electrospinning and solution blowing and their applications". In: *Fibers* 6.3 (2018), pp. 1–53. DOI: 10.3390/fib6030045.

[30] Daristotle, J. L., Behrens, A. M., Sandler, A. D., and Kofinas, P. "A Review of the Fundamental Principles and Applications of Solution Blow Spinning". In: *ACS Applied Materials & Interfaces* 8.51 (Dec. 2016), pp. 34951–34963. DOI: 10.1021/acsami.6b12994.

[31] Cowie, J. M. G. and Arrighi, V. *Polymers : Chemistry and Physics of Modern Materials, Third Edition*. 3rd ed. CRC Press LLC, 2007.

[32] Zhang, J., Kitayama, H., and Gotoh, Y. "High strength ultrafine cellulose fibers generated by solution blow spinning". In: *European Polymer Journal* 125.January (2020). DOI: 10.1016/j.eurpolymj.2020.109513.

[33] Zhang, J., Kitayama, H., Gotoh, Y., Potthast, A., et al. "Non-woven fabrics of fine regenerated cellulose fibers prepared from ionic-liquid solution via wet type solution blow spinning". In: *Carbohydrate Polymers* 226.April (2019), p. 115258. DOI: 10.1016/j.carbpol.2019.115258.

[34] Bajpai, P. "Structure and Properties of Cellulose and Nanocellulose". In: *Pulp and Paper Industry*. Ed. by P. Bajpai. Elsevier, 2017. Chap. 3, pp. 27–40. DOI: 10.1016/b978-0-12-811101-7.00003-4.

[35] Paquin, F., Rivnay, J., Salleo, A., Stingelin, N., et al. "Multi-phase semicrystalline microstructures drive exciton dissociation in neat plastic semiconductors". In: *J. Mater. Chem. C* 3 (2015), pp. 10715–10722. DOI: 10.1039/b000000x.

[36] Gericke, M., Fardim, P., and Heinze, T. "Ionic liquids - Promising but challenging solvents for homogeneous derivatization of cellulose". In: *Molecules* 17.6 (2012), pp. 7458–7502. DOI: 10.3390/molecules17067458.

[37] Smith, R. L. J., Qi, X., and Fang, Z. *Production of Biofuels and Chemicals with Ionic Liquids*. 1st ed. Dordrecht, Netherlands: Springer Netherlands, 2014.

[38] Wertz, J.-L., Mercier, J. P., and Bédué, O. *Cellulose Science and Technology*. 1st ed. EPFL Press, 2010. DOI: 10.1201/b16496. URL: https://www.taylorfrancis.com/books/9781439807996.

[39] Zhang, J., Zhang, H., Wu, J., Zhang, J., et al. "NMR spectroscopic studies of cellobiose solvation in EmimAc aimed to understand the dissolution mechanism of cellulose in ionic liquids". In: *Physical Chemistry Chemical Physics* 12.8 (2010), p. 1941. DOI: 10.1039/b920446f.

[40] Le, K. A., Rudaz, C., and Budtova, T. "Phase diagram, solubility limit and hydrodynamic properties of cellulose in binary solvents with ionic liquid". In: *Carbohydrate Polymers* 105.1 (2014), pp. 237–243. DOI: 10.1016/j.carbpol.2014.01.085.

[41] Härdelin, L., Thunberg, J., Perzon, E., Westman, G., et al. "Electrospinning of cellulose nanofibers from ionic liquids: The effect of different cosolvents". In: *Journal of Applied Polymer Science* 125.3 (Aug. 2012), pp. 1901–1909. DOI: 10.1002/app.36323.

[42] DeArmitt, C. "Functional Fillers for Plastics". In: *Applied Plastics Engineering Handbook*. Ed. by M. Kutz. 1st ed. Elsevier, 2011. Chap. 26, pp. 455–468. DOI: 10.

1016/C2010-0-67336-6. URL: https://www.researchgate.net/publication/298525344_Applied_Plastics_Engineering_Handbook.

[43] Spahr, M. E., Gilardi, R., and Bonacchi, D. "Carbon Black for Electrically Conductive Polymer Applications". In: *Fillers for Polymeric Applications. Polymers and Polymeric Composites: A Reference Series*. Ed. by R. Rothon. Springer, Cham, 2017. Chap. 19, pp. 375–400.

[44] Bautista-Quijano, J. R., Pötschke, P., Brünig, H., and Heinrich, G. "Strain sensing, electrical and mechanical properties of polycarbonate/multiwall carbon nanotube monofilament fibers fabricated by melt spinning". In: *Polymer* 82 (2016), pp. 181–189. DOI: 10.1016/j.polymer.2015.11.030.

[45] Spahr, M. E. and Rothon, R. "Carbon Black as a Polymer Filler". In: *Fillers for Polymeric Applications. Polymers and Polymeric Composites: A Reference Series*. Ed. by R. Rothon. Springer, Cham, 2017. Chap. 14, pp. 261–291.

[46] Singh, R., Gautam, N., Mishra, A., and Gupta, R. "Heavy metals and living systems: An overview". In: *Indian Journal of Pharmacology* 43.3 (2011), p. 246. DOI: 10.4103/0253-7613.81505.

[47] Lund, A., Velden, N. M. van der, Persson, N. K., Hamedi, M. M., et al. "Electrically conducting fibres for e-textiles: An open playground for conjugated polymers and carbon nanomaterials". In: *Materials Science and Engineering R: Reports* 126 (2018), pp. 1–29. DOI: 10.1016/j.mser.2018.03.001.

[48] Delft University of Technology. *Database Idematapp*. Date accessed: 12 June 2020. URL: https://www.ecocostsvalue.com/EVR/model/theory/subject/5-data.html.

[49] Rothon, R. "Sustainable and Recycled Particulate Fillers". In: *Fillers for Polymeric Applications. Polymers and Polymeric Composites: A Reference Series*. Ed. by R. Rothon. Springer, Cham, 2017. Chap. 22, pp. 439–461. DOI: 10.1007/978-3-319-28117-9. URL: http://link.springer.com/10.1007/978-3-319-28117-9.

[50] Langenhove, L. V. A. N. and Hertleer, C. "Conductivity Based Sensors for Protection and Healthcare". In: *Intelligent Textiles for Personal Protection and Safety : Intelligent Textiles for Personal Protection and Safety*. Ed. by S. Jayaraman, P. Kiekens, and A. Grancaric. Vol. 3. Amsterdam: IOS Press, 2019, pp. 89–105.

[51] Zhu, F., Hu, J., Zhang, H., Shi, J., et al. "Breathing measurement on the basis of contact resistance of cross-overlapping conductive yarns". In: *Fibers and Polymers* 18.2 (2017), pp. 369–375. DOI: 10.1007/s12221-017-6629-6.

[52] Li, L., Liu, S., Ding, F., Hua, T., et al. "Electromechanical analysis of length-related resistance and contact resistance of conductive knitted fabrics". In: *Textile Research Journal* 82.20 (2012), pp. 2062–2070. DOI: 10.1177/0040517512447519.

[53] Guo, L., Bashir, T., Bresky, E., and Persson, N. K. "Electroconductive textiles and textile-based electromechanical sensors-integration in as an approach for smart textiles". In: *Smart Textiles and Their Applications*. Elsevier Ltd, 2016, pp. 657–693. DOI: 10.1016/B978-0-08-100574-3.00028-X.

[54] Wang, L., Wang, X., and Lin, T. "Conductive coatings for textiles". In: *Smart Textile Coatings and Laminates*. Ed. by W. C. Smith. Woodhead Publishing, 2010, pp. 155–188. DOI: 10.1533/9781845697785.2.155. URL: https://linkinghub.elsevier.com/retrieve/pii/B9781845693794500067.

[55] Osswald, T. A. and Rudolph, N. "Introduction to rheology". In: *Polymer Rheology: Fundamentals and Applications*. Cincinnati: Carl Hanser Verlag GmbH & Co. KG, 2015. Chap. 1, pp. 1–24.

[56] Osswald, T. A. and Rudolph, N. "Viscoelasticity". In: *Polymer Rheology: Fundamentals and Applications*. Cincinnati: Carl Hanser Verlag GmbH & Co. KG, 2015. Chap. 5, pp. 143–185.

[57] Osswald, T. and Rudolph, N. "Structure and Properties of Deforming Polymers". In: *Polymer Rheology: Fundamentals and Applications*. Cincinnati: Carl Hanser Verlag GmbH & Co. KG, 2015. Chap. 2, pp. 25–58.

[58] Wu, D., Zhang, Y., Zhang, M., and Yu, W. "Selective localization of multiwalled carbon nanotubes in poly($\epsilon$-caprolactone)/polylactide blend". In: *Biomacromolecules* 10.2 (2009), pp. 417–424. DOI: 10.1021/bm801183f.

[59] Kashi, S., Gupta, R. K., Baum, T., Kao, N., et al. "Phase transition and anomalous rheological behaviour of polylactide/graphene nanocomposites". In: *Composites Part B: Engineering* 135.October (2018), pp. 25–34. DOI: 10.1016/j.compositesb.2017.10.002.

[60] Pan, Y. and Li, L. "Percolation and gel-like behavior of multiwalled carbon nanotube/polypropylene composites influenced by nanotube aspect ratio". In: *Polymer* 54.3 (2013), pp. 1218–1226. DOI: 10.1016/j.polymer.2012.12.058.

[61] Garzon, C., Wilhelm, M., Abbasi, M., and Palza, H. "Effect of Carbon-Based Particles on the Mechanical Behavior of Isotactic Poly(propylene)s". In: *Macromolecular Materials and Engineering* 301.4 (2016), pp. 429–440. DOI: 10.1002/mame.201500380.

[62] Hutten, I. M. "Testing of Nonwoven Filter Media". In: *Handbook of Nonwoven Filter Media*. 1st ed. Amsterdam: Elsevier Science Ltd, 2007. Chap. 6, pp. 245–290. DOI: 10.1016/B978-1-85617-441-1.50012-3.

[63] Saville, B. P. "Strength and elongation tests". In: *Physical Testing of Textiles*. Cambridge, England: Woodhead Publishing, 2002, pp. 115–167. URL: https://app.knovel.com/web/view/khtml/show.v/rcid:kpPTT00003/cid:kt003HTE71/viewerType:khtml//root_slug:5-strength-and-elongation-tests/url_slug:strength-elongation-tests?b-q=Physical%20Testing%20of%20Textiles&sort_on=default&b-group-by=true&b-sort-on=default&b.

[64] Pourdeyhimi, B., Maze, B., Farukh, F., and Silberschmidt, V. V. *Nonwovens-Structure-process-property relationships*. 2nd ed. Elsevier Ltd., 2019, pp. 109–143. DOI: 10.1016/B978-0-08-102619-9.00004-3. URL: http://dx.doi.org/10.1016/B978-0-08-102619-9.00004-3.

[65] Tausif, M., Pliakas, A., O'Haire, T., Goswami, P., et al. "Mechanical properties of nonwoven reinforced thermoplastic polyurethane composites". In: *Materials* 10.6 (2017). DOI: 10.3390/ma10060618.

[66] Cheema, S., Shah, T., Anand, S., and Soin, N. "Development and Characterisation of Nonwoven Fabrics for Apparel Applications". In: *Journal of Textile Science & Engineering* 08.03 (2018), pp. 4–7. DOI: 10.4172/2165-8064.1000359.

[67] Thommes, M., Kaneko, K., Neimark, A. V., Olivier, J. P., et al. "Physisorption of gases, with special reference to the evaluation of surface area and pore size distribution (IUPAC Technical Report)". In: *Pure and Applied Chemistry* 87.9-10 (2015), pp. 1051–1069. DOI: 10.1515/pac-2014-1117.

[68] Askelund, D. R., Haddleton, F., Green, P., and Robertson, H. *The Science & Engineering of Materials*. 1st ed. New York, NY: Springer US, 1996. URL: http://search.ebscohost.com/login.aspx?direct=true&AuthType=sso&db=cat07472a&AN=clec.SPRINGERLINK9781489928955&site=eds-live&scope=site.

[69] GESTIS Substance database. *Carbon Black*. Date accessed: 29 May 2020: IFA Institute for Occupational safety and Health of the German Social Accident Insurance. URL: http://gestis-en.itrust.de/nxt/gateway.dll/gestis_.

[70] Härdelin, L., Perzon, E., Hagström, B., Walkenström, P., et al. "Influence of molecular weight and rheological behavior on electrospinning cellulose nanofibers from ionic liquids". In: *Journal of Applied Polymer Science* 130.4 (2013), pp. 2303–2310. DOI: 10.1002/app.39449.

[71] Bishop, C. A. "Process Diagnostics and Coating Characteristics". In: *Vacuum Deposition Onto Webs, Films and Foils*. Ed. by C. A. Bishop. 3rd ed. William Andrew Publishing, 2015. Chap. 5, pp. 85–128. DOI: 10.1016/b978-0-323-29644-1.00005-0.

[72] Yang, Y. P., Zhang, Y., Lang, Y. X., and Yu, M. H. "Structural ATR-IR analysis of cellulose fibers prepared from a NaOH complex aqueous solution". In: *IOP Conference Series: Materials Science and Engineering* 213.1 (2017). DOI: 10.1088/1757-899X/213/1/012039.

[73] Lei, L., Lindbråthen, A., Sandru, M., Gutierrez, M. T. G., et al. "Spinning cellulose hollow fibers using 1-ethyl-3-methylimidazolium acetate-dimethylsulfoxide cosolvent". In: *Polymers* 10.9 (2018), pp. 1–11. DOI: 10.3390/polym10090972.

[74] Han, S. O., Son, W. K., Youk, J. H., Lee, T. S., et al. "Ultrafine porous fibers electrospun from cellulose triacetate". In: *Materials Letters* 59.24-25 (2005), pp. 2998–3001. DOI: 10.1016/j.matlet.2005.05.003.

[75] Lu, P. and Hsieh, Y. L. "Multiwalled carbon nanotube (MWCNT) reinforced cellulose fibers by electrospinning". In: *ACS Applied Materials and Interfaces* 2.8 (2010), pp. 2413–2420. DOI: 10.1021/am1004128.

[76] Bedford, N. M., Pelaez, M., Han, C., Dionysiou, D. D., et al. "Photocatalytic cellulosic electrospun fibers for the degradation of potent cyanobacteria toxin microcystin-LR". In: *Journal of Materials Chemistry* 22.25 (2012), pp. 12666–12674. DOI: 10.1039/c2jm31597a.

[77] Ben Yahia, M., Ben Torkia, Y., Knani, S., Hachicha, M. A., et al. "Models for type VI adsorption isotherms from a statistical mechanical formulation". In: *Adsorption Science and Technology* 31.4 (2013), pp. 341–357. DOI: 10.1260/0263-6174.31.4.341.

[78] Deng, L., Young, R. J., Kinloch, I. A., Abdelkader, A. M., et al. "Supercapacitance from cellulose and carbon nanotube nanocomposite fibers". In: *ACS Applied Materials and Interfaces* 5.20 (2013), pp. 9983–9990. DOI: 10.1021/am403622v.

[79] Zhang, S., Lum, C., and Pan, N. "Enhanced performance of carbon/carbon supercapacitors upon graphene addition". In: *Nanotechnology for Environmental Engineering* 2.1 (2017), pp. 1–8. DOI: 10.1007/s41204-017-0020-0.

# Appendices

# Appendix A "Original" Method

The "original" method that was to be improved is summarized in this appendix, Appendix A. The same materials as mentioned in section 3.1 were used in this method. The carbon black was ball milled together with the DMSO for 2 days into a sticky paste. The cellulose and high MW tunicate cellulose was dissolved in EMIMAc at 70 °C for 1 h. The sticky carbon black/DMSO paste was then added into the dissolved cellulose, and the solution was ball milled and stirred overnight at room temperature. The solution was then centrifuged, at 2000 rpm for 5 min, to remove any air bubbles. The solution was solution blown at a pump speed of 11.8 mm/min and an air pressure of 0.2 bar at room temperature. The distance between the coagulation bath, 0.1 wt% SDS in water, and the die was 50 cm. The produced nonwoven was soaked in water overnight and then put in ethanol for a few hours before it was pinned to a styrofoam board while drying. The composition of the solution is given in Table A-1. The percentage of high MW cellulose to cellulose is 5 wt%, the ratio of CB:Cellulose is 33:67 and the ratio of solvents, EMIMAc:DMSO, is 50:50. The lowest measured sheet resistance for nonwovens produced using the "original" method was 760 Ω/□.

Table A-1: "Original" recipe for 120 ml of total solvent

| | Cellulose | High MW Cellulose | EMIMAc | DMSO | Carbon black |
|---|---|---|---|---|---|
| Mass (g) | 4 | 0.2 | 60 | 60 | 2 |
| Weight percentage (%) | 3.17 | 0.16 | 47.54 | 47.54 | 1.58 |
| Dry weight percentage (%) | 65 | 3 | - | - | 32 |

# Appendix B Components in Solution

Calculations of the amounts of CB, cellulose pulp, high MW tunicate cellulose, EMIMAc, and DMSO, were made in order to prepare the solutions for rheological testing and solution blow spinning. The CB to cellulose concentration and the EMIMAc:DMSO ratio was varied between solutions. The concentration of cellulose in solvent was kept constant, and so was the ratio between cellulose pulp and high MW cellulose.

- The CB to cellulose concentration: 0, 33, 42, and 50 wt% CB, based on the total amount of CB and cellulose
- The ratio of EMIMAc:DMSO: 50:50, 40:60, 30:70, and 20:80 wt/wt
- Cellulose in solvent: 4 wt%
- High MW cellulose to cellulose pulp: 5 wt%, based on the total amount of cellulose

The mass of the components needed for a CB/cellulose solution containing 100 ml of solvent, with 42 wt% CB and 70 % DMSO, is shown in Table B-1. The weight percentage in the total solution is also shown for each component, as well as the dry weight percentage for the celluloses and CB. Example calculations of the components for the solution are also shown. The densities of the solvents are approximately 1 g/cm$^3$.

Table B-1: Recipe of CB/cellulose solution with 42 wt% CB and 70% DMSO. The volume of solvent is 100 ml.

| | Cellulose pulp | High MW cellulose | EMIMAc | DMSO | Carbon black |
|---|---|---|---|---|---|
| Mass (g) | 3.96 | 0.21 | 70 | 30 | 3.02 |
| Weight percentage (%) | 3.69 | 0.19 | 27.99 | 65.31 | 2.83 |
| Dry weight percentage (%) | 22.90 | 55.10 | - | - | 42 |

Example calculation:

*DMSO (g)* = Total amount of solvent (g) × (Percentage of DMSO ÷ 100) =
$100ml \times (70\% \div 100) = 70g$

*EMIMAc (g)* = Total amount of solvent (g) - DMSO (g) =
$100g - 70g = 30g$

*Cellulose (g)* $= \frac{\text{(Percentage of cellulose} \div 100) \times \text{Total amount of solvent (g)}}{1-\text{(Percentage of cellulose} \div 100)} =$
$\frac{(4\% \div 100) \times 100g}{1-(4\% \div 100)} \approx 4.17g$

*High MW cellulose (g)* = Cellulose (g) × (Percentage of High MW cellulose ÷ 100) =
$4.17g \times (5\% \div 100) \approx 0.21g$

*Cellulose pulp (g)* = Cellulose (g) - High MW cellulose (g) =
$4.17 - 0.21 \approx 3.96g$

*Carbon black, CB, (g)* $= \frac{\text{(Percentage of CB} \div 100) \times \text{Cellulose (g)}}{1-\text{(Percentage of CB} \div 100)} =$
$\frac{(42\% \div 100) \times 4.17g}{1-(42\% \div 100)} \approx 3.02g$

The volume percentage of carbon black can also be calculated using: cellulose density = 1.5 g/cm$^3$, carbon black density = 1.8 g/cm$^3$.[68, 69] The volume of the components can be calculated as the mass of component ÷ density of component, Table B-2.

Table B-2: Volume of components for CB/cellulose solution with 42 wt% CB and 70% DMSO. The volume of solvent is 100 ml.

| | Cellulose pulp | High MW cellulose | EMIMAc | DMSO | Carbon black |
|---|---|---|---|---|---|
| Volume (ml) | 2.64 | 0.14 | 70 | 30 | 1.68 |
| Volume percentage (%) | 2.53 | 0.13 | 28.72 | 67.02 | 1.61 |

# Appendix C Solution Blow Parameters

The solution blowing parameters, extrusion speed and sample collection time, were calculated to i) change the fibre diameter while maintaining a constant surface density of the sample and ii) change the surface density while maintaining the fibre diameter. The extrusion speed for the custom-made fibre spinning pump is calculated from the pump speed and the area of the cylinder used, Equation C-1. The pump speed itself is calculated from the knob position on the custom-made pump, Equation C-2.

$$\text{Extrusion speed (ml/min)} = \text{Pump speed (mm/min)} \times \text{Cylinder area(mm}^2\text{)} \div 1000 \quad \text{(C-1)}$$

$$\text{Pump speed (mm/min)} = \text{Knob position} \times 1.1217 - 1.175 \quad \text{(C-2)}$$

The volume of solution, needed to collect a sample of specified surface density, can be calculated from the area, dry weight percentage of the solution, and the desired surface density, of the sample, Equation C-3 and C-4. The dry mass of sample, needed to achieve the surface density of choice, is calculated by Equation C-4. For calculations it is assumed that the density of the solution is 1 g/ml.

$$\text{Volume of solution (ml)} = \text{Dry mass of sample (g)} \div \text{Dry mass percentage in solution} \quad \text{(C-3)}$$

$$\text{Dry mass of sample (g)} = \text{Area of sample (cm}^2\text{)} \times \text{Surface density (g/cm}^2\text{)} \quad \text{(C-4)}$$

The collection time needed to collect a given volume of solution is given by the volume of solution and the calculated extrusion speed, Equation C-5.

$$\text{Collection time (min)} = \text{Volume of solution (ml)} \div \text{Extrusion speed (ml/min)} \quad \text{(C-5)}$$

For the experiment with 42 wt% CB, a cylinder with a diameter of 32 mm was used and the dry mass percentage of the solution was 6.7%. An air pressure of 0.8 bar was used with a distance of 30 cm between the collection bath and the die. An approximation of the area of the sample collected, using a collector with a circumference of 25 cm and a die with 9 capillaries (Biax Fiberfilms, Greenville, WI, USA), was made to 25 cm x 1.5 cm, resulting in an area of 37.5 $cm^2$ for the collected sample.

The desired surface density for the samples in test i), where the fibre diameter was changed by changing the extrusion speed, was 0.02 $g/cm^2$. For all samples in test i), the calculated dry mass of the sample, with an area of 37.5 $cm^2$ and a surface density of 0.02 $g/cm^2$, was 0.75 g, calculated by Equation C-4. The volume of the solution was calculated by

Equation C-3, with the dry percentage in solution of 6.7%, to 11.2 ml. The extrusion speed was chosen in the range of 5.72 - 8.72 where previous experiments had shown that it was possible to spin fibre. The pump speed, knob position and collection time for the selected extrusion speeds were calculated using Equation C-1,C-2 and C-5, for values see Table.C-1. An example calculation of the knob position and collection time to collect 11.2 ml of solution at an extrusion speed of 5.72 ml/min is shown, referred to as Example calculation i). A cylinder with the diameter 32 mm was used.

Example calculation i):

$$Pump\ speed = 5.72ml/min \div (\pi \times 16^2)mm^2 \times 1000 = 7.11mm/min$$

$$Knob\ position = (7.11ml/min + 1.175) \div 1.1217 \approx 7.40$$

$$Collection\ time = 11.2ml \div 5.72 = 1.96min$$

Table C-1: Calculated solution blow parameters to change the fibre diameter by changing the extrusion speed, i)

| Extrusion speed (ml/min) | Collection time (min) | Pump speed (mm/min) | Knob position |
|---|---|---|---|
| 5.72 | 1.96 | 7.12 | 7.40 |
| 6.72 | 1.67 | 8.37 | 8.51 |
| 7.72 | 1.45 | 9.61 | 9.62 |
| 8.72 | 1.28 | 10.86 | 10.73 |

For test ii), the surface density of the samples were changed by changing the collection time, and the fibre diameter was maintained by keeping the extrusion speed constant, at 5.72 ml/min. The collection time was calculated for the desired surface density values of the surface density (0.03, 0.025 and 0.02 g/cm$^2$) using Equation C-3, C-4 and C-5, for values see Table C-2.

Table C-2: Calculated solution blow parameters to change the surface density by changing the collection time, ii)

| Extrusion speed (ml/min) | Collection time (min) | Pump speed (mm/min) | Knob position | Surface density (g/cm$^2$) |
|---|---|---|---|---|
| 5.72 | 2.94 | 7.12 | 7.40 | 0.030 |
| 5.72 | 2.45 | 7.12 | 7.40 | 0.025 |
| 5.72 | 1.96 | 7.12 | 7.40 | 0.020 |

An example calculation (Example calculation ii)) is shown, used to calculate the collection time for a set knob position of 7.40, for a nonwoven with a desired surface density of 0.02 g/cm$^2$ an area of 37.6 cm$^2$ and a dry weight percentage of 6.7% in the solution, using a cylinder with a diameter 32 mm.

Example calculation ii):

$$Dry\ mass\ of\ sample = 37.5cm^2 \times 0.02g/cm^2 = 0.75g$$

$$Volume\ of\ solution = 0.75g \div 0.067 = 11.2g$$

$Pump\ speed = 7.40 \times 1.1217 - 1.175 = 7.12 mm/min$

$Extrusion\ speed = 7.12 mm/min \times (\pi \times 16^2) mm^2 \div 1000 = 5.72 ml/min$

$Collection\ time = 11.2 ml \div 5.72 ml/min = 1.96 min$

A pure cellulose nonwoven sample was also produced with the desire to achieve the same fibre diameter, and the same surface density, as for one of the CB/cellulose nonwovens made. The dry weight percentage of the pure cellulose solution was 5.8 wt%. Choosing the same extrusion speed to 6.72 ml/min the collection time could be calculated using Equation C-3 and C-5 to achieve the same dry mass of sample as for the CB/cellulose nonwoven 0.75 g. The calculation is shown in Example calculation iii).

Example calculation iii):

$Volume\ of\ solution = 0.75 g \div 0.058 = 12.9 g$

$Collection\ time = 12.9 ml \div 6.72 ml/min = 1.92 min$

# Appendix D Pressure Sensor Testing Set Up

Measurements of the resistance with changing pressure on the nonwoven were conducted. The measurements were conducted manually with the aim of giving an indication whether the material could work as a potential pressure sensor. Two different tests were performed one the nonwoven material, one dynamic test which showed the materials potential to return to its original state after being exerted to pressure, and one test where the pressure was added continuously, more clearly showing the change in resistance with pressure.

The set-up of the pressure-resistance test is shown in Figure D-1c. Measurements of the sample and weight used is shown in Figure D-1b. The nonwoven samples were cut into strips with a width of 1 cm and a minimum length of 5 cm. The sample was placed on the template, Figure D-1a, and the positive and negative probe was clamped to the material, 5 cm apart, using crocodile clips. Weights with a diameter of 3 cm were (Figure D-1b were placed onto the nonwoven at the marked out spot on the template, Figure D-1a. The weights had to be balanced on the nonwoven, making sure the weight only contacted the nonwoven, and not the surface underneath, which could otherwise affect the pressure exerted on the sample by the weight.

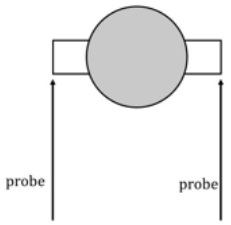


(a) Template for placement of components during measurement

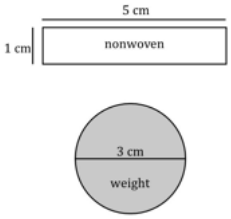


(b) Measurements of sample and weight used

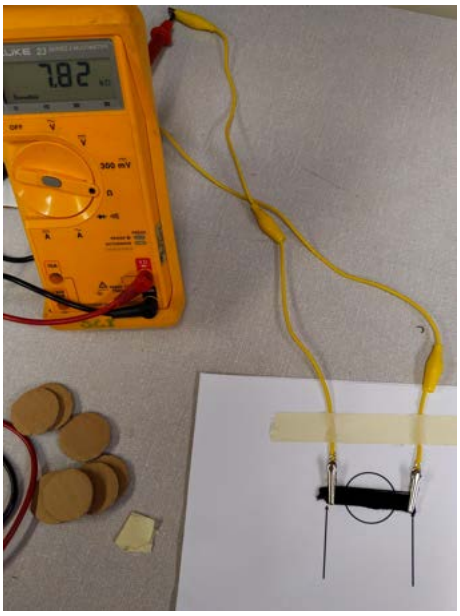


(c) Photo of pressure-resistance measurement set up

Figure D-1: Template a), measurements of components b) and set up c) for pressure resistance measurement on nonwoven sample

# Appendix E Rheology of Solutions

Rheology was performed on solutions with 33, 42, and 50 wt% carbon black, based on the total amount of filler and cellulose. The ratio between DMSO and EMIMAc was varied between 50, 60, 70 and 80 wt% DMSO. The cellulose content in solvent was kept constant at 4 wt%. The solutions are referred to as CBX_DMSOY, where X is the concentration of CB, and Y is the concentrations of DMSO in the solvent. The complex viscosity, G', G", and the phase angle, in the frequency range 0.01 to 20 Hz, obtained from an oscillatory shear test, is shown for all the prepared solutions, CBX_DMSOY. Solutions CB0_DMSOY are shown in Figure E-1, CB33_DMSOY in Figure E-2, CB42_DMSOY in Figure E-3 and CB50_DMSOY in Figure E-4.

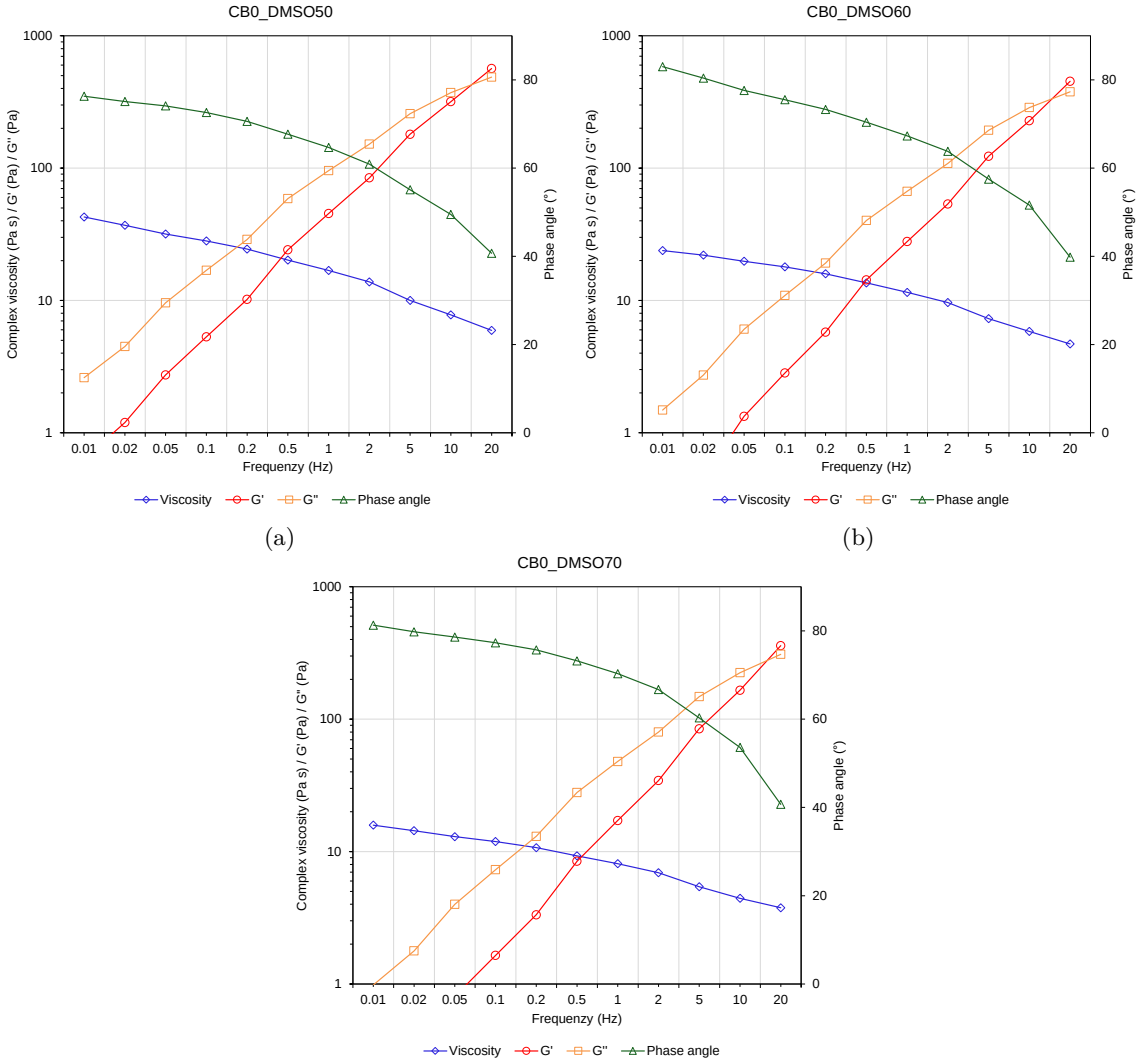


Figure E-1: Viscosity (blue diamond), G' (red circle), G" (yellow square), and phase angle (green triangle), in the frequency range 0.01 to 20 Hz for solutions CB0_DMSO50, a, CB0_DMSO60, b, CB0_DMSO70, c.

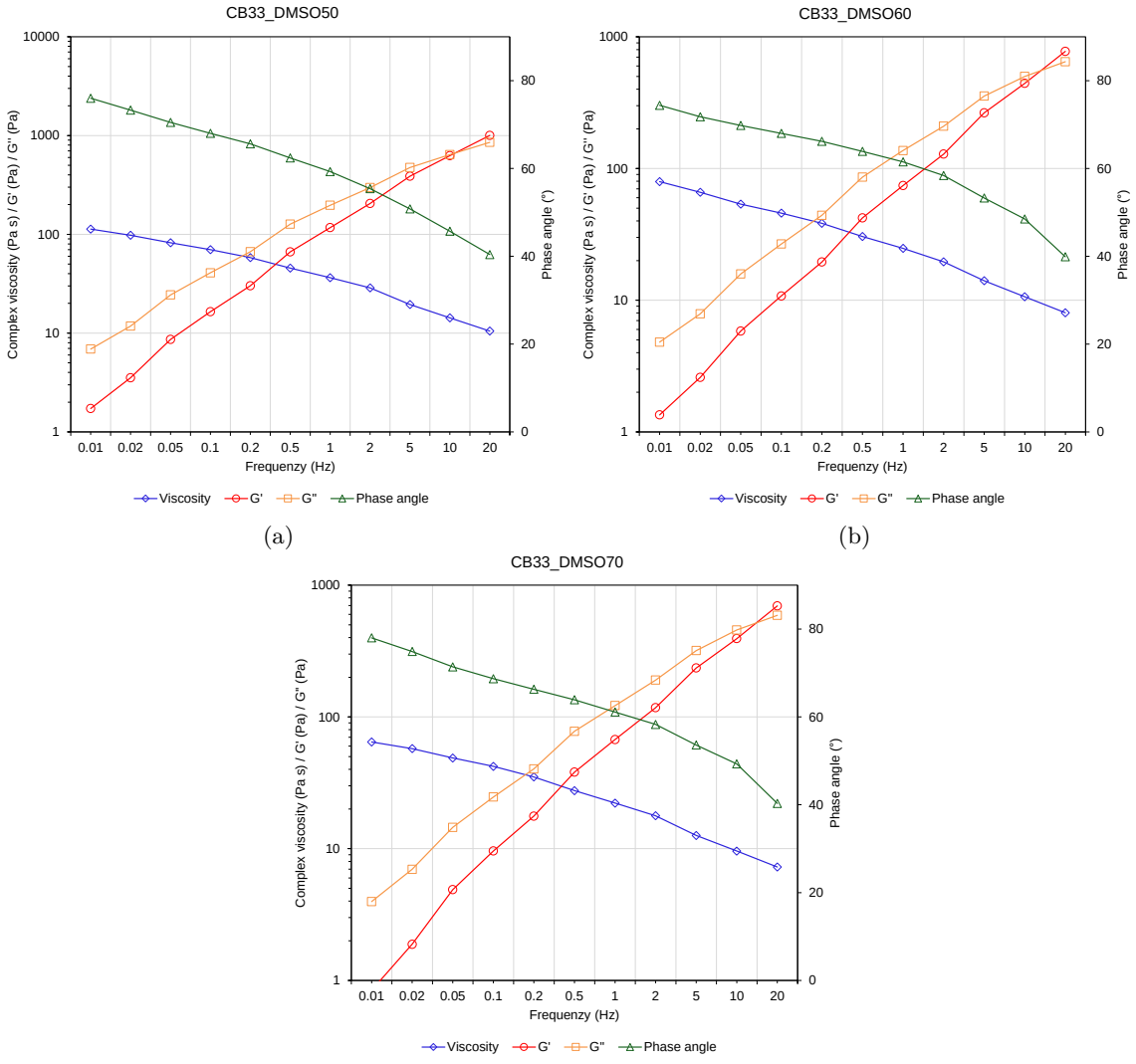


Figure E-2: Viscosity (blue diamond), G' (red circle), G" (yellow square), and phase angle (green triangle), in the frequency range 0.01 to 20 Hz for solutions CB33_DMSO50, a, CB33_DMSO60, b, CB33_DMSO70, c.

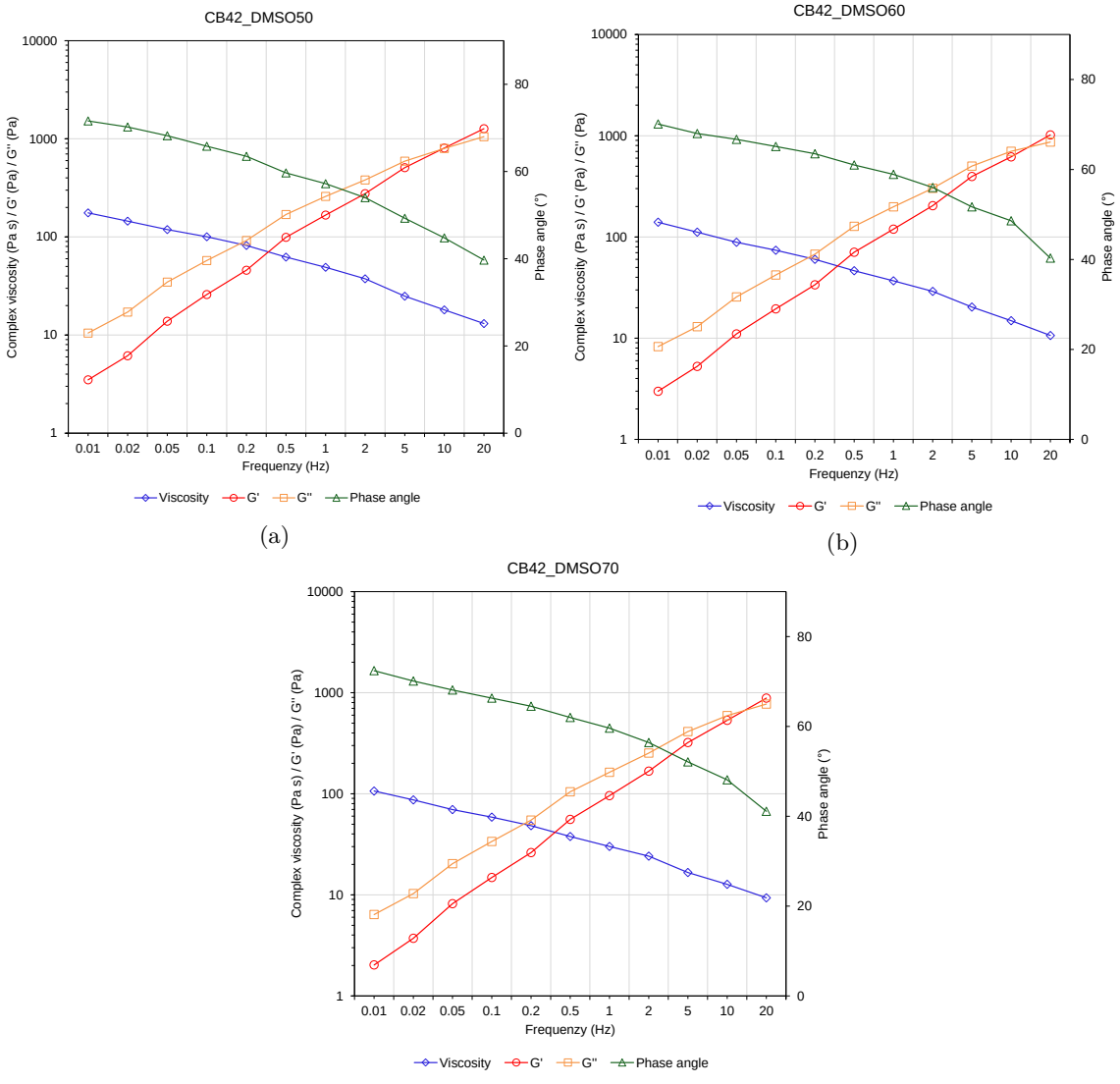


Figure E-3: Viscosity (blue diamond), G' (red circle), G" (yellow square), and phase angle (green triangle), in the frequency range 0.01 to 20 Hz for solutions CB42_DMSO50, a, CB42_DMSO60, b, CB42_DMSO70, c.

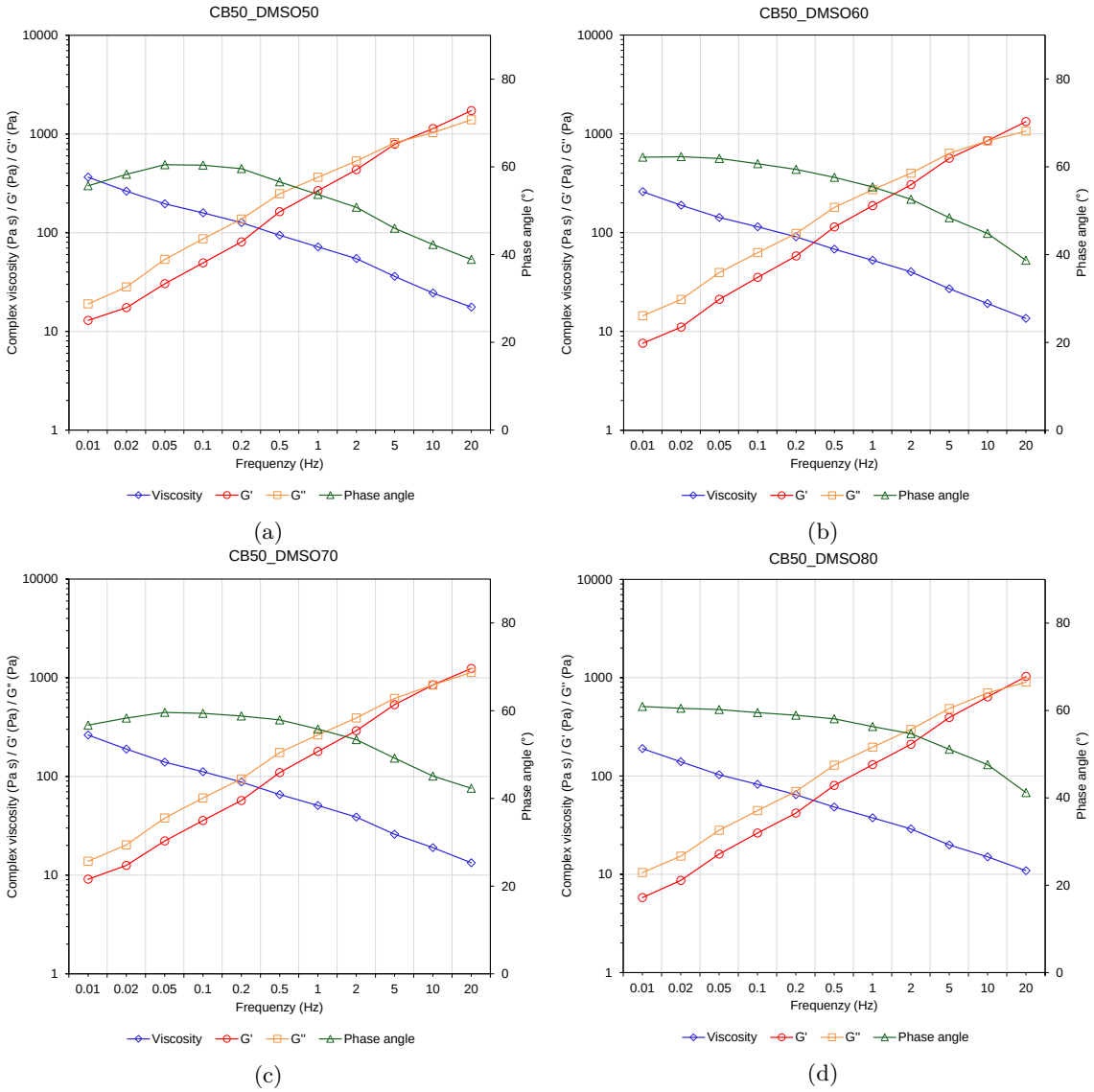


Figure E-4: Viscosity (blue diamond), G' (red circle), G" (yellow square), and phase angle (green triangle), in the frequency range 0.01 to 20 Hz for solutions CB50_DMSO50, a, CB50_DMSO60, b, CB50_DMSO70, c, CB50_DMSO80, d.

# Appendix F Light Microscopy Images of Nonwoven Fibres

Light microscopy imaging was used to visualize individual fibres in the nonwoven. The mean fibre diameter was measured in light microscopy images where the nonwoven had been separated to easier visualize individual fibres. Light microscopy images are shown for the produced nonwovens of varying surface density (NW_surfdens17, NW_surfdens21 and NW_surfdens33), Figure F-1, and varying fibre diameter (NW_fibdim14, NW_fibdim16, NW_fibdim25, NW_fibdim28), Figure F-2, in the "parameter"-test. Light microscopy images are shown in both a magnification of x4 and x10. The fibre diameter distribution for each sample is presented in the form of a histogram, Figure F-3.


(a) NW_surfdens17, x4 magnification.


(b) NW_surfdens17, x10 magnification.

(c) NW_surfdens21, x4 magnification.


(d) NW_surfdens, x10 magnification.


(e) NW_surfdens33, x4 magnification.

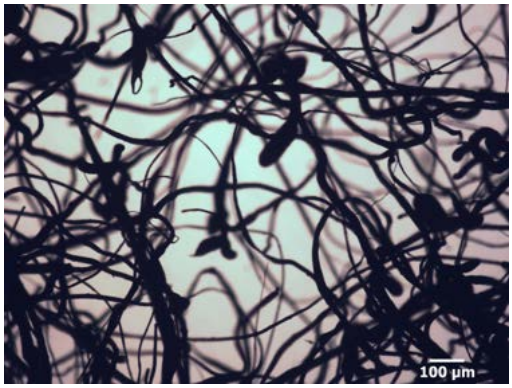


(f) NW_surfdens33, x10 magnification.

Figure F-1: Light microscopy images of fibres in nonwoven samples NW_surfdens17, a-b, NW_surfdens21, c-d, NW_surfdens33, e-f, at a magnification of x4 and x10.

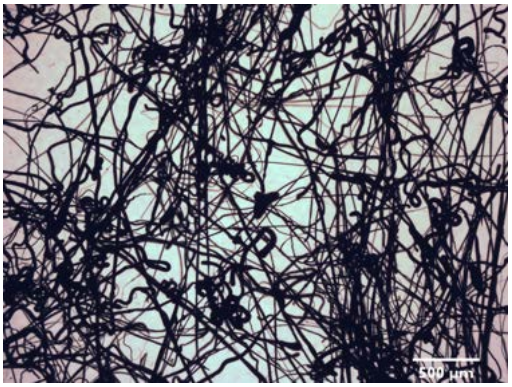


(a) NW_fibdim14, x4 magnification.


(b) NW_fibdim14, x10 magnification.


(c) NW_fibdim16, x4 magnification.

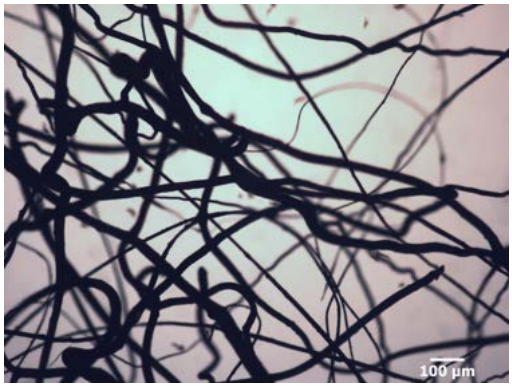


(d) NW_fibdim16, x10 magnification.

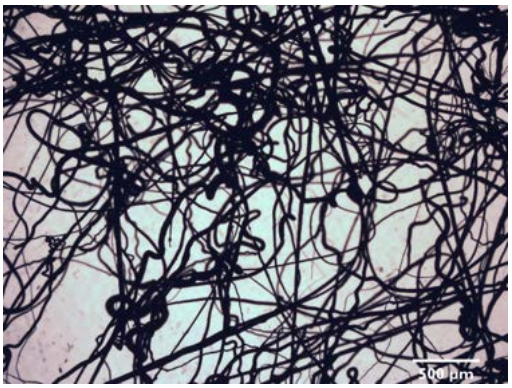


(e) NW_fibdim25, x4 magnification.

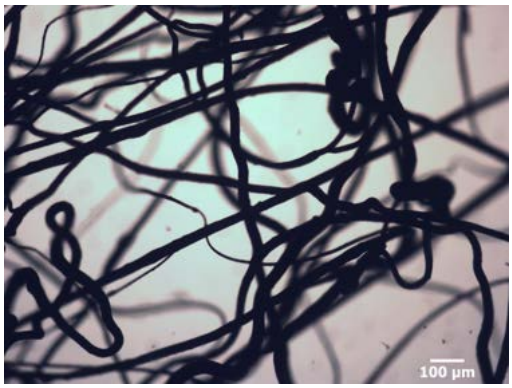


(f) NW_fibdim25, x10 magnification.


(g) NW_fibdim28, x4 magnification.

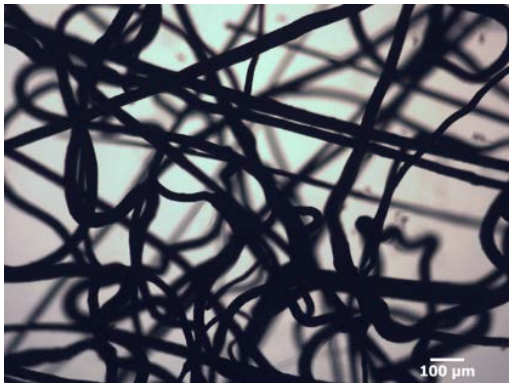


(h) NW_fibdim28, x10 magnification.

Figure F-2: Light microscopy images of fibres in nonwoven samples NW_fibdim14, a-b, NW_fibdim16, c-d, NW_fibdim25, e-f, NW_fibdim28, g-h at a magnification of x4 and x10.

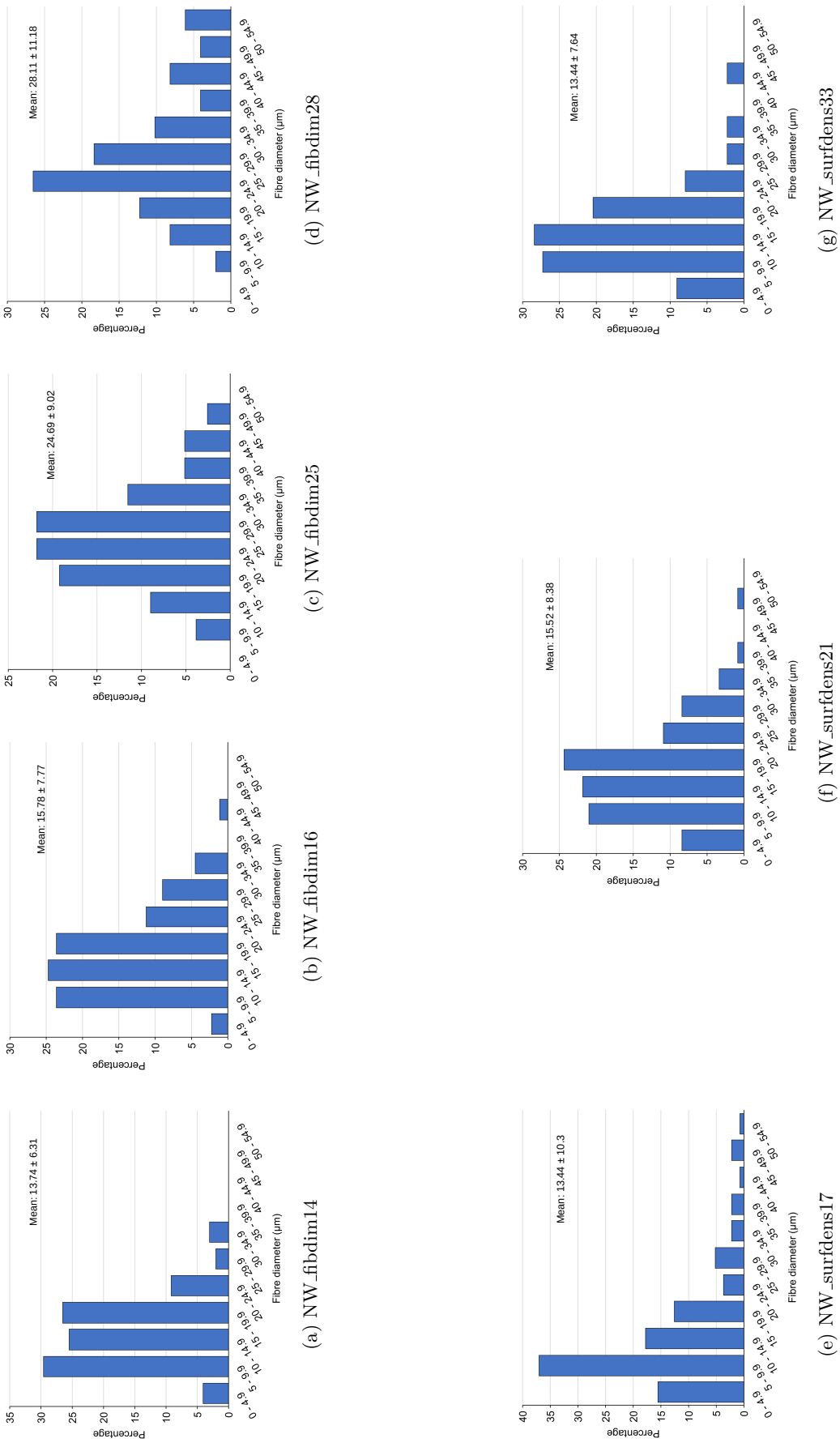


(a) NW_fibdim14 (b) NW_fibdim16 (c) NW_fibdim25 (d) NW_fibdim28

(e) NW_surfdens17 (f) NW_surfdens21 (g) NW_surfdens33

Figure F-3: Histogram representation of the fibre diameter distribution in nonwoven samples NW_fibdim14, a, NW_fibdim16, b, NW_fibdim25, c, NW_fibdim28, d, NW_surfdens17, e, NW_surfdens21, f and NW_surfdens33, g.

# Appendix G Surface- and Volume Density

The surface density is often used as a measurement for nonwovens, as their thickness can be difficult to measure. The nonwoven surface density is defined as the mass of the nonwoven divided by its surface area, according to Equation 3 ($m \div (w \times l)$), where m is the mass, w is the width, and l is the length, of the nonwoven sample). The nonwoven was cut into a rectangular shape, to easier measure the length and width of the samples. Table G-1 shows the obtained length, width, and mass, as well as the calculated area and surface density, for nonwoven samples with 42 wt% CB (NW_fibdim14-28 and NW_surfdens17-33).

Table G-1: Calculated surface density for nonwovens with 42 wt% carbon black.

| | Length (cm) | Width (cm) | Mass (g) | Area ($cm^2$) | Surface density ($g/cm^2$) |
|---|---|---|---|---|---|
| NW_fibdim14 | 22.2 | 1.5 | 0.721 | 33.3 | 0.02165 |
| NW_fibdim16 | 21.0 | 1.5 | 0.662 | 31.5 | 0.02102 |
| NW_fibdim25 | 23.4 | 1.5 | 0.729 | 35.1 | 0.02077 |
| NW_fibdim28 | 18.0 | 1.5 | 0.542 | 27.0 | 0.02007 |
| NW_surfdens17 | 21.8 | 1.5 | 0.544 | 32.7 | 0.01664 |
| NW_surfdens21 | 19.9 | 2.0 | 0.823 | 39.8 | 0.02068 |
| NW_surfdens33 | 17.0 | 1.7 | 0.955 | 28.9 | 0.03304 |

The volume density of the samples can also be calculated, provided that the thickness can be measured. The volume density is calculated as the surface density divided by the thickness. The thickness of the nonwovens, with 42 wt% CB, was measured using digital vernier calipers. The measurements were performed without pressing the nonwoven together, to get a value of the thickness in the nonwoven's original shape. Due to the unevenness of the nonwovens, six measurements were made at different places along each sample to calculate a mean value for the thickness, Table G-2. The calculated volume density, from the surface density and mean thickness, is shown in Table G-3.

Table G-2: Measured thickness of nonwovens with 42 wt% carbon black.

| Sample | Thickness (mm) | | | | | | Mean thickness (mm) |
|---|---|---|---|---|---|---|---|
| NW_fibdim14 | 5.81 | 5.89 | 5.58 | 5.95 | 5.56 | 5.23 | 5.67 ± 0.27 |
| NW_fibdim16 | 4.24 | 4.05 | 4.55 | 4.57 | 4.57 | 4.94 | 4.49 ± 0.31 |
| NW_fibdim25 | 5.33 | 5.27 | 5.56 | 5.37 | 5.12 | 5.6 | 5.38 ± 0.18 |
| NW_fibdim28 | 4.33 | 4.38 | 4.43 | 4.41 | 4.29 | 4.53 | 4.40 ± 0.08 |
| NW_surfdens17 | 3.78 | 3.5 | 3.86 | 3.57 | 3.85 | 4.01 | 3.76 ± 0.19 |
| NW_surfdens21 | 5.11 | 6.13 | 6.63 | 5.86 | 5.78 | 5.33 | 5.81 ± 0.55 |
| NW_surfdens33 | 6.48 | 6.64 | 6.79 | 6.7 | 8.14 | 7.58 | 7.06 ± 0.66 |

Table G-3: Calculated volume density for nonwovens with 42 wt% carbon black.

| | Mean thickness (mm) | Surface density ($mg/cm^2$) | Volume density ($mg/cm^3$) |
|---|---|---|---|
| NW_fibdim14 | 5.67 | 21.65 | 38.18 |
| NW_fibdim16 | 4.49 | 21.02 | 46.82 |
| NW_fibdim25 | 5.38 | 20.77 | 38.64 |
| NW_fibdim28 | 4.40 | 20.77 | 47.20 |
| NW_surfdens17 | 3.76 | 16.64 | 44.26 |
| NW_surfdens21 | 5.81 | 20.68 | 35.59 |
| NW_surfdens33 | 7.06 | 33.04 | 46.83 |

# Appendix H Surface Resistance and Conductivity

A four-point bar measurement, of the surface resistance for nonwoven samples, was performed by collaborators at RISE Norrköping using a prototype probe fixture. The surface resistance of the CB/cellulose nonwovens, with 42 wt% CB, were measured at six different places along each nonwoven and a mean value for the surface resistance of the nonwoven was calculated. The measurements of surface resistance for nonwovens with 42 wt% CB is shown in Table H-1

Table H-1: Measured surface resistance for nonwovens with 42 wt% carbon black.

| Sample | Surface resistance (Ω/□) | | | | | Mean Surface resistance (Ω/□) |
|---|---|---|---|---|---|---|
| NW_fibdim14 | 108.5 | 111.6 | 102.6 | 114 | 116.2 | 110.6 ± 5.3 |
| NW_fibdim16 | 83.6 | 100.4 | 99.7 | 82.6 | 99.03 | 93.1 ± 9.1 |
| NW_fibdim25 | 80.32 | 72 | 85.32 | 87.2 | 73.3 | 79.6 ± 6.9 |
| NW_fibdim28 | 87.9 | 102.3 | 83.8 | 77.7 | 74.1 | 85.2 ± 11 |
| NW_surfdens17 | 106.6 | 108.4 | 116 | 100 | 106 | 107.4 ± 5.8 |
| NW_surfdens21 | 70.6 | 72.3 | 67.9 | 73.6 | 75 | 71.9 ± 2.8 |
| NW_surfdens33 | 48.03 | 48.5 | 52.7 | 69.8 | 65.6 | 56.9 ± 10.1 |

The conductivities of the nonwovens were estimated in order to compare the conductivity to other porous conductive textiles. The conductivity of the CB/cellulose nonwovens, produced with 42 wt%, was estimated using Equation H-1, where $\sigma_{\text{est}}$ is the estimated conductivity, $\rho$ is the resistivity, $R_{\text{surf}}$ is the surface resistance and t is the thickness.[71]

$$\sigma_{est} = \frac{1}{\rho} = \frac{1}{R_{surf} \times t} \tag{H-1}$$

The conductivity, estimated from the mean surface density and the mean thickness, is shown in Table H-2. The conductivity for all samples is between 0.016 and 0.025 S/cm. The mean conductive over all samples is 0.023 S/cm ± 0.003.

Table H-2: Estimated conductivity of nonwovens with 42 wt% CB, based on the mean surface resistance and the mean thickness of the samples

| Sample | Surface resistance (Ω/□) | Mean thickness (mm) | Estimated conductivity (S/cm) |
|---|---|---|---|
| NW_fibdim14 | 110.6 | 5.67 | 0.016 |
| NW_fibdim16 | 93.1 | 4.49 | 0.024 |
| NW_fibdim25 | 79.6 | 5.38 | 0.023 |
| NW_fibdim28 | 85.2 | 4.40 | 0.027 |
| NW_surfdens17 | 107.4 | 3.76 | 0.025 |
| NW_surfdens21 | 71.9 | 5.81 | 0.024 |
| NW_surfdens33 | 56.9 | 7.06 | 0.025 |

# Appendix I Tensile testing

Tensile testing was performed on nonwovens NW_fibdimX, NW_surfdensY, with 42 wt% CB, and pure cellulose nonwoven, NW_cell. Two specimens for each nonwoven was tested. The strain at max load, Young's modulus and force at max load was measured by the software Bluehill (Instron), found in Table I-1, Table I-2, and Table I-3 respectively. The effective stress at max load, Table 4, was calculated according to Equation 4, where the surface density, $\rho_{surf}$, was calculated as the mass of the sample divided by its surface area. The density of the fibres were approximated to 1.5 g/cm$^3$, for the pure cellulose nonwoven, and 1.61 g/cm$^3$ for 42 wt% CB/cellulose nonwovens (approximations were made using: cellulose density = 1.5 g/cm$^3$, carbon black density = 1.8 g/cm$^3$)[68, 69]

Table I-1: Strain at max load.

| | Strain at max load (%) | | |
|---|---|---|---|
| | Specimen 1 | Specimen 2 | Mean |
| NW_fibdim14 | 4.57 | 4.09 | 4.33 ± 0.34 |
| NW_fibdim16 | 4.65 | 4.93 | 4.79 ± 0.20 |
| NW_fibdim25 | 5.13 | 8.44 | 6.79 ± 2.34 |
| NW_fibdim28 | 5.32 | 6.59 | 5.96 ± 0.90 |
| NW_surfdens17 | 2.72 | 2.27 | 2.50 ± 0.32 |
| NW_surfdens21 | 3.87 | 4.94 | 4.41 ± 0.76 |
| NW_surfdens33 | 6.03 | 5.53 | 5.78 ± 0.35 |
| NW_cell | 6.28 | 4.22 | 5.25 ± 1.46 |

Table I-2: Young's modulus

| | Young's modulus (MPa) | | |
|---|---|---|---|
| | Specimen 1 | Specimen 2 | Mean |
| NW_fibdim14 | 1.75 | 1.78 | 1.77 ± 0.02 |
| NW_fibdim16 | 1.82 | 2.80 | 2.31 ± 0.70 |
| NW_fibdim25 | 3.30 | 0.96 | 2.13 ± 1.65 |
| NW_fibdim28 | 1.58 | 2.40 | 1.99 ± 0.57 |
| NW_surfdens17 | 2.76 | 4.22 | 3.49 ± 1.03 |
| NW_surfdens21 | 2.14 | 2.11 | 2.12 ± 0.02 |
| NW_surfdens33 | 4.91 | 4.58 | 4.75 ± 0.23 |
| NW_cell | 24.40 | 33.75 | 29.07 ± 6.61 |

Table I-3: Max load and calculated effective stress at max load.

| | Max load (N) | | | Effective stress at max load (MPa) | | |
|---|---|---|---|---|---|---|
| | Specimen 1 | Specimen 2 | Mean | Specimen 1 | Specimen 2 | Mean |
| NW_fibdim14 | 3.53 | 3.13 | 3.33 ± 0.28 | 2.63 | 2.33 | 2.48 ± 0.21 |
| NW_fibdim16 | 3.10 | 4.54 | 3.82 ± 1.02 | 2.38 | 3.48 | 2.93 ± 0.78 |
| NW_fibdim25 | 6.17 | 2.83 | 4.50 ± 2.36 | 4.79 | 2.20 | 3.49 ±1.83 |
| NW_fibdim28 | 3.14 | 4.38 | 3.76 ± 0.88 | 2.44 | 3.40 | 2.92 ± 0.68 |
| NW_surfdens17 | 2.11 | 3.14 | 2.63 ± 0.73 | 2.05 | 3.04 | 2.55 ± 0.71 |
| NW_surfdens21 | 3.88 | 4.50 | 4.19 ± 0.44 | 3.03 | 3.51 | 3.27 ± 0.34 |
| NW_surfdens33 | 13.21 | 9.49 | 11.35 ± 2.63 | 6.45 | 4.63 | 5.54 ± 1.28 |
| NW_cell | 8.68 | 12.40 | 10.54 ± 2.63 | 5.94 | 8.49 | 7.21 ± 1.80 |

**DEPARTMENT OF CHEMISTRY AND CHEMICAL ENGINEERING**
**CHALMERS UNIVERSITY OF TECHNOLOGY**
Gothenburg, Sweden
www.chalmers.se


CHALMERS
UNIVERSITY OF TECHNOLOGY